

Salinization of soil moisture in Dutch coastal regions based on field data and the LHM model



MSc thesis by Ageeth de Haan

February 2024

**Soil Physics and
Land Management Group**



WAGENINGEN UNIVERSITY
WAGENINGEN **UR**

Salinization of soil moisture in Dutch coastal regions based on field data and the LHM model

cover photo made by Ageeth de Haan during the fieldwork campaign

Master thesis Soil Physics and Land Management Group
submitted in partial fulfillment of the degree of Master of
Science in Earth and Environment at Wageningen University,
the Netherlands

Study program:

MSc Earth and Environment

Student registration number:

1030148

SLM 80336

Supervisors:

WU Supervisor: dr.ir. JC (Jos) van Dam

Host supervisors: ir. I (Ilja) America - van den Heuvel (Deltares)
dr.ir. JR (Joost) Delsman (Deltares)

Examinator:

ing. G (George) Bier

Date:

24/02/24

Soil Physics and Land Management Group, Wageningen University

Acknowledgements

First, I want to thank everyone who played a role in my thesis. Among them, there are several individuals who have significantly influenced my research journey. I wish to say some words to express my appreciation to them.

I am really thankful for my main supervisors at Deltares, Ilja America and Joost Delsman. Your guidance introduced me to the complexities of salinization, learnt me research skills and provided me with valuable feedback on my work. Ilja, a special thank you for helping me starting with this thesis, guiding me through the initial fieldwork day, and offering interesting new insights when I faced some challenges. Thank you for making me feel welcome at the company Deltares.

Next, I would like to extend my gratitude to Jos van Dam, my main supervisor from the university, for connecting me with Deltares, sharing valuable knowledge and providing guidance and feedback throughout various stages of my research and writing.

I also want to acknowledge the contributions of my colleagues at Deltares: Perry de Louw, Vince Kaandorp, Eva Schoonderwoerd, Janneke Pouwels and other researchers at Deltares. Your suggestions for measurement locations, knowledge and data you shared were really helpful in shaping my thesis. Special thanks to Perry de Louw, Vince Kaandorp and others for bringing samples from Terschelling and Zeeuws-Vlaanderen. Also special thanks to Eva Schoonderwoerd and Janneke Pouwels for your assistance during the fieldwork on Schouwen-Duiveland.

Moreover, I appreciate the help from the company Aequator for providing me with measurement locations on Goeree-Overflakkee, contributing to larger spatial coverage of the measurements. Next to that, I would like to thank the farmers and field-owners who allowed me to conduct research on their fields. Your cooperation not only provided necessary and interesting locations for my research, but you also offered valuable insights in the local area. Without you I would not have this many locations to take my soil samples.

A special appreciation goes to my fellow students as well, especially those within the thesis rings, and supervisors leading these thesis rings. Your advice on writing, visualization of results and general improvements enriched my work and improved my research capacities. It was also interesting to talk to fellow thesis students to share experiences.

Lastly, I express my gratitude to my family, friends and roommates. Even while some of you were unfamiliar with my research topic, your patience in listening to me talking about my thesis, especially during busy days, have been a great support for me.

As I finish this thesis now, I am grateful for the opportunity to take some rest, reunite with family and friends, before I will start my next thesis for my second master, Geo-Information science. The lessons which I learned during this research will undoubtedly help me with my next thesis. Thank you all who contributed to this. I can use this knowledge and these lessons my whole life which is still lying ahead of me.

Abstract

This research investigates salinization in the root zone of coastal areas within the Netherlands. Currently, there is insufficient field data and understanding regarding root zone salinity in humid areas like the Netherlands. Validation of salinization models (e.g., the National Hydrological Model - LHM) relies on field data, highlighting the importance of field measurements in the root zone in order to understand salinization processes in the root zone. To address this gap, soil sample measurements were collected at 57 locations along the Dutch coast, at 25 cm intervals up to 150 cm depth. Subsequently, electrical conductivity (EC) measurements of soil moisture were done using the adjusted saturated paste method, aiming to identify salinization in the root zone. The results show significant spatial variability in soil moisture salinity, generally increasing with depth.

The coastal zone of the Netherlands contains two types of polders: deep polders in Flevoland, North Holland and South Holland, and sub-recent transgression areas in Groningen, Friesland and the South West delta. Results show that salinities are generally low in infiltration areas within sub-recent transgression areas. Seepage areas in both sub-recent transgression areas and deep polders show generally higher, but varying salinity levels, influenced by the depth of the fresh-saline interface. High concentrations are found locally in deep polders due to saline groundwater upwelling through preferential seepage via boils.

Field results were compared to the TRANSOL model, a sub-model of the LHM model. Salt fronts were generally indicative of subsoil salinity, where locations with shallow fronts and high concentrations generally match locations where high salinity in soil moisture is measured as well. However, the model simulated no salt in the root zone for almost the entire coastal area, which contradicts the soil moisture measurements. Notably, saline soil moisture is found in a large part of the coastal area, but soil samples show significant spatial variability in salinity.

To enhance understanding of salinization in the root zone of Dutch coastal areas, additional field measurements with increased spatial and temporal coverage are recommended. These field measurements are essential to validate and improve the existing models, in order to accurately simulate salinization dynamics in the soil moisture, to consequently identify risk zones for salinization and salt damage in agriculture.

Table of Contents

Acknowledgements	i
Abstract	ii
List of Figures	v
List of Tables	viii
Lists of Location Codes, Abbreviations and Symbols	ix
<i>List of location codes</i>	<i>ix</i>
<i>List of Abbreviations</i>	<i>x</i>
<i>List of symbols</i>	<i>x</i>
1 Introduction	1
1.1 <i>Context and Background</i>	<i>1</i>
1.2 <i>Research Gap</i>	<i>3</i>
1.3 <i>Research Questions and Objective</i>	<i>3</i>
1.4 <i>Hypothesis</i>	<i>3</i>
2 System Description of Relevant Salinization Sources in the Netherlands	5
2.1 <i>Seepage</i>	<i>6</i>
2.2 <i>Rainwater Lenses</i>	<i>8</i>
3 Methodology	9
3.1 <i>Study Area</i>	<i>9</i>
3.1.1 <i>Waddenzee Coast</i>	<i>9</i>
3.1.2 <i>Flevoland Coast</i>	<i>10</i>
3.1.3 <i>Holland Coast</i>	<i>10</i>
3.1.4 <i>Delta Coast</i>	<i>10</i>
3.2 <i>Study Design</i>	<i>11</i>
3.2.1 <i>Data Collection</i>	<i>11</i>
3.2.2 <i>Sample Analysis</i>	<i>12</i>
3.2.3 <i>External Data Collection</i>	<i>12</i>
3.2.4 <i>Model Analysis</i>	<i>15</i>
4 Results	17
4.1 <i>Salinity in the Field Measurements</i>	<i>17</i>
4.1.1 <i>Waddenzee Coast</i>	<i>19</i>
4.1.2 <i>Flevoland Coast</i>	<i>24</i>
4.1.3 <i>Holland Coast</i>	<i>27</i>
4.1.4 <i>Delta Coast</i>	<i>30</i>
4.2 <i>Salinity in the Model Results</i>	<i>36</i>
4.2.1 <i>Salinity Index</i>	<i>36</i>
4.2.2 <i>Salt Fronts and Concentrations</i>	<i>37</i>
4.2.3 <i>Salt Concentrations in the Root Zone</i>	<i>40</i>
5 Discussion and recommendations	42
5.1 <i>Discussion Relevant Processes</i>	<i>42</i>
5.1.1 <i>Soil Moisture Salinity Levels</i>	<i>42</i>
5.1.2 <i>Saturation Level Dependency</i>	<i>42</i>
5.1.3 <i>Drain Locations</i>	<i>43</i>

5.1.4	Ditch Dependence.....	43
5.1.5	EC as Salinity Indicator	43
5.2	<i>Recommendations</i>	44
5.2.1	Spatial and Temporal Variability.....	44
5.2.2	Saturated Paste Method	44
5.2.3	Seepage-Infiltration Map	44
5.2.4	TEC-Probe Data	45
5.2.5	Bulk Density	45
5.2.6	TRANSOL Simulations.....	45
6	Conclusion	47
	References	48
	Appendices	55
	<i>Appendix A</i>	55
	<i>Appendix B</i>	70
	<i>Appendix C</i>	75

List of Figures

Figure 1: Depth of the fresh-salt interface (Janssen et al., 2023).	1
Figure 2: Schematic representation of two important seepage systems in the Dutch delta: a) preferential saline seepage in deep polders via boils causing saltwater upconing of deeper and more saline groundwater, (b) saline seepage in sub-recent transgression areas resulting in thin rainwater lenses (P. G. B. de Louw, 2013).....	7
Figure 3: Principle of rainwater lenses above the brackish groundwater (P. G. B. de Louw, 2013).	8
Figure 4: The four coastal zones in the Netherlands classified based on their location and polder types.....	9
Figure 5: Supply of fresh surface water in the Netherlands (Donkers & Köbben, 2018).	9
Figure 6: Soil sample locations along the Dutch coast.....	11
Figure 7: Resistance layer between model layer 1 and 2 implemented in the model (Janssen et al., 2023).	15
Figure 8: Salinity index for 2019 as calculated from the LHM model (Delsman & America, 2022).	15
Figure 9: Measured EC_{sw} (mS/cm) for soil samples over the Dutch coastal area at 25 to 150 cm depth in the autumn of 2023.	17
Figure 10: Measured EC_w values (mS/cm) for ditches over the coastal area of the Netherlands in the autumn of 2023.....	18
Figure 11: Seepage-infiltration map for the Netherlands (Janssen et al., 2020).	18
Figure 12: Map showing the locations along the Waddenzee coast, and maps zooming in on the locations on the seepage-infiltration map (Janssen et al., 2020). The numbering a-f corresponds with the numbering in Figure 13.....	19
Figure 13: EC_{sw} values over depth for various locations along the Waddenzee coast during the autumn of 2023.....	20
Figure 14: Depth for the fresh-saline interface on Terschelling for a chloride concentration of 8 g/L (Data from Internal Database Deltares, n.d.; Kok et al., 2010).	22
Figure 15: Digital Terrain Model showing the elevation and measured EC_{sw} values at 150 cm depth on Terschelling, with an old tidal creek being encircled (Data Feed - Digital Terrain Model (DTM) 0,5m, 2023).	22
Figure 16: Digital Terrain Model showing the elevation and measured EC_{sw} values at 150 cm depth near Holwerd and Ternaard (Data Feed - Digital Terrain Model (DTM) 0,5m, 2023).....	22
Figure 17: Map showing the locations along the Flevoland coast, and maps zooming in on the locations on the seepage-infiltration map (Janssen et al., 2020). The numbering a-f corresponds with the numbering in Figure 18.....	24
Figure 18: EC_{sw} values over depth for various locations along the Flevoland coast during the autumn of 2023.	25
Figure 19: TEC-probe data showing the EC_{sw} values in depth for a location near Swifterbant, FL-SWB-L1 for September 2023, including soil sample measurements.	26
Figure 20: Map showing the locations along the Holland coast, and maps zooming in on the locations on the seepage-infiltration map (Janssen et al., 2020). The numbering a-f corresponds with the numbering in Figure 21.....	27
Figure 21: EC_{sw} values over depth for various locations along the Holland coast during the autumn of 2023.	28
Figure 22: TEC-probe data showing the EC_{sw} values in depth for locations near Anna Paulowna (NH-APL-L1 and NH-APL-L2) for September 2023 (Data from Project - “Zoetwaterboeren” 2022 - 2025. n.d.), including soil sample measurements.	28

Figure 23: Map showing the locations along the Delta coast, and maps zooming in on the locations on the seepage-infiltration map (Janssen et al., 2020). The numbering a-f corresponds with the numbering in Figure 24. 30

Figure 24: EC_{sw} values over depth for various locations along the Delta coast during the autumn of 2023. 31

Figure 25: Ditch EC_w values (mS/cm) for Goeree-Overflakkee (Data from Internal Database Deltares, n.d.) and Digital Terrain Model showing the elevation on Goeree-Overflakkee (Data Feed - Digital Terrain Model (DTM) 0,5m, 2023). 32

Figure 26: Depth of the fresh-saline interface on Zeeland for a chloride concentration of 1 g/L (FRESHM Zeeland Grensvlakken, 2017). 33

Figure 27: TEC-probe data showing the EC_{sw} values in depth for locations in Zeeland near Kerkwerve, the Papeweg (ZL-KWP-L1, ZL-KWP-L2 and ZL-KWP-L3) for September 2023 (Data from Project - “Samenwerken Voor Zoetwater: Innovatieve Drainage Demonstreren, Monitoren En Evalueren” 2022-2024. n.d.), including soil sample measurements. 34

Figure 28: TEC-probe data showing the EC_{sw} values in depth for locations in Zeeland near Kerkwerve, the Verseputseweg (ZL-KWV-L1 and ZL-KWV-L2) for May 2023 (Data from Project - “Samenwerken Voor Zoetwater: Innovatieve Drainage Demonstreren, Monitoren En Evalueren” 2022-2024, n.d.), including soil sample measurements. 34

Figure 29: Measured EC_{sw} (mS/cm) for soil samples over the Dutch coastal area at 100 cm depth in the autumn of 2023 overlying the salinity index for 2019 as calculated from the LHM model (Delsman & America, 2022). 36

Figure 30: Average salt front depth and concentration over 2010-2019 for the locations of the soil sample measurements as output from the TRANSOL model, grey indicates locations where soil moisture measurements indicated a salinization risk (EC_{sw} larger than 4 mS/cm), and dark grey indicates locations where both TRANSOL and soil moisture measurements indicated a salinization risk (EC_{sw} larger than 4 mS/cm and salt front shallower than 4 meters) (Janssen et al., 2023). 37

Figure 31: Yearly averaged solute concentrations in the root zone over 2010-2019 for the locations of the soil sample measurements as output from the TRANSOL model (Janssen et al., 2023). 40

Figure 32: Solute concentrations in the root zone for locations in Flevoland: Eendenweg location 2 (FL-LSE-L2) and Vogelweg location 1 (FL-LSV-L1) as output from the TRANSOL model (Janssen et al., 2023). 40

Figure 33: Solute concentration in the root zone for the Netherlands as output from the TRANSOL model (Janssen et al., 2023). 41

Figure 34: Precipitation and evapotranspiration during the fieldwork period from a weather station in de Bilt (Dagwaarden van Weerstations (25-08-2023 to 11-10-2023) - de Bilt, n.d.). 69

Figure 35: Hydrological cross-section, showing the area with mudflats (slikken) and salt marshes (schorren), and the more saline ‘seepage’ ditches close to the dike (America et al., 2023). 70

Figure 36: Results routing October 2021, showing seepage in the southern (horizontal) ditch and seepage in the encircled western (vertical) ditch (Schipper et al., 2022). 71

Figure 37: Simulated seepage and salt load for the Wieringermeerpolder in mm/d for the current situation. Upper figure shows the seepage-infiltration map, lower figure shows the salt load map for the mean summer and winter situation (Velstra et al., 2013). 72

Figure 38: Depth of 1500 mg/L chloride concentration for the Hedwigepolder, with MP4 being ZL-ZVL-L3, MP5 being ZL-ZVL-L2 and MP6 being ZL-ZVL-L1 (P. G. B. de Louw & Bootsma, 2020). 73

Figure 39: Conductivity of the subsurface with depth for mp4: ZL-ZVL-L3 (P. G. B. de Louw & Bootsma, 2020). 74

Figure 40: Conductivity of the subsurface with depth for mp5: ZL-ZVL-L2 (P. G. B. de Louw & Bootsma, 2020). 74

Figure 41: Conductivity of the subsurface with depth for mp6: ZL-ZVL-L1 (P. G. B. de Louw & Bootsma, 2020)..... 74

Figure 42: Solute concentrations modelled in depth for FL-SWB-L1L2 for three moments in time, at the start of the timeseries, the end of the timeseries and a measurement in September 2019 (Janssen et al., 2023)..... 75

Figure 43: Solute concentrations modelled in depth for FR-PBR-L1L2 for three moments in time, at the start of the timeseries, the end of the timeseries and a measurement in September 2019 (Janssen et al., 2023)..... 75

Figure 44: Solute concentrations modelled in depth for FR-TRS-L1 for three moments in time, at the start of the timeseries, the end of the timeseries and a measurement in September 2019 (Janssen et al., 2023). 75

Figure 45: Solute concentrations modelled in depth for FR-TRS-L3 for three moments in time, at the start of the timeseries, the end of the timeseries and a measurement in September 2019 (Janssen et al., 2023). 75

Figure 46: Solute concentrations modelled in depth for GR-RTT-L1 for three moments in time, at the start of the timeseries, the end of the timeseries and a measurement in September 2019 (Janssen et al., 2023). 75

Figure 47: Solute concentrations modelled in depth for NH-APL-1 for three moments in time, at the start of the timeseries, the end of the timeseries and a measurement in September 2019 (Janssen et al., 2023). 75

Figure 48: Solute concentrations modelled in depth for NH-APL-L2L3 for three moments in time, at the start of the timeseries, the end of the timeseries and a measurement in September 2019 (Janssen et al., 2023)..... 76

Figure 49: Solute concentrations modelled in depth for NH-SLD-L1L2 for three moments in time, at the start of the timeseries, the end of the timeseries and a measurement in September 2019 (Janssen et al., 2023)..... 76

Figure 50: Solute concentrations modelled in depth for NH-ZSC-L1 for three moments in time, at the start of the timeseries, the end of the timeseries and a measurement in September 2019 (Janssen et al., 2023). 76

Figure 51: Solute concentrations modelled in depth for NH-ZSC-L2 for three moments in time, at the start of the timeseries, the end of the timeseries and a measurement in September 2019 (Janssen et al., 2023). 76

Figure 52: Solute concentrations modelled in depth for ZL-KWP-L1L2L3 for three moments in time, at the start of the timeseries, the end of the timeseries and a measurement in September 2019 (Janssen et al., 2023)..... 76

Figure 53: Solute concentrations modelled in depth for ZL-ZVL-L1L2 for three moments in time, at the start of the timeseries, the end of the timeseries and a measurement in September 2019 (Janssen et al., 2023). 76

Figure 54: Yearly averaged root zone depths over 2010-2019 for the locations of the soil sample measurement as output from the TRANSOL model (Janssen et al., 2023)..... 77

Figure 55: Solute concentrations in the root zone for a location in Flevoland: Swifterbant location 1 and 2 (FL-SWB-L1L2) and a location in Groningen: Uithuizermeeden location 1 (GR-UHM-L1) (Janssen et al., 2023). 78

Figure 56: Solute concentrations in the root zone for locations in Flevoland: Marknesse location 1 (FL-MRK-L1) and location 2 (FL-MRK-L2) (Janssen et al., 2023)..... 78

List of Tables

Table 1: Soil moisture salinity classification and effects on crop growth (Abrol et al., 1988).....	5
Table 2: Formation factors (FF) for different lithological units (P. G. B. de Louw et al., 2011).....	13
Table 3: TEC-probe locations and dates from other projects within Deltares.	13
Table 4: Soil sample measurements (each 25 cm): EC values (mS/cm) for the coastal zone of the Netherlands including coordinates.	55
Table 5: Comments for the soil sample measurements (each 25 cm) for the coastal zone of the Netherlands.....	58
Table 6: Ditch measurements: EC values (mS/cm) for the coastal zone of the Netherlands.....	65
Table 7: Ditch EC values (mS/cm) for the coastal zone of the Netherlands from external sources.	67
Table 8: FRESHM and SkyTEM results for measurement locations (Data from Internal Database Deltares, n.d.; FRESHM Zeeland Grensvlakken, 2017; Kok et al., 2010).	68
Table 9: Fieldwork dates per location.	69

Lists of Location Codes, Abbreviations and Symbols

List of location codes

The locations have specific codes based on their location. The first 2 letters are based on the province name, the next 3 letters are based on the location, street and/or neighborhood name. The last part indicates the location number for this location. The coordinates of these locations are specified in Table 4 in Appendix A for soil sample locations, and Table 6 in Appendix A for ditch measurement locations.

FL-AED-L1	=	Flevoland, Aeres Dronten, Location 1
FL-LSE-L1	=	Flevoland, Lelystad Eendenweg, Location 1
FL-LSE-L2	=	Flevoland, Lelystad Eendenweg, Location 2
FL-LSV-L1	=	Flevoland, Lelystad Vogelweg, Location 1
FL-LSV-L2	=	Flevoland, Lelystad Vogelweg, Location 2
FL-MRK-L1	=	Flevoland, Marknesse, Location 1
FL-MRK-L2	=	Flevoland, Marknesse, Location 2
FL-SWB-L1	=	Flevoland, Swifterbant, Location 1
FL-SWB-L2	=	Flevoland, Swifterbant, Location 2
FR-HLK-L1	=	Friesland, Holwerd Kletterbuurt, Location 1
FR-HLW-L1	=	Friesland, Holwerd West, Location 1
FR-PBR-L1	=	Friesland, Pietersbierum, Location 1
FR-PBR-L2	=	Friesland, Pietersbierum, Location 2
FR-PNG-L1	=	Friesland, Pingjum, Location 1
FR-PNG-L2	=	Friesland, Pingjum, Location 2
FR-TRN-L1	=	Friesland, Ternaard Noord, Location 1
FR-TRN-L2	=	Friesland, Ternaard Noord, Location 2
FR-TRS-L1	=	Friesland, Terschelling, Location 1
FR-TRS-L2	=	Friesland, Terschelling, Location 2
FR-TRS-L3	=	Friesland, Terschelling, Location 3
FR-TRT-L1	=	Friesland, Ternaard Teijeburen, Location 1
GR-KLB-L1	=	Groningen, Kloosterburen, Location 1
GR-RTT-L1	=	Groningen, Rottum, Location 1
GR-RTT-L2	=	Groningen, Rottum, Location 2
GR-UHM-L1	=	Groningen, Uithuizermeeden, Location 1
GR-UHM-L2	=	Groningen, Uithuizermeeden, Location 2
NH-APL-L1	=	North Holland, Anna Paulowna, Location 1
NH-APL-L2	=	North Holland, Anna Paulowna, Location 2
NH-APL-L3	=	North Holland, Anna Paulowna, Location 3
NH-SLD-L1	=	North Holland, Slootdorp, Location 1
NH-SLD-L2	=	North Holland, Slootdorp, Location 2
NH-ZSC-L1	=	North Holland, Zuid-Schermer, Location 1
NH-ZSC-L2	=	North Holland, Zuid-Schermer, Location 2
ZH-BSK-L1	=	South Holland, Boskoop, Location 1
ZH-BSK-L2	=	South Holland, Boskoop, Location 2
ZH-BSK-L3	=	South Holland, Boskoop, Location 3
ZH-BSK-L4	=	South Holland, Boskoop, Location 4
ZH-GFB-L1	=	South Holland, Goeree-Overflakkee Boutweg, Location 1
ZH-GFB-L2	=	South Holland, Goeree-Overflakkee Boutweg, Location 2
ZH-GFG-L1	=	South Holland, Goeree-Overflakkee Groeneweg, Location 1
ZH-GFG-L2	=	South Holland, Goeree-Overflakkee Groeneweg, Location 2
ZH-GFW-L1	=	South Holland, Goeree-Overflakkee Westduinweg, Location 1
ZH-GFW-L2	=	South Holland, Goeree-Overflakkee Westduinweg, Location 2

ZL-AAG-L1	=	Zeeland, Aagtekerke, Location 1
ZL-AAG-L2	=	Zeeland, Aagtekerke, Location 2
ZL-HKK-L1	=	Zeeland, Hoedekenskerke, Location 1
ZL-HKK-L2	=	Zeeland, Hoedekenskerke, Location 2
ZL-KMP-L1	=	Zeeland, Kamperland, Location 1
ZL-KMP-L2	=	Zeeland, Kamperland, Location 2
ZL-KWP-L1	=	Zeeland, Kerkwerve Papeweg, Location 1
ZL-KWP-L2	=	Zeeland, Kerkwerve Papeweg, Location 2
ZL-KWP-L3	=	Zeeland, Kerkwerve Papeweg, Location 3
ZL-KWV-L1	=	Zeeland, Kerkwerve Verseputseweg, Location 1
ZL-KWV-L2	=	Zeeland, Kerkwerve Verseputseweg, Location 2
ZL-ZVL-L1	=	Zeeland, Zeeuws Vlaanderen, Location 1
ZL-ZVL-L2	=	Zeeland, Zeeuws Vlaanderen, Location 2
ZL-ZVL-L3	=	Zeeland, Zeeuws Vlaanderen, Location 3

List of Abbreviations

BRO	=	Basisregistratie Ondergrond
DPZW	=	Delta Program Fresh Water (Delta Programma Zoet Water)
DTM	=	Digital Terrain Model
EC	=	Electrical Conductivity
FF	=	Formation Factors
LHM	=	National Hydrological Model (Landelijk Hydrologisch Model)
NHI	=	Dutch Hydrological Instrumentarium (Nederlands Hydrologische Instrumentarium)
TEC-probe	=	Temperature and Electrical Conductivity probe
TRANSOL	=	TRANsport of SOLutes model

List of symbols

c	=	Resistance layer
Cl	=	Chloride concentration
CVES	=	Continuous Vertical Electrical Sounding
$\Delta\phi$	=	Pressure difference between the hydraulic head of the aquifer and the phreatic water level
EC_{dil}	=	Electrical Conductivity of the extracted water from the diluted paste
EC_{sw}	=	Electrical Conductivity of soil moisture (soil water)
EC_w	=	Electrical Conductivity of water
F_{dil}	=	Dilution factor for the saturation paste method
$M_{demiwater}$	=	Mass of the added demineralized water
M_{dry}	=	Mass of the oven-dry sample in the foil container
M_{field}	=	Mass of the sample in the foil container
$M_{saturation}$	=	Mass of the saturated sample in the foil container
M_{sw}	=	Mass of the soil moisture (soil water) present in the sample
M_{water_total}	=	Mass of the total amount of water (added demineralized water and soil moisture)
q_z	=	Vertical groundwater flux; seepage (positive; upward) or infiltration flux (negative; downward)

1 Introduction

1.1 Context and Background

Coastal areas commonly contain saline to brackish surface- and groundwater. Most groundwater and surface waters in the Dutch coastal region are brackish or salt, as is shown by the depth of the fresh-salt interface of groundwater in Figure 1. Coastal groundwater is significantly more saline than groundwater land inward, which can be seen by the shallower depth of the interface, showing that saline groundwater is found closer to the surface. Currently, these areas are becoming more saline over time: salinization takes place. Salinization is already a problem in many, especially drier, regions in the world (Rengasamy, 2006), because crops, animals, humans and nature need freshwater to survive. In the Netherlands this is becoming more of a problem as well (Boer & Radersma, 2011). This problem is increasing on the one hand by climate change in terms of drought and increasing sea levels, on the other hand by soil subsidence and artificial lowering of groundwater tables (Oude Essink, 2007; Stuyfzand, 2007). The coastal zones of the Netherlands are mainly used for agriculture (CORINE Land Cover - CLC 2018, 2019), which requires availability of freshwater. However, with the expected salinization issues in the Netherlands, future agriculture might be in danger (Boer & Radersma, 2011).

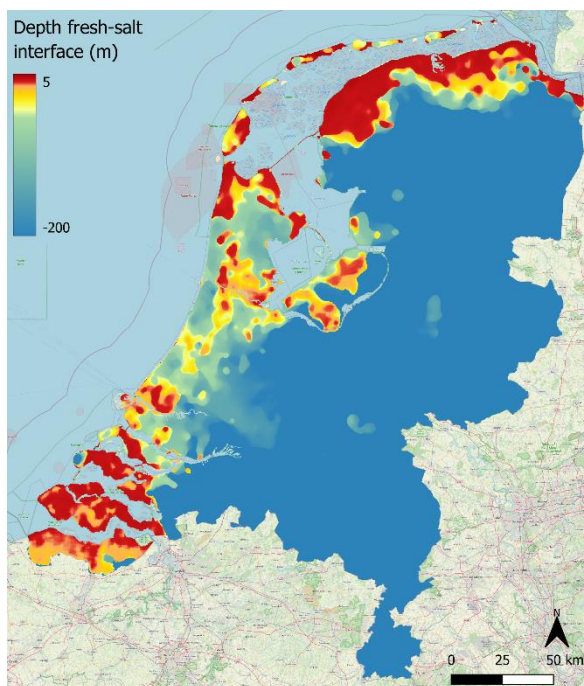


Figure 1: Depth of the fresh-salt interface (Janssen et al., 2023).

About one-third of the Netherlands is below sea level, but without the protection by dunes, dikes and pumps, even 65% would be flooded (Hoeksema, 2007). This makes the Netherlands susceptible to salinization. Salinization is the increase of salt concentrations in the soil, soil moisture and groundwater, leading to a decreased freshwater availability. Salinization is not an immediate problem for the Netherlands due to the humid climate, where precipitation usually provides sufficient fresh water for plants. Lots of research is available about salinization in semi-arid regions, but due to the different climate, this is not relevant in the Netherlands, where generally enough water is available for plants, but over time soil moisture might become more saline, which can endanger crop growth in the Netherlands where crops are generally not salt-tolerant (Kroes & Supit, 2011; Raats, 2015; van Alphen et al., 2022). Therefore, over time with the expected climate change and increasing freshwater demands for vegetation, it can endanger the crop growth in Dutch agriculture (Stofberg et al., 2017).

There are multiple sources of salinization. The first one is intrusion of water from the North Sea to the groundwater. Groundwater flow and seepage lead to a flow of saline seawater land inward with an intrusion front of 1.5 up to 6 kilometers (Stuyfzand, 2007), depending on the hydraulic conductivity of the top layer, the thickness and hydraulic conductivity of the aquifer, and the hydraulic head difference between the sea and low-lying polders (Costall et al., 2020). Next to that, there is mobilization of deep old marine groundwater below the land surface. This salt groundwater comes up through seepage, leading to salinization in a strip of 25 to 75 kilometers along the coast (Stuyfzand, 2007). The seepage processes are further elaborated in section 2.1. Furthermore, seawater intrudes through river mounds connected to the sea. This depends on sea water levels, river water discharge, surface levels and the wind direction (Boer & Radersma, 2011; Jacobs, 2007). Because of the changing climate with decreasing river discharge and increasing sea water levels, this problem is expected to increase as the salt-fresh balance in estuaries is disturbed (KNMI, 2014; van den Brink et al., 2019). The intrusion of seawater and mobilization of marine groundwater are strengthened by soil subsidence and subsequently lower phreatic groundwater levels as well, either due to compaction, peat oxidation, tectonics, isostasy, or gas and salt extraction (Fokker et al., 2018; Hoeksema, 2007).

Furthermore, a different balance in water availability over the seasons is expected due to climate change. During winter, precipitation rates are expected to increase, with larger river water discharges. During summer on the other hand, the freshwater availability is expected to decrease, due to decreased precipitation rates and increased evapotranspiration rates, leading to decreased river discharges (Jacobs, 2007; KNMI, 2014). Together, climate change and soil subsidence can result in a double amount of salinization in the northern part of the Netherlands (Boer & Radersma, 2011; Stuurman et al., 2006). Salinization is expected to become more of a problem during the summer, when precipitation rates are lower. Crops are dependent on freshwater availability, and vegetation's demand for freshwater is expected to increase due to increasing temperatures (Condon et al., 2020). The lower rainfall amounts, and higher evapotranspiration rates will increase the drought risk and capillary rise in the summer growing season.

Agriculture needs freshwater for plant growth. In coastal areas, water used for agriculture comes from rainwater lenses above the brackish groundwater, which are fed by precipitation (De Louw, 2013; Stuurman et al., 2006). These rainwater lenses lay above brackish groundwater, as salt water has a higher density, and therefore sinks, leaving a rainwater lens on top (De Louw, 2013; Schot et al., 2004). The principle of rainwater lenses is further elaborated in section 2.2. However, the rainwater lenses and fresh groundwater are depleted by agriculture, industries, and for drinking water practices, thereby decreasing the freshwater availability (De Louw, 2013). These rainwater lenses are threatened to disappear completely, due to the decreasing thickness and mixing at the salt-fresh interface (P. G. B. de Louw, Eeman, et al., 2013; Stofberg et al., 2017). This can lead to capillary rise from the salty subsurface towards the root zone, causing salinization problems in soil moisture in the root zone (P. G. B. de Louw, Eeman, et al., 2013). Together with the increasing salinization of the groundwater, this can reduce freshwater availability. In agricultural fields, plants get stressed by brackish water, which negatively affects plant growth. Even though there are some salt tolerant plants, these plants get salt stressed as well if salt concentrations increase significantly (Dajic, 2006; Stofberg et al., 2017). At the same time, during the growing season, precipitation amounts are expected to decrease and temperatures to increase due to climate change. This increases the plant's need for good-quality soil moisture, while soil moisture quality is deteriorating at the moment.

1.2 Research Gap

Currently, the salinization in the groundwater is quite well investigated both by models and field measurements, but salinization of soil moisture in the root zone requires more research. There are only some models available about salinization in the root zone, lacking sufficient research to provide field measurements to validate these models, especially in temperate regions like the Netherlands (P. G. B. de Louw, Eeman, et al., 2013; Delsman & America, 2022; Stofberg et al., 2017; Velstra et al., 2011)

Therefore, this research is focused on the salinization of soil moisture in the root zone in coastal areas of the Netherlands. Knowledge of salinization in the root zone is important, as water from this zone is taken up by plants (Ritchie, 1981) and salt concentrations in the topsoil are more variable than in surface waters and groundwater (P. G. B. de Louw, Eeman, et al., 2013; Velstra et al., 2011). Salinization in the root zone is affected by seepage and capillary rise from groundwater, irrigation, and irregular, seasonal precipitation and evapotranspiration patterns (Stofberg et al., 2017). Salt comes into the root zone by capillary rise and remains in the soil after evapotranspiration. Precipitation does not flush all salts towards the groundwater due to preferential flow, leading to higher concentrations in the topsoil.

However, the variability of salt concentrations in the root zone requires more in-detail research (P. G. B. de Louw, Eeman, et al., 2013; Stofberg et al., 2017). The seasonality and variability make it more difficult to investigate this, but also more interesting and important to obtain these results. A model is developed by the Dutch Hydrological Instrumentarium (Nederlands Hydrologische Instrumentarium – NHI), which simulates the transport of salt within the unsaturated soil column (Janssen et al., 2023). The output of this National Hydrological Model (Landelijk Hydrologisch Model – LHM), and the sub-model TRANSOL, predicts which areas are prone to salinization. However, this model is currently not used because of absence of field measurements to validate this model. The data obtained in this research can be used to validate the TRANSOL output within the LHM model.

1.3 Research Questions and Objective

In order to fill this research gap, this research aimed to identify salinization in the root zone in Dutch coastal areas. This research is therefore focused on the following research question: To what extent is salinization found in the root zone in Dutch coastal areas? Together with the following sub-questions: i) In which areas along the Dutch coast does salt occur in soil moisture in the root zone? ii) To what extent do the measured locations with salt in the root zone match the modelled saline locations? The objective was to measure salinity concentrations in the soil moisture in Dutch coastal areas, and to use earlier field measurements and studies, to identify in which areas along the Dutch coast salt occurs in the root zone.

1.4 Hypothesis

Salinization was expected to play a significant role in the soil moisture in the root zone of Dutch coastal areas (Boer & Radersma, 2011; Stofberg et al., 2017). Especially in areas close to the coast, where the availability of freshwater is low. Parts of the Dutch coast have no freshwater availability next to the rainwater lenses, which are elaborated in Figure 5 in section 3.1. However, with the expected climate change, precipitation rates are expected to decrease, and evapotranspiration rates are expected to increase, therefore drought is expected to become a larger problem. This was expected to decrease the water availability in rainwater lenses, and thereby the freshwater availability in these parts of the coast was expected to decrease significantly (Stofberg et al., 2017). Also, salinization was expected in the soil moisture of seepage areas in the coastal zone of the Netherlands, which can be quite local dependent on local seepage processes in deep polders, the shallow depth of the fresh-salt interface with small rainwater lenses in sub-recent transgression areas and the soil composition (P. G. B. de Louw, 2013).

However, salt concentrations in the root zone can be quite variable (P. G. B. de Louw, Eeman, et al., 2013; Velstra et al., 2011), this made it difficult to predict whether the field measurements would match the risk zones for salinization as simulated by the LHM model (Delsman & America, 2022). Especially because the LHM model is not validated yet by field measurements. Processes influencing the root zone salinity may involve partial dissolution of salts, resulting in some salts not leaching towards the groundwater during precipitation events (P. G. B. de Louw, Eeman, et al., 2013), or high evaporation rates leading to more salt accumulating in the root zone (Zhang et al., 2022). Salt concentrations were expected to vary significantly with depth, depending on processes affecting salt concentrations in the root zone, like precipitation, irrigation, evapotranspiration, capillary rise and seepage (P. G. B. de Louw, Eeman, et al., 2013; Stofberg et al., 2017; Velstra et al., 2011; Zhang et al., 2022). These processes were expected to cause a mismatch between the model and field results.

2 System Description of Relevant Salinization Sources in the Netherlands

As this research is focused on salinity concentrations in the soil moisture in the root zone and the processes affecting these concentrations, this system description is focused on the relevant salinization processes in the Netherlands. It is known that seepage and infiltration processes are the most important factors for the existence of rainwater lenses. When these lenses decrease in size, the implications for soil salinization become more pronounced. Therefore, a detailed elaboration of these sources is provided here.

When dealing with salinization in the root zone, it is important to consider the salinity of water. The measurements in this report uses Electrical Conductivity (EC) values, an indicator for the salinity of the water. Higher values mean that the water is more conductive, and thus that there are more salts dissolved in the water. In this report, the classification as is shown in Table 1 is used in order to understand the magnitude of the salinity values. Other research or model results might use the chloride concentration (Cl) as salinity indicator. To convert the chloride concentrations to EC values, different relationships can be applied. A simple relationship to convert chloride concentrations from external sources to the EC of water (EC_w) is given by P. G. B. de Louw et al. (2011), and is only valid for values larger than 2 mS/cm, where chloride and sodium dominate. For smaller values other dominant anions are dominating the conductivity (P. G. B. de Louw et al., 2011; P. G. B. de Louw, Vandenbohede, et al., 2013; Delsman et al., 2018).

$$Cl (g L^{-1}) = EC_w (mS cm^{-1}) * 0.36 - 0.45$$

The EC_w is expected to be similar to the EC values of the soil water (EC_{sw}) as resulting from the saturated paste method, as a dilution factor is used to get the EC_{sw} , which is elaborated in section 3.2.2. These EC values can thus be compared to each other. Soil moisture salinity can be classified based EC values and its effects on crop growth (Abrol et al., 1988), which are converted using the relationship given by P. G. B. de Louw et al. (2011). The classification as is shown in Table 1 can be used to understand the salinity of the subsurface in the Netherlands.

Table 1: Soil moisture salinity classification and effects on crop growth (Abrol et al., 1988).

	EC_{sw} (mS/cm)	Cl (mg/L)	Effect on crops
Non-saline	0 – 2	0 – 270	Salinity effects negligible
Slightly saline	2 – 4	270 – 1000	Yields of sensitive crops may be restricted
Moderately saline	4 – 8	1000 – 2500	Yields of many crops are restricted
Strongly saline	8 – 16	2500 – 5300	Only tolerant crops yield satisfactorily
Very strongly saline	> 16	> 5300	Only a few very tolerant crops yield satisfactorily

2.1 Seepage

Saline groundwater can reach the surface in low-lying coastal areas like the Netherlands when the hydraulic heads of aquifers exceed phreatic water levels. This depends on the hydraulic resistivity of the soil above, and the pressure of the aquifer below. Seepage can be expected for low resistivities, which occurs by conductive and thin soil layers, and higher pressures of the aquifer below (Maljaars et al., 2006). This leads to a groundwater flow from the aquifer towards the Holocene confining layer near the surface. This process is called seepage (P. G. B. de Louw, 2013). Different seepage processes are playing a role in the Netherlands. The Netherlands consists of several coastal areas in which seepage is expected, formed by different processes and during different periods. These areas can be divided into two kinds of polders: deep polders and sub-recent transgression areas. Deep polders can be found in Flevoland and the Holland coast, sub-recent transgression areas can be found along the Waddensee coast and the Delta coast (see Figure 4 in section 3.1).

Deep polders are reclaimed lake areas, laying 4 to 7 meters below sea level, significantly lower in elevation compared to their surroundings, with artificially controlled surface water levels at around 5 to 8 meters below sea level (*Data Feed - Digital Terrain Model (DTM) 0,5m*, 2023; P. G. B. de Louw, 2013). These areas have preferential saline seepage through boils from the deeper groundwater, which is often more saline compared to shallower groundwater, leading to more saline seepage and thus higher salinity concentrations are found in these deep polders (P. G. B. de Louw, 2013; Post et al., 2003). Due to the lower elevation, groundwater in aquifers flows from the more elevated surroundings towards these deep polders (P. G. B. de Louw, 2013), which is nicely illustrated in Figure 2a. Seepage comes up through boils from deep groundwater, as is indicated at several locations in the deep polders and in the drained lake. This shows that the seepage can be quite local. Due to high pressures within the aquifer compared to the Holocene confining layer above, cracks are created in the soil of this Holocene confining layer, creating flow paths through the more impermeable aquitards. This creates boils, where saline groundwater comes up as seepage, connecting the lower aquifer with the surface (P. G. B. de Louw, 2013). This explains that salinization can be quite local in these deep polders, dependent on the locations of these boils. These boils, and thus most of the seepage is expected in the ditches in these deep polders, as the pressure of the aquifer is higher than the layer above, leading to groundwater coming up at these locations (P. G. B. de Louw, 2013).

Sub-recent transgression areas are mainly reclaimed tidal flats, with less variation in elevation compared to the deep polders and their surroundings (BRO Geomorfologische Kaart (GMM) WMS, 2023; *Data Feed - Digital Terrain Model (DTM) 0.5m*, 2023). The elevation differences in these areas are either due to dunes, dikes, and tidal creek ridges. The reclaimed salt marches are laying in between these creek ridges (*BRO Geomorfologische Kaart (GMM) WMS*, 2023). Rainwater infiltrates at these more elevated areas, especially in dunes and tidal creek ridges, whereas saline groundwater comes up as seepage in the reclaimed salt marches, as is clearly illustrated in Figure 2b. Saline groundwater is occurring at much shallower depth in these areas compared to the deep polders (P. G. B. de Louw, 2013; Post et al., 2003). In the reclaimed tidal salt marches, some fresh rainwater lenses are developing below the agricultural fields. Agricultural fields are separated by ditches and drains, where seepage is coming up. Ditches and drains have a thinner upper soil layer compared to parcels, which decreases the pressure of the soil on the aquifers below compared to the agricultural fields. Together with the high pressure of the aquifer by high hydraulic heads compared to the lower phreatic water levels, more groundwater comes up by seepage especially in ditches, leading to salinization (P. G. B. de Louw, 2013; Maljaars et al., 2006). This decreases the size of rainwater lenses significantly, and thus the availability of freshwater in these areas. The principle of rainwater lenses will be elaborated in more detail in section 2.2.

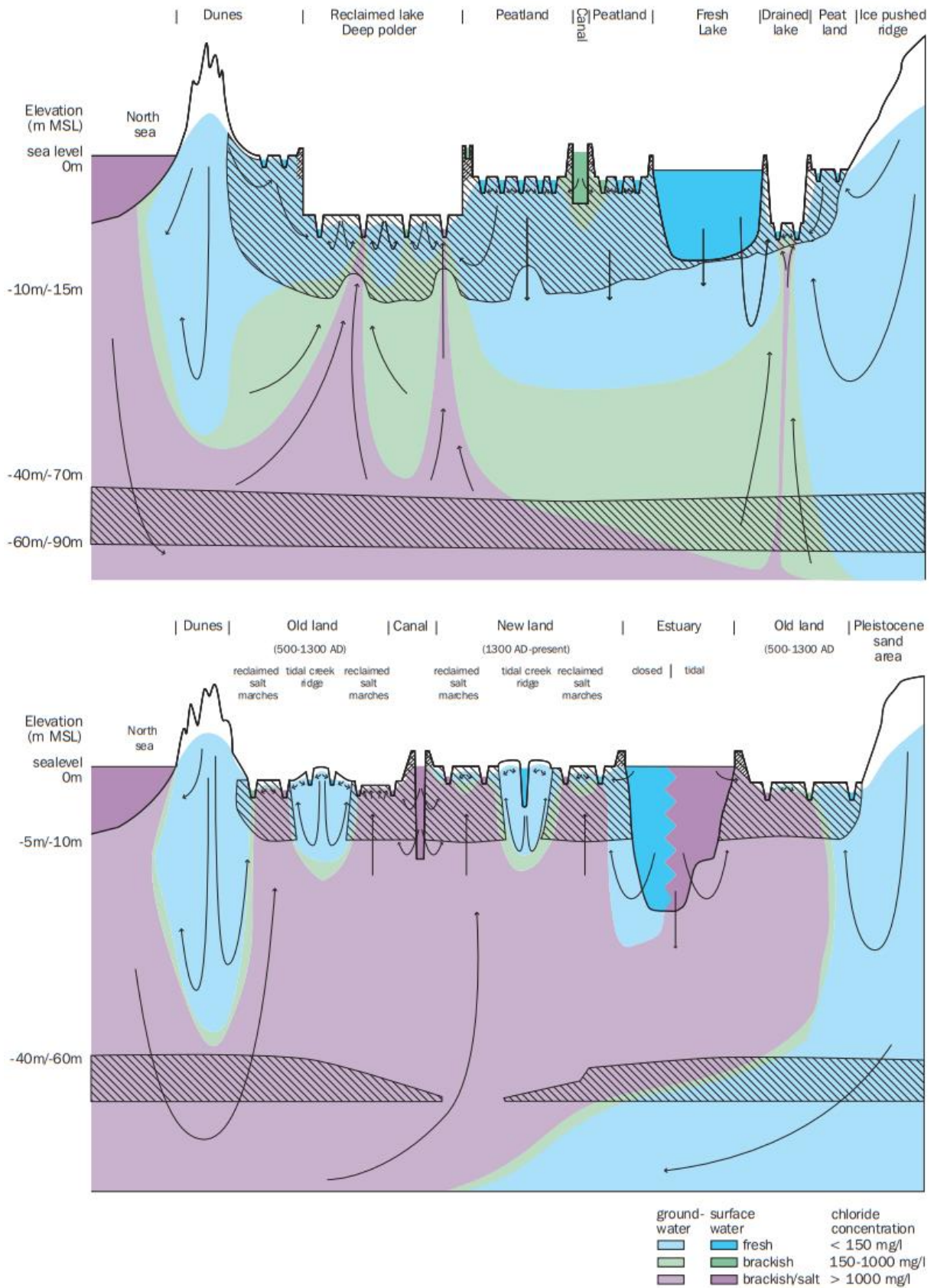


Figure 2: Schematic representation of two important seepage systems in the Dutch delta: a) preferential saline seepage in deep polders via boils causing saltwater upconing of deeper and more saline groundwater, b) saline seepage in sub-recent transgression areas resulting in thin rainwater lenses (P. G. B. de Louw, 2013).

2.2 Rainwater Lenses

In many coastal areas of the Netherlands, rainwater lenses are the only source of freshwater. These rainwater lenses can especially be found in more elevated areas along the coast, like dunes, and tidal creek ridges. However, also within agricultural fields small rainwater lenses can originate (P. G. B. de Louw, Eeman, et al., 2013; Oude Essink et al., 2018). Excess precipitation water infiltrates the soils in these areas, creating these rainwater lenses on top of the more saline groundwater. Salt water has a higher density than freshwater, this explains how the freshwater floats on top of the saline water (P. G. B. de Louw, 2013; Schot et al., 2004). However, more saline groundwater comes up as seepage in these areas as well, limiting the penetration depth of infiltrating rainwater, and thus limiting the growth of rainwater lenses, which is illustrated in Figure 3 (P. G. B. de Louw, 2013). This decreases the freshwater availability, especially during dry periods when there is limited precipitation which can infiltrate, while more seepage is reaching the root zone (P. G. B. de Louw, 2013; Maljaars et al., 2006).

The size of rainwater lenses differs between dunes or creek ridges, and agricultural fields. Within dunes and creek ridges, there is more space for water to infiltrate, and the pressure from the upper soil layer is higher, which counteracts the high pressure of the aquifer. This decreases the amount of seepage in these areas, and therefore larger rainwater lenses are found in these areas (P. G. B. de Louw, 2013; Oude Essink et al., 2018). In lower-lying agricultural fields on the other hand, for example in reclaimed salt marches, the pressure of the upper soil layer is lower compared to the pressure of the aquifer below, due to hydraulic heads of aquifers exceeding the phreatic water levels. This increases the seepage in these areas, and thus the size of rainwater lenses is significantly smaller (P. G. B. de Louw, 2013; Oude Essink et al., 2018). Next to that, the size of rainwater lenses is limited by ditches and drains in these agricultural fields, in which the pressure of the upper soil layer is even lower, and thus more seepage is coming up at these locations (P. G. B. de Louw, 2013; Eeman et al., 2011; Oude Essink et al., 2018). This is also illustrated in Figure 3 by the red arrows pointing upwards at drain and ditch locations. This explains why the size of rainwater lenses can be significantly different between these different locations, and thus how the soil moisture salinity can be affected by these processes. Therefore, it is also important to take the locations of soil samples into account.

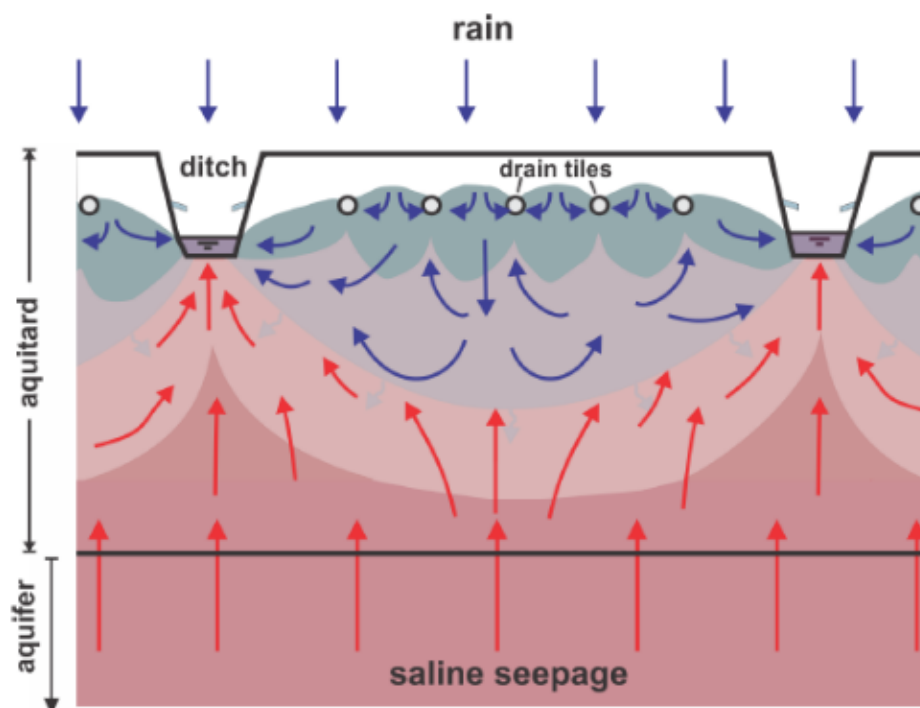


Figure 3: Principle of rainwater lenses above the brackish groundwater (P. G. B. de Louw, 2013).

3 Methodology

3.1 Study Area

This study focusses on the coastal zone in the Netherlands. This is the region where salinization plays a role and where groundwater and/or surface waters are saline. The coastal zone covers the provinces of Groningen, Friesland, Flevoland, North Holland, South Holland and Zeeland. The soil and hydrology are differing over the country. Coastal zones are mainly formed by polder reclamation. In these polders, a Holocene clayey and peaty layer is found above a Pleistocene sandy aquifer layer (Delsman, 2015).

A distinction is made between the deep polders in the Holland and the Flevoland coastal area, and the sub-marine transgression areas along the Waddenzee coast and the Delta coast (see Figure 4). The polders were formed during different periods, and different processes play a role, as the source of freshwater is different per region. The lake IJsselmeer and several rivers provide freshwater to the polders. For this research, the coastal zone of the Netherlands is divided into four areas, as shown in Figure 4: the Waddenzee coast, the Flevoland coast, the Holland coast and the Delta coast. Figure 5 shows the supply of fresh surface waters in the Netherlands, demonstrating that part of the area does not have supply of freshwater, whereas other areas have freshwater available. This supply of freshwater is either used to increase groundwater levels, as is shown by the light blue arrows, or to counter salinization and algae growth, as is shown by the red arrows. The freshwater sources are elaborated in the study area description of the individual coastal areas in section 3.1.1 to 3.1.4. Figure 5 shows that there is also saline water intrusion in the whole coastal area of the Netherlands, as is shown by the dark blue arrows.

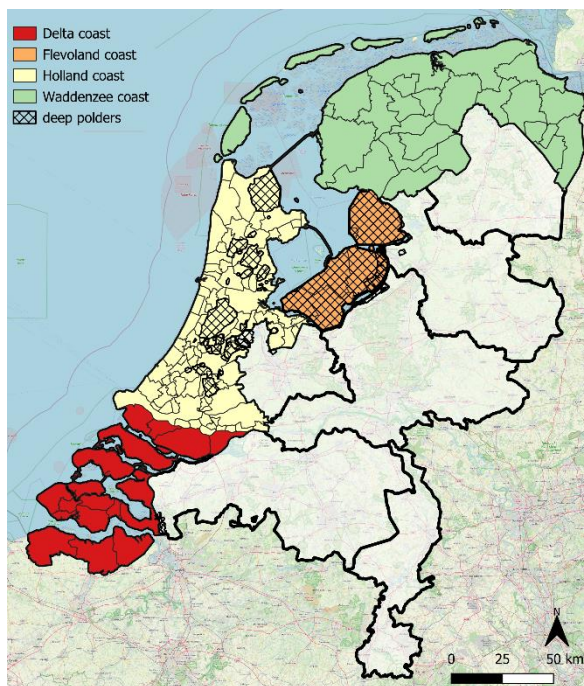


Figure 4: The four coastal zones in the Netherlands classified based on their location and polder types.

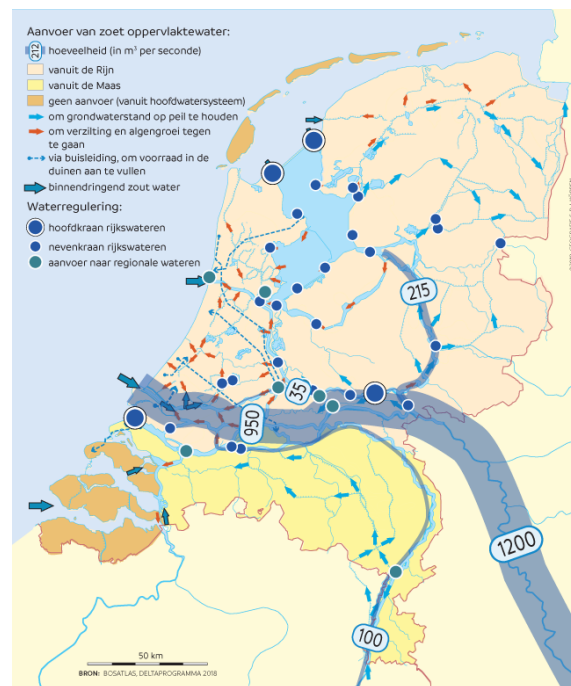


Figure 5: Supply of fresh surface water in the Netherlands (Donkers & Köbben, 2018).

3.1.1 Waddenzee Coast

In the Northern part of the Netherlands, mainly reclaimed tidal flats are found in sub-recent transgression areas, which have formed shallow polders (P. G. B. de Louw, 2013). These shallow clayey polders can be found along the Waddenzee. These polders have saline to brackish ground- and surface waters (Boer & Radersma, 2011). The upper soil consists mainly of clay with sandy aquifers underneath. These aquifers were especially formed in former tidal gullies, which are filled with sand.

Next to some rainwater lenses above the groundwater, the only freshwater source in this area is the IJsselmeer which is fed by Rhine water. This lake is used to flush ditches in order to provide freshwater during dry periods to regulate salinization (Donkers & Köbber, 2018; Hilarides, 2019; Ritzema & Stuyt, 2015). This region also has intrusion of saline water from the Waddenzee (Donkers & Köbber, 2018).

3.1.2 Flevoland Coast

Flevoland is a deep clayey polder reclaimed from the Zuiderzee. A freshwater lake was left after the reclamation, the IJsselmeer. Flevoland receives saline water by seepage from groundwater, leading to salinization (Boer & Radersma, 2011; Verburg et al., 2011). There are some freshwater sources, as freshwater from the IJsselmeer is pumped into the area. There is also some fresh groundwater in this area (Donkers & Köbber, 2018; Oude Essink et al., 2008). However, due to the usage of this fresh groundwater, salinization is expected to become a bigger problem here as well (Vogelzang et al., 2019).

3.1.3 Holland Coast

The coast in North and South Holland consists of various deep polders with peaty and clayey soils and with relatively low chloride concentrations in the surface waters and groundwater (Boer & Radersma, 2011; Oude Essink et al., 2004). Surface water levels are artificially kept shallow during summer, to prevent peat oxidation. In winter there are waterlogged conditions with excess rainfall (Ritzema & Stuyt, 2015). This is a groundwater discharge area, which receives freshwater from nearby sandy recharge areas, for example the dunes and more to the south also the Pleistocene uplands like the Utrechtse Heuvelrug (Minnema et al., 2004; Stuyfzand, 1995). The southern part of the area also has rivers, the Rhine and Meuse, as freshwater source, but during low river discharges, seawater intrudes these rivers, leading to salinization of the river, especially in the Nieuwe Waterweg (Boer & Radersma, 2011; Donkers & Köbber, 2018; Jacobs, 2007). This river water is also infiltrating, leading to fresh surface water pushing back the seepage of brackish groundwater, depending on the local geology and hydrology (Oude Essink et al., 2004). The northern part of the area is also flushed with IJsselmeer water, being a freshwater source in this area (Bonte & Biesheuvel, 2006; Donkers & Köbber, 2018). The availability and quality of freshwater in this area is uncertain due to fluctuations in the quantity and quality of river water discharge and inlet of IJsselmeer water (Boer & Radersma, 2011). Next to that, seepage with saline water is coming up by boils from deeper groundwater, leading to salinization (P. G. B. de Louw, 2013).

3.1.4 Delta Coast

In the southwestern delta of the Netherlands, in Zeeland and a part of South Holland, mainly reclaimed tidal flats are found in sub-recent transgression areas, which have formed shallow polders (P. G. B. de Louw, 2013). After impoldering, peat began to form, and clay settled down. Also, filled tidal channels and dunes are found in Zeeland, which are sandier. These polders have saline to brackish groundwater and surface waters (Boer & Radersma, 2011; Goes et al., 2009). Part of this delta has no freshwater sources, only some thin fresh rainwater lenses above the groundwater, and fresh groundwater in the coastal dune area. Other parts of the delta have freshwater from the Volkerak-Zoommeer, the Haringvliet and from the Maas river (de Vries & Veraart, 2009; Donkers & Köbber, 2018; van Duinen et al., 2015; Veraart & Klostermann, 2013). These freshwater sources are also used to flush the ditches and water systems, in order to prevent salinization (van Duinen et al., 2015). However, as there are large open water mouths in the Schelde, seawater intrudes this area, leading to salinization during low river discharges. Salinization in this area has a more irregular pattern compared to other parts of the Netherlands due to the lower freshwater availability and intrusion of seawater in the estuaries (Boer & Radersma, 2011; Donkers & Köbber, 2018; Jacobs, 2007).

3.2 Study Design

3.2.1 Data Collection

Measurements were taken at the end of summer in 2023, when salt concentrations peak due to precipitation shortages, resulting in decreased soil moisture levels (see Table 9 in Appendix A for exact dates). This is expected to increase EC_{sw} values when salts accumulate in the soil. The measurements were done at locations where high salinity concentrations were expected in the soil moisture in the root zone. This was based on the LHM model results (Delsman & America, 2022), which are based on shallow groundwater locations and seepage areas. Also, water boards were asked for relevant areas, where agriculture experiences problems with salinization. Water boards have more knowledge about the study area in general, and are in contact with farmers, therefore they can indicate which areas are prone to salinization. Within the field, locations were chosen at least 300 meters from a dike where possible, as either more freshwater might be found closer to dikes due to rainwater lenses (Ernst, 1969), or more saline water due to saline seepage directly behind the dike (America et al., 2023). Preferably measurements were done close to a drainage pipe, as saline seepage is expected here (Velstra et al., 2011). Where possible, measurements were taken 50 meters from a ditch, to have comparable field characteristics for the separate parcels.

Samples were taken at several locations along the Dutch coast, as is shown in Figure 6. For some of these locations, multiple samples were taken. Soil samples were taken using an Edelman auger at each 25 cm depth, up to a maximum depth of 150 cm. For some locations where the soil became too saturated to take deeper samples, samples were taken as deep as possible. The samples were stored in a fridge in closed bags, to analyze later on in the laboratory. The soil type (clay, clayey sand, sandy clay, sand or peat), soil characteristics (gley, shells, or other characteristics) and, if measurable, depth of saturation were noted. The EC_w was measured in an adjacent ditch as well, using a WTW Cond 3310 EC meter.

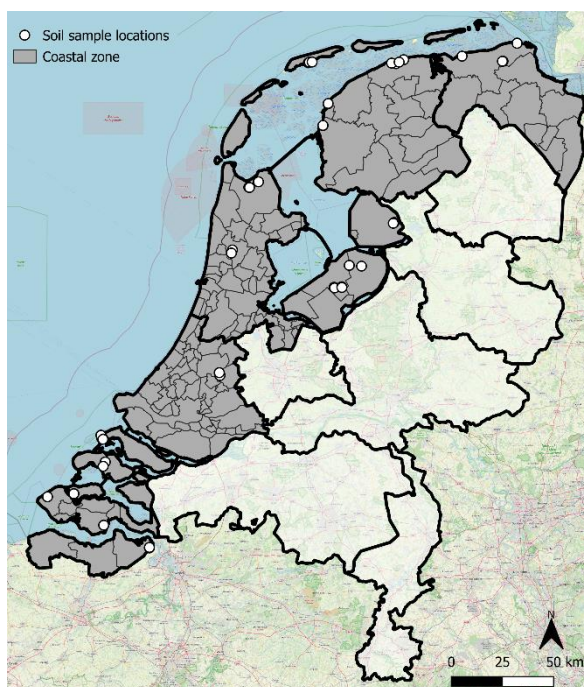


Figure 6: Soil sample locations along the Dutch coast.

3.2.2 Sample Analysis

The salinity of the soil samples was analyzed in the laboratory to determine the total of dissolved salt, based on the adjusted saturated paste method (Oude Essink et al., 2018), which is adjusted relative to the original saturated paste method (Rhoades et al., 1989). This method determines the total amount of dissolved salt from a saturated soil solution, which could be applied to disturbed soil samples.

First the mass of the foil container was measured, next the sample was put in the foil container, and the field mass of the sample in the foil container (M_{field}) was measured. Next, demineralized water was added to saturate the sample. It took some time for the water to infiltrate the complete sample and for the salts to dissolve. Then the mass of the saturated sample in the foil container ($M_{\text{saturation}}$) was determined. The mass of the added demineralized water ($M_{\text{demiwater}}$) was then calculated by:

$$M_{\text{demiwater}} = M_{\text{saturation}} - M_{\text{field}}$$

Subsequently, the sample was mixed until a mud substance is formed, which is called a saturated paste. This saturated paste did rest for 24 hours to let all the salts dissolve, and afterwards some soil moisture with dissolved salts was extracted via a rhizon and a vacuum pump. Next, the EC of the extracted water from the diluted paste (EC_{dil}) was measured using a WTW LF 300 EC meter. Then, the sample was dried in an oven at 105 °C for at least 24 hours, and the dry weight of the sample in the foil container (M_{dry}) was determined. The mass of the soil moisture (M_{sw}) present in the sample was then determined by:

$$M_{\text{sw}} = M_{\text{field}} - M_{\text{dry}}$$

The mass of the total amount of water ($M_{\text{water_total}}$) was then determined by:

$$M_{\text{water_total}} = M_{\text{sw}} + M_{\text{demiwater}}$$

The dilution factor (F_{dil}) was determined by:

$$F_{\text{dil}} = \frac{M_{\text{water_total}}}{M_{\text{sw}}}$$

The EC, and thus the salinity of the soil moisture in the field (EC_{sw}) was determined by:

$$EC_{\text{sw}} = EC_{\text{dil}} * F_{\text{dil}}$$

These steps for determining the salinity were followed for all soil samples, so on all different depths for the various locations. The total dissolved salt content is an indicator of the salinity of the soil samples. Afterwards, the EC_{sw} values, and thus the salinities, were compared to each other using QGIS. Thereby, the salinity was analyzed over depth, and various locations were compared to each other.

3.2.3 External Data Collection

The measured salinity values over depth are compared to existing field measurements from the past, subsoil information and findings from other studies, in order to understand and explain the salinity distribution of salt in the root zone along the Dutch coast. A wide range of data sources is used, including Temperature and Electrical Conductivity data in the subsurface, EC values and chloride concentrations in ditches from water boards, the intern Deltares dataset and data from previous research, the fresh-salt groundwater distribution from Terschelling (SkyTEM) and Zeeland (FRESHM), the elevation map of the Netherlands, the soil and geomorphological map of the Netherlands, and the seepage map from the LHM model. In the next sections, the various data and diverse sources are described.

Temperature and Electrical Conductivity (TEC-)Probe Data

The TEC-probe is used to measure temperatures and EC values each 10 centimeters, from the groundwater table until a maximum depth of 4 meters, to indicate the fresh-saline interface for some of the locations. The measured EC must be corrected for the temperature, and a correction factor is used to obtain the correct EC of the groundwater, the EC_w , to compare it to other measurements, by taking into account the soil type as is indicated in Table 2 (P. G. B. de Louw et al., 2011). TEC-probe data is available for some of the locations from this research and originates from other projects within Deltares. Also, during the field campaign for this research, some measurements were done in collaboration with researchers from other projects within Deltares. Several TEC-probe data is available for different dates. Table 3 shows the projects and dates from which TEC-probe data is used. The EC_{sw} values from the unsaturated zone, as obtained during the field measurements, were plotted above the TEC-probe profiles from the saturated zone, to compare the whole conductivity-depth profiles.

Table 2: Formation factors (FF) for different lithological units (P. G. B. de Louw et al., 2011).

Lithology	Average FF
Peat	2.1
Clay	2.5
Sandy clay/clayey sand	2.8
(Clayey) fine sand	3.2

Table 3: TEC-probe locations and dates from other projects within Deltares.

Location	Date	Project
Anna Paulowna (NH-APL-L1; NH-APL-L2; NH-APL-L3)	27-03-2023	(Data from Project - "Zoetwaterboeren" 2022 - 2025. n.d.)
Kerkwerpe: (ZL-KWP-L1; ZL-KWP-L2; ZL-KWP-L3; ZL-KWV-L1; ZL-KWV-L2)	03-05-2023 and 14-09-2023	(Data from Project - "Samenwerken Voor Zoetwater: Innovatieve Drainage Demonstreren, Monitoren En Evalueren" 2022-2024. n.d.)
Swifterbant (FL-SWB-L1)	11-09-2023	(Data from Internal Database Deltares, n.d.)

Salinity Concentrations in Ditches

The ditch EC_w values were measured within the field adjacent to the parcels where soil samples were taken, but not for all locations ditches could be reached, or no water was present in the ditches. Therefore, ditch data from external sources was gathered, preferably close to the location and date of the measurements of this research. This data is used to compare the soil sample salinities with the ditch data, in order to understand whether the ditches affect the soil moisture salinity, and to explain the spatial variability between various locations. Water boards measure the EC values or chloride concentrations in ditches within their management area. For Friesland, measurements were available by Wetterskip Fryslân (*Chloridekaart - Wetterskip Fryslân*, 2014), for Flevoland measurements were available by water board Zuiderzeeland (*Zoutgehalte - Waterschap Zuiderzeeland*, 2022) and for part of South Holland measurements were available from water board Hollandse Delta (*Meetpunten Chloride - Waterschap Hollandse Delta*, 2019). For Groningen (water board Noordzijlvest), part of North Holland (water board Hollands Noorderkwartier) and part of South Holland (Water board Rijnland) no relevant measurements were available. Next to that, salinity data is available from previous research or projects, including projects in Zeeland and Terschelling (Data from Internal Database Deltares, n.d.; Data from Project - "Samenwerken Voor Zoetwater: Innovatieve Drainage Demonstreren, Monitoren En Evalueren" 2022-2024. n.d.; Data from Project - "Toekomstperspectief Polder Terschelling" 2021-2026. n.d.; Data from Project - "Zoetwaterboeren" 2022 - 2025. n.d.; Deltares Nitrate App, n.d.; EC Metingen - Provincie Zeeland, n.d.; Schipper et al., 2022).

Fresh-Saline Groundwater Distribution

Detailed data is available about the salinity of the groundwater on Terschelling (SkyTEM) and in Zeeland (FRESHEM), which is obtained by helicopters measuring the geo-electrical resistivity of the subsoil. The depth of the fresh-saline interfaces is obtained from this data. The FRESHEM data is online available (*FRESHEM Zeeland Grensvlakken*, 2017), the SkyTEM data (Kok et al., 2010) and the interpolated map of the fresh-saline interface is available in the internal database of Deltares (*Data from Internal Database Deltares*, n.d.). This fresh-saline interface is used to understand the salinity of the subsoil, and to explain the salinity values of the soil moisture in the root zone.

Elevation Map

The Digital Terrain Model (DTM) with a resolution of 0.5 meters can be used to understand the elevation of the measurement locations and the surroundings (Data Feed - Digital Terrain Model (DTM) 0.5m, 2023). The elevation affects the groundwater flow and surface water runoff. Also, seepage is dependent on the elevation and thereby the salinity of the soil moisture.

Subsurface Data

Seepage is also dependent on the subsurface composition by the horizontal and vertical conductivity, and thus how easily water can flow through the subsoil. This is dependent on the soil type. Together with the elevation, the subsurface composition affects the salinity of the soil moisture. The subsurface composition is obtained from the Basisregistratie Ondergrond (BRO) soil map (*BRO Bodemkaart (SGM) WMS*, 2023). Next to that, the BRO geomorphology map (*BRO Geomorfologische Kaart (GMM) WMS*, 2023) is used to understand the geomorphology of the Netherlands.

Precipitation and Evapotranspiration Data

Precipitation and evapotranspiration data is used as it is expected to influence the results significantly. Evapotranspiration dries the soil leaving salts in the soil, while precipitation dilutes salts and flushes salts towards the subsoil (P. G. B. de Louw, 2013). Daily precipitation and evapotranspiration data is used from a weather station in de Bilt, situated in the center of the Netherlands, to gain insights into the weather conditions during the field sampling period (*Dagwaarden van Weerstations (25-08-2023 to 11-10-2023) - de Bilt*, n.d.).

LHM Seepage-Infiltration Map

The LHM model simulates in which areas seepage are expected. The yearly-averaged seepage-infiltration map from 2011 to 2018, as output from the LHM 4.1 model (Janssen et al., 2020), is used to understand the seepage and infiltration processes over the Netherlands. Areas with saline seepage generally have higher salinity concentrations in ditches and soil moisture compared to infiltration areas where non-saline precipitation water is infiltrating the soils (Velstra et al., 2011). This model output is compared to the salinity values in the soil moisture. In this way, the spatial variability in salinity concentrations in the soil moisture is tried to be explained by the spatial variability in seepage processes over the coastal zone of the Netherlands.

This external data is used to understand and explain the water flow and water composition along the Dutch coast. This data is compared to the soil sample measurements, in order to understand the variability in salinity over the coastal zone of the Netherlands, but also the variability on a smaller scale on parcel level. In the next part of the research, the salinities were compared to model results, to analyze whether the field measurements match the modeled results.

3.2.4 Model Analysis

National Hydrological Model (Landelijk Hydrologisch Model - LHM)

The National Hydrological Model (LHM) has been developed to identify risk zones for salinization and salt damage in agriculture (Delsman & America, 2022). The LHM is used within the Delta Program Fresh Water (Delta Programma Zoet Water - DPZW) to quantify and visualize effects of various policy choices within the water system. This numerical model describes the hydrology of groundwater, unsaturated zone and surface waters for the Netherlands. LHM is based on several coupled sub-models: a distribution model for surface water (DM), a surface water model of regional water systems (MOZART), a groundwater model (MODFLOW), a model of the unsaturated zone (MetaSWAP) and a salt transport model for shallow groundwater and the unsaturated zone (TRANSOL). Salt flow and concentrations are calculated by the sub-models DM, MOZART and TRANSOL (Delsman et al., 2022). This research is only focused the 1D model for the TRANsport of SOLutes (TRANSOL), which simulates the storage and flow of salt in the unsaturated and shallow saturated zone. This model is based on several vertical layers, where transport of salt is simulated via convection by water flow, diffusion and dispersion. Horizontal transport to water courses and drains is simulated by horizontal flow paths (Kroes & Rijtema, 1996).

The model output of the LHM is used to calculate a salinity risk. Important parameters are the depth of the fresh-salt interface and the resistance of the subsoil. The depth of the fresh-saline interface is shown in Figure 1 in section 1.1, where a higher value indicates saline water closer to the surface. The resistance (c) together with the pressure difference between the hydraulic head of the aquifer and the phreatic water level ($\Delta\phi$) indicates the seepage flux (q_z), according to $q_z = \frac{\Delta\phi}{c}$. The resistance layer of the top system, implemented between the two upper layers in the model (see Figure 7) is an indicator for seepage chance, where a low resistance leads to more seepage. If there is more seepage together with a shallow depth of the fresh-salt interface, a higher salinization index is expected (see Figure 8), and is based on both the risk for disappearing of the rainwater lenses, and the risk of salinization due to irrigation with saline surface waters (Delsman & America, 2022).

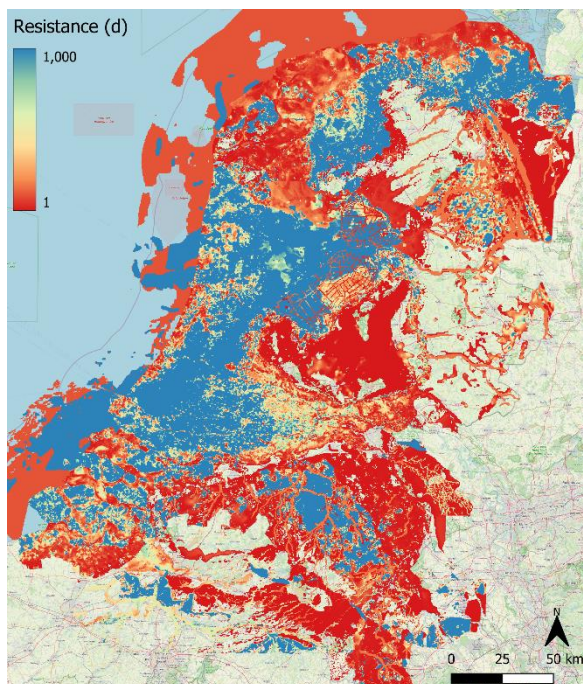


Figure 7: Resistance layer between model layer 1 and 2 implemented in the model (Janssen et al., 2023).

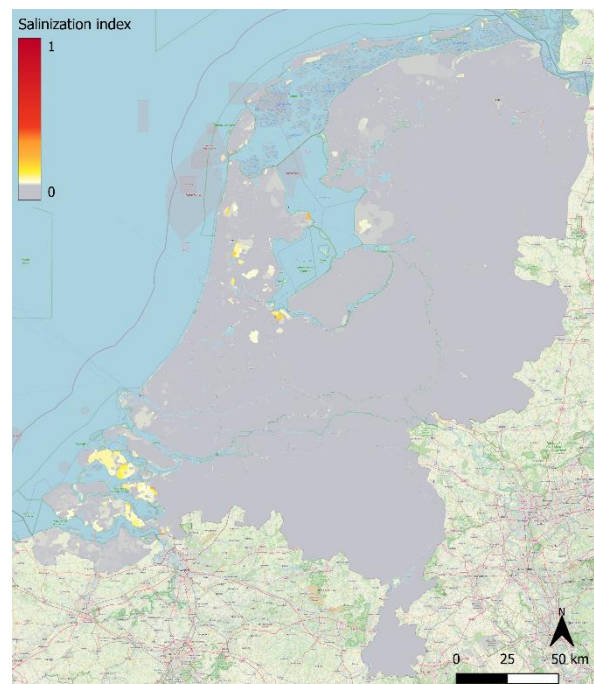


Figure 8: Salinity index for 2019 as calculated from the LHM model (Delsman & America, 2022).

Model Analysis

Relevant soil sample locations were partly obtained from the salinity index map, and partly by discussing with the local water boards for relevant locations. The soil moisture measurements are compared to the critical locations for salinization, by using the simulated salinity index for 2019 from the LHM model, to compare whether field measurements indeed match the simulated risk zones as obtained from the salinity index. Next to the salinity index, various kinds of TRANSOL model outputs are compared to the field measurements, to understand individual factors which might cause salinization, and underlying processes within the model.

The TRANSOL model simulates timeseries of the salt concentrations in depth from 2010 to 2019, for certain locations which were given as input, including the locations from this research. Next to that, the depth of the salt front is simulated for each location and is averaged over this time period. This salt front is an indicator for the depth of the fresh-saline interface (van Walsum, 2023), and is given at the depth where a strong increase in salinity concentration is modeled, indicating a fresh-saline interface. The solute concentration for this depth is averaged over time as well, to investigate the concentration of the salt front per location. Locations where salinization is expected to be a problem are elaborated in more detail, by zooming in to the simulated concentration profiles in depth. These are either locations with moderately to strongly saline soil moisture in the field measurements, so EC values larger than 4 mS/cm, or locations which are assumed to be risk zones according to the TRANSOL model. This is expected for moderate solute concentrations, larger than 1 g/L (corresponding to an EC larger than 4 mS/cm), with a salt front shallower than 4 meters.

Furthermore, timeseries of salt concentrations in the root zone from 2010 to 2019 are simulated for certain locations, including the locations from this research. The root zone is dynamic over the year, which is simulated as well. The solute concentration in the root zone is yearly-averaged per location, to have one averaged value to investigate critical locations for salinization in the root zone. Locations which appear to be critical are investigated in more detail, by investigating the timeseries of solute concentration in the root zone to compare this to field measurements.

4 Results

4.1 Salinity in the Field Measurements

Salinity concentrations of 330 soil samples were collected and measured in the autumn of 2023 (see Figure 9 and the measurement details in Table 4 and Table 5, Appendix A). Samples were taken from 57 point-locations at various depths (see section 3.2). Location codes are detailed in the List of location codes and in sections 4.1.1 to 4.1.4. The salinity classification of soil moisture is detailed in section 2. Note that these results are only valid for these specific locations, at this specific moment in time. The measurements might not be representative for their surroundings and might contain temporal variation in salinity values.

EC_{sw} values of soil moisture in the root zone varied significantly across the Dutch coastal area, showing significant differences over short distances and within parcels. Generally, EC values increase with depth. However, in the topsoil at 25 cm depth, soil moisture concentrations are higher compared to the measurement below for some locations in North Holland, the Flevopolder and on Goeree-Overflakkee, possibly due to irrigation with saline surface water (Chen et al., 2010) and root water extraction, leading to salt accumulation in the root zone (Blanco & Folegatti, 2002; Nishida & Shiozawa, 2010). Soil moisture in Zeeland, South Holland, part of Friesland and the Noordoostpolder appears to be slightly saline, while in deep polders of North Holland and Flevoland, and certain locations in Friesland and Groningen, it is moderately to strongly saline. However, deviations on field scale are found both in depth and spatially. The salinity for specific locations and the variability over depth is elaborated in sections 4.1.1 to 4.1.4.

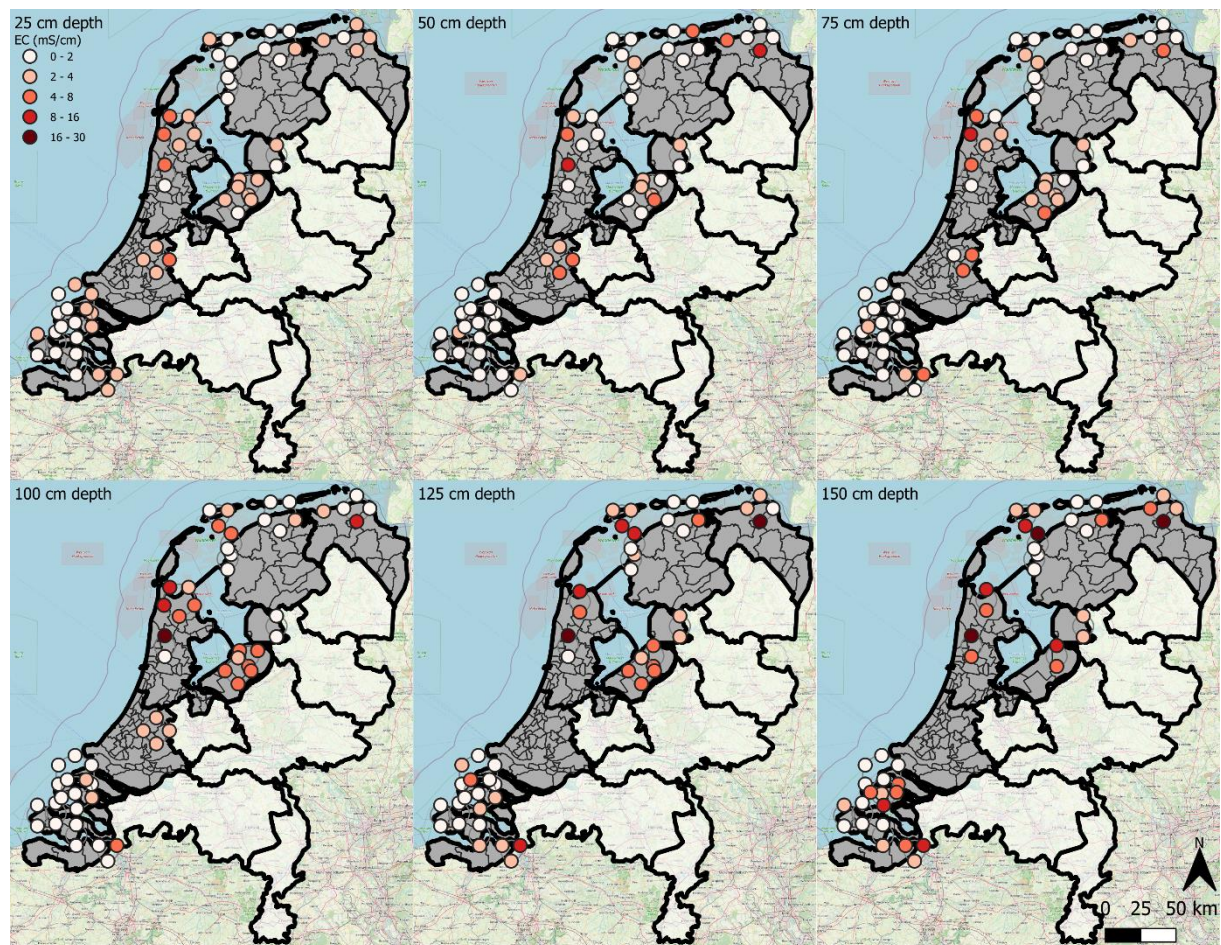


Figure 9: Measured EC_{sw} (mS/cm) for soil samples over the Dutch coastal area at 25 to 150 cm depth in the autumn of 2023.

EC_w measurements were conducted in accessible ditches adjacent to the measurement locations (see Figure 10). However, in some areas, water was inaccessible due to low water levels or vegetation blocking the ditch. Strongly saline ditches were observed in Groningen, the north-western part of Friesland, the Schermer area and a part of Goeree-Overflakkee. Ditches around Boskoop, Anna Paulowna and the Noordoostpolder showed slightly to moderately saline levels. Non-saline ditches were found in the northeastern part of Friesland, parts of the Boskoop area, parts of Zeeland, parts of Goeree-Overflakkee, and the Flevopolder.

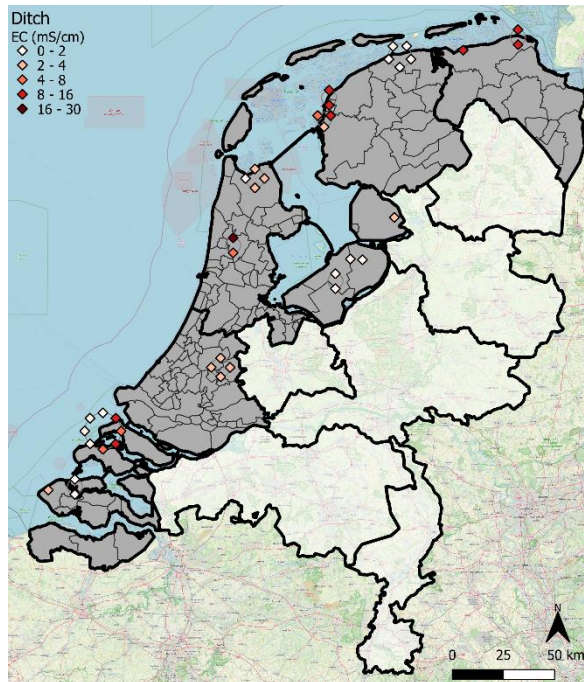


Figure 10: Measured EC_w values (mS/cm) for ditches over the coastal area of the Netherlands in the autumn of 2023.

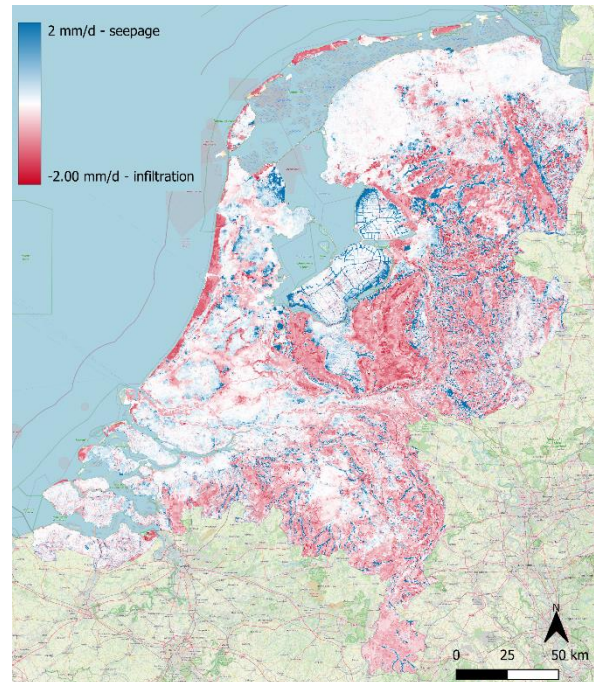


Figure 11: Seepage-infiltration map for the Netherlands (Janssen et al., 2020).

In parts of Groningen, the Wieringermeer and Schermerpolder (North Holland), soil moisture measurements show moderately to strongly saline conditions (5-26 mS/cm) with ditch measurements showing similar trends (3-17 mS/cm, higher in Groningen and Schermer polder). Conversely, Boskoop (South-Holland) showed one moderately saline parcel for soil moisture (4-6 mS/cm for location 1 and 2 at 50-75 cm depth), compared to non- to slightly saline values (1.7-2.2 mS/cm for location 3 and 4 at 50-75 cm depth), along with corresponding ditch measurements (2.6-3.0 mS/cm for location 1 and 2, and 2.0-2.3 mS/cm for location 3 and 4). Similarly, Goeree-Overflakkee shows non-saline to slightly saline conditions in the soil moisture (up to 3-4 mS/cm at 150 cm depth for the Boutweg, compared to 1-2 mS/cm at 150 cm depth for the Groenedijk and Westduinweg) and moderately saline in the ditch measurements (7-8 mS/cm for the Boutweg, compared to 0.5-1.3 mS/cm for the Groenedijk and Westduinweg). Parts of Zeeland show moderately to strongly saline soil moisture, particularly in Schouwen-Duivenland (up to 9 mS/cm at 150 cm depth) and the Hedwigepolder in Zeeuws-Vlaanderen (up to 13 mS/cm at 150 cm depth). Other parts of Zeeland show non-saline to slightly saline soil moisture (0.9-2.8 mS/cm at 150 cm depth) and ditch measurements (1.5-3.7 mS/cm). The moderately saline values (up to 5-6 mS/cm at 150 cm depth) as found in the soil moisture in the Flevopolder are not found in ditches (0.3-0.6 mS/cm). The Noordoostpolder showed moderately saline soil moisture (2.4-2.9 mS/cm at 150 cm depth). Friesland showed non-saline soil moisture, (1.3-1.7 mS/cm at 150 cm depth) with only two moderately to strongly saline locations (up to 7 and 18 mS/cm at 150 cm depth). Ditches in northwest Friesland were strongly saline (Pingjum up to 8.9 mS/cm, Pietersbierum up to 12 mS/cm). Terschelling has one strongly saline location (up to 15 mS/cm at 150-200 cm depth).

The seepage map from the LHM model indicates yearly averaged seepage (blue) and infiltration areas (red). Saline water is expected in seepage areas near the coast, while infiltration of fresh rainwater is expected in infiltration areas (see Figure 11). Seepage areas are mainly found in deep polders (Flevoland, Wieringermeerpolder, Schermer area and the polder close to Boskoop). Both infiltration and seepage areas are found in sub-recent transgression areas (Friesland, Groningen and Zeeland).

In the next part of the research, the soil samples were analyzed over depth, and by zooming in on the locations, measurements can be compared to seepage and elevation maps and external data.

4.1.1 Waddenzee Coast

The locations along the Waddenzee are shown in Figure 12. By zooming in to the specific locations, the seepage-infiltration map is shown (Janssen et al., 2020), to compare these maps to the salinity profiles of the soil moisture in depth (see Figure 13) with similar indices.

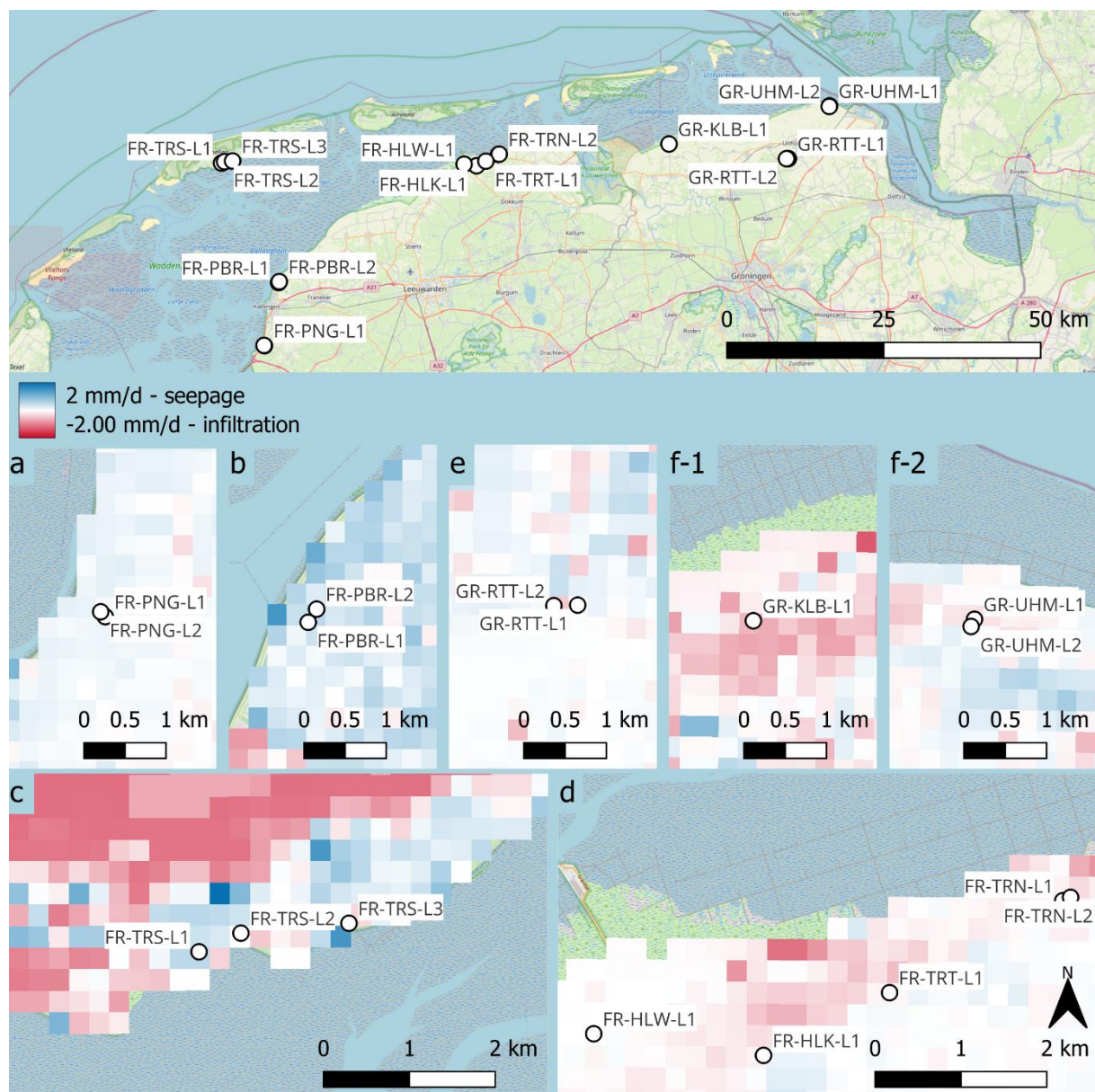


Figure 12: Map showing the locations along the Waddenzee coast, and maps zooming in on the locations on the seepage-infiltration map (Janssen et al., 2020). The numbering a-f corresponds with the numbering in Figure 13.

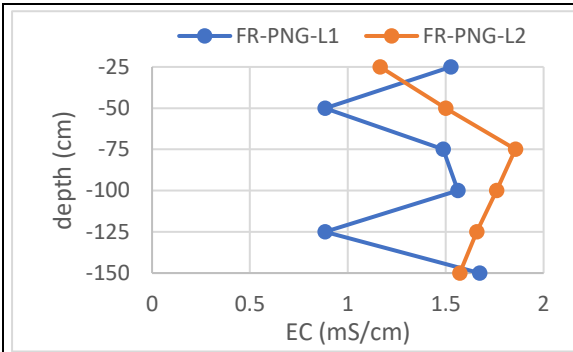


Figure 13a: EC_{sw} values for locations in Friesland (FR) around Pingjum (PNG).

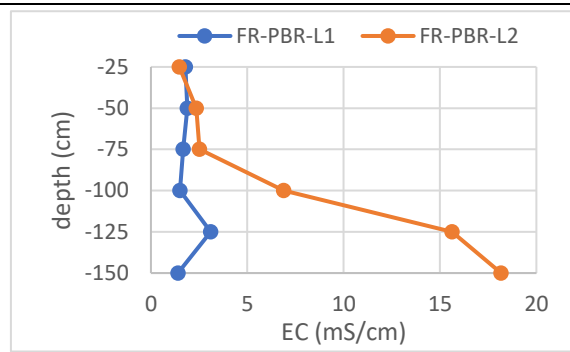


Figure 13b: EC_{sw} values for locations in Friesland (FR) around Pietersbierum (PBR).

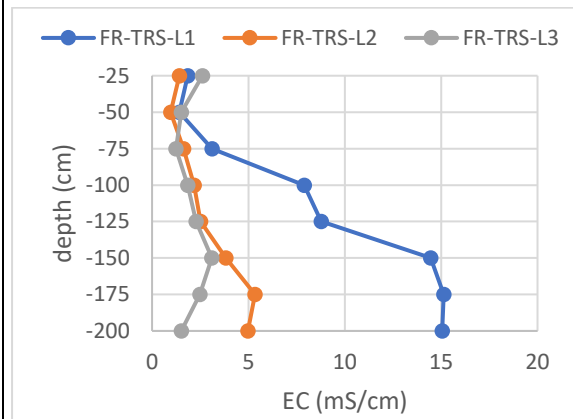


Figure 13c: EC_{sw} values for locations in Friesland (FR) on Terschelling (TRS).

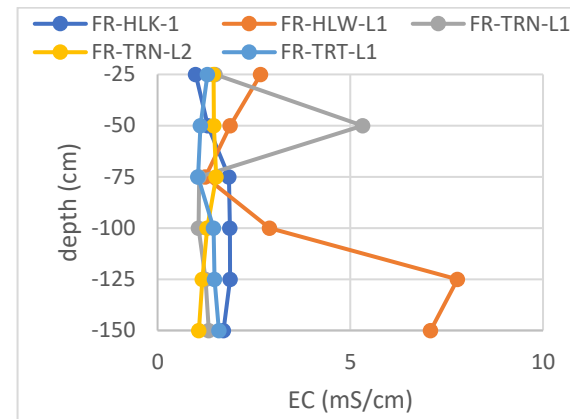


Figure 13d: EC_{sw} values for locations in Friesland (FR) around Holwerd (HLK and HLW) and Ternaard (TRN and TRT).

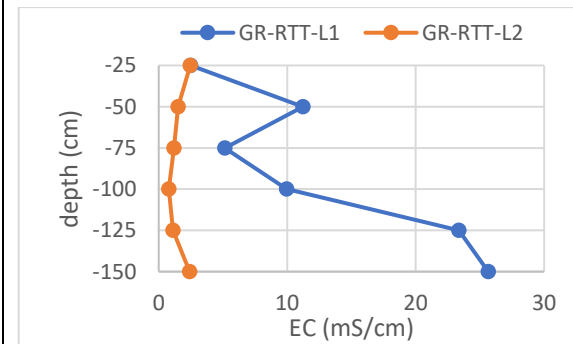


Figure 13e: EC_{sw} values for locations in Groningen (GR) around Rottum (RTT).

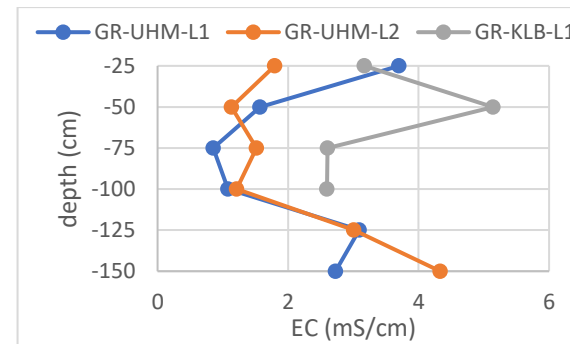


Figure 13f: EC_{sw} values for locations in Groningen (GR) around Uithuizermeeden (UHM) and Kloosterburen (KLB).

Figure 13: EC_{sw} values over depth for various locations along the Waddenzee coast during the autumn of 2023.

The soil moisture as measured near Pingjum (FR-PNG-L1 and FR-PNG-L2) shows non-saline conditions with no clear pattern in depth (see Figure 13a). There is no significant difference in salinity between the two locations. Both locations are situated on a tidal levee (*BRO Geomorfologische Kaart (GMM) WMS, 2023; Data Feed - Digital Terrain Model (DTM) 0,5m, 2023*). Together with the low salinities this would suggest infiltration. However, the seepage-infiltration map shows minimal infiltration or seepage (see Figure 12a), suggesting negligible processes. Location 1 reached saturation at 125 cm, while location 2, positioned in a lower elevated dug drain, did not reach saturation (see Table 5, Appendix A).

In Pietersbierum (FR-PBR-L1 and FR-PBR-L2), salinity differs significantly between locations. Location 2 shows increasing salinity with depth, up to a 15 mS/cm difference at 150 cm depth, with very saline conditions (see Figure 13b) suggesting saline seepage. Location 1 does not show a pattern with depth, with non-saline to slightly saline soil moisture, suggesting infiltration. However, both locations are situated in a lower elevated area with tidal deposits, suggesting seepage (*BRO Geomorfologische Kaart (GMM) WMS, 2023; Data Feed - Digital Terrain Model (DTM) 0,5m, 2023*). This matches the predicted seepage from the seepage-infiltration map (see Figure 12b). Both locations have comparable locations in the field with similar elevation (*Data Feed - Digital Terrain Model (DTM) 0.5m, 2023*) and similar soil types (see Table 5, Appendix A). Even though no drainage data is available, it might be that location 1 is located in between drainage pipes, leading to a rainwater lens, while location 2 might be located at a drainage pipe, leading to seepage and thus higher concentrations (Maljaars et al., 2006; Velstra et al., 2011). However, location 1 was saturated at 110 cm, whereas location 2 was saturated at 125 cm depth. Additionally, location 2 showed gley starting at 50 centimeters, whereas no gley was observed for location 1 (see Table 5, Appendix A). Therefore, local iron-rich seepage might be expected at location 2, while no seepage is expected at location 1. This indicator for local gley in location 2 might possibly explain the higher salinity, as is elaborated in section 5.1.2, even though location 1 showed shallower saturation levels (van Enk, 2016).

The salinity profiles for Terschelling (FR-TRS-L1, FR-TRS-L2 and FR-TRS-L3) are comparable on shallow depth, but increase in salinity towards the west at greater depths (see Figure 13c and Figure 15). Location 1 shows significantly higher salinity levels compared to location 2 and 3, increasing with depth, reaching strongly saline values. The higher salinity in location 1 is possibly influenced by local seepage, matching the seepage-infiltration map (see Figure 12c), and a shallower fresh-salt interface (see Figure 12c and Figure 14). The fresh-salt interface is obtained from SkyTEM data (*Data from Internal Database Deltares, n.d.; Kok et al., 2010*), and is shown in Figure 14. Table 8 in Appendix A shows the depth of this interface for the soil sample locations as obtained from this map. The interface is quite deep for location 2 and 3, while a shallower interface is found for location 1. The deeper interfaces for location 2 and 3 match the non-saline to moderately saline soil moisture. Location 2 and 3 are situated in drained parcels (see Figure 15). Location 2 is found at a drain location, which could suggest local seepage, while location 3 is found in between drains, which could indicate infiltration towards a rainwater lens (Maljaars et al., 2006; Velstra et al., 2011). This possibly explains the higher salinity at 150 cm depth for location 2 compared to location 3.

Comparing TEC-probe data for locations 2 and 3 on Terschelling on the 31st of May 2023 (see Table 7, Appendix A), both ditch measurements and TEC-probe measurements in the saturated zone show slightly saline values, with location 3 being somewhat more saline compared to location 2. This contradicts the measured salinities in the soil moisture, where location 2 is found somewhat more saline at 150 cm depth. However, location 3 is found in a lower elevated, old tidal creek, as visible by the encircled dark blue areas north of location 2 in the direction of location 3 (see Figure 15). This old tidal creek could suggest seepage, matching the seepage as found in the seepage-infiltration map (see Figure 12c). This might explain higher salinity concentrations as measured by the TEC-probe at location 3. However, the use of average TEC-probe values introduces some uncertainty, particularly when comparing specific locations or depths, as values are depth-averaged, and no depth-specific data is available at these locations.

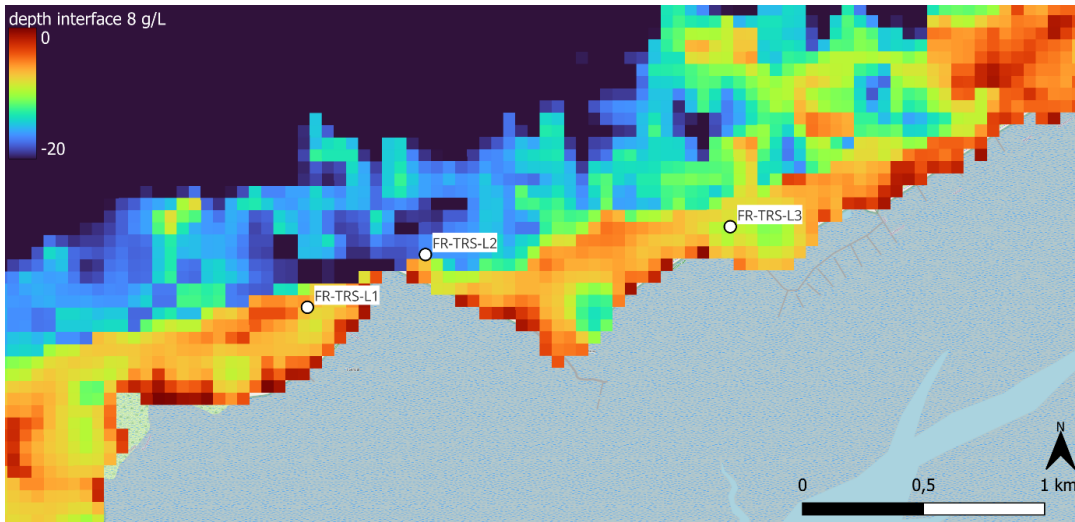


Figure 14: Depth for the fresh-saline interface on Terschelling for a chloride concentration of 8 g/L (Data from Internal Database Deltares, n.d.; Kok et al., 2010).

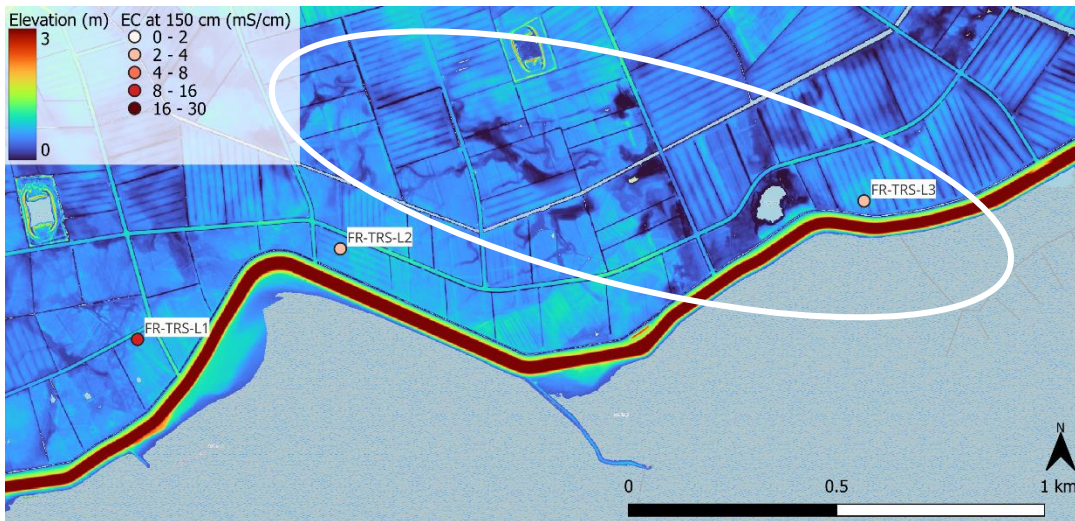


Figure 15: Digital Terrain Model showing the elevation and measured EC_{sw} values at 150 cm depth on Terschelling, with an old tidal creek being encircled (Data Feed - Digital Terrain Model (DTM) 0,5m, 2023).

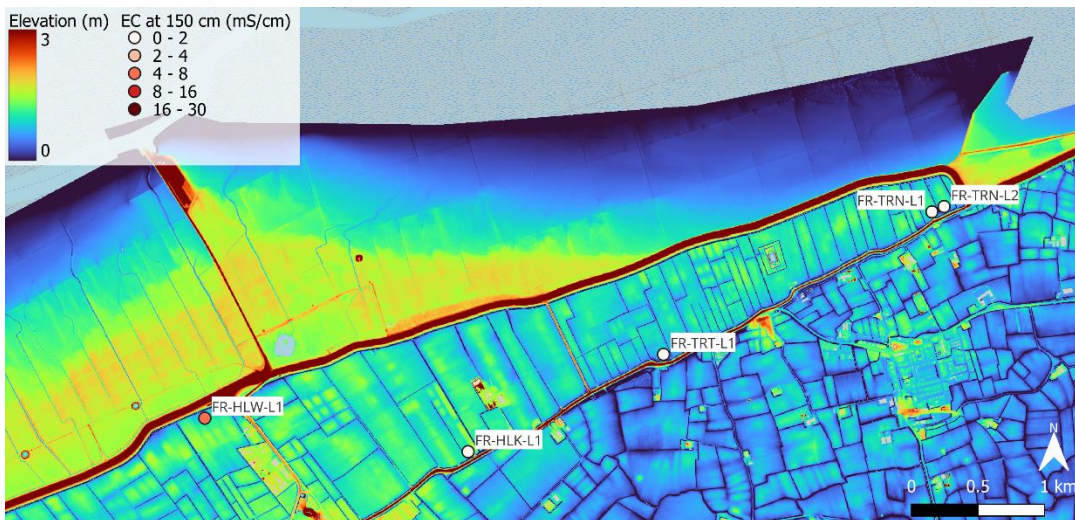


Figure 16: Digital Terrain Model showing the elevation and measured EC_{sw} values at 150 cm depth near Holwerd and Ternaard (Data Feed - Digital Terrain Model (DTM) 0,5m, 2023).

Soil moisture along the dike between Ternaard and Holwerd shows non-saline conditions, except for the most western location near Holwerd (FR-HLW-L1), which reaches moderately saline values, especially at greater depths (see Figure 13d and Figure 16). The low salinities and the position at a higher elevated salt marsh terrace (see Figure 16), would suggest an infiltration zone (*BRO Geomorfologische Kaart (GMM) WMS, 2023; Data Feed - Digital Terrain Model (DTM) 0,5m, 2023*). This matches the zone with high infiltration rates from the seepage-infiltration map (see Figure 12d) for the eastern locations with lower salinities (FR-HLK-L1, FR-TRT-L1, FR-TRN-L1 and FR-TRN-L2). However, the western location with higher salinities (FR-HLW-L1) is located somewhat closer to the Waddensee dike, with a larger area of mudflats and salt marshes behind the dike (see the green to orange colors north of the dike in Figure 16). This area behind the dike is expected to have a smaller seepage flux due to higher hydraulic resistance. However, on the inland side of the dike, the seepage flux increases compared to areas without mudflats and salt marshes (America et al., 2023). This is also observed by the seepage-infiltration map, which does not show a clear infiltration or seepage zone at the measurement location (see Figure 12d). This could possibly explain the higher salinity, as this is the only measurement location in the neighborhood with mudflat and salt marsh areas behind the dike, which also shows higher salinity. Next to that, the deep 'seepage ditch' located close to the measurement location prevents higher seepage fluxes more land inwards. However, the parcel next to this deep seepage ditch could have a shallower, or even disappeared rainwater lens (America et al., 2023), explaining the higher salinity for this location (see Figure 35, Appendix B).

In Rottum (GR-RTT-L1 and GR-RTT-L2), location 1 shows significantly higher salinity, reaching very strong salinity at greater depths, compared to location 2, which remains non-saline to slightly saline (see Figure 13e). Saturation was only reached for location 1, at 100 cm (see Table 5, Appendix A). Below this level the salinity increased with 10 to 15 mS/cm, to a very strong salinity of 25 mS/cm. Location 2 was quite stable in depth with non-saline to slightly saline soil moisture in the root zone. The absence of a salinity pattern in depth would suggest infiltration at location 2: freshwater and eventually some salt from occasional seepage or capillary rise infiltrates towards the groundwater (P. G. B. de Louw, Eeman, et al., 2013; Patel et al., 2000). The higher salinity at location 1 could be attributed to the 40 cm lower elevation compared to location 2, suggesting seepage at location 1 (Data Feed - Digital Terrain Model (DTM) 0.5m, 2023). This matches the seepage-infiltration map (see Figure 12e).

The measurement in Kloosterburen (GR-KLB-L1) indicates slightly saline conditions (see Figure 13f), with saturation reached at 90 cm depth. Due to saturation and starting thunder in the field during the moment of sampling, no deeper measurements or additional locations in the parcel were possible (see Table 5, Appendix A). The low salinity values in the soil moisture, even at saturation level, and the location at the border of a higher-elevated salt marsh terrace (*BRO Geomorfologische Kaart (GMM) WMS, 2023; Data Feed - Digital Terrain Model (DTM) 0,5m, 2023*), would suggest infiltration, matching the infiltration area in the seepage-infiltration map (see Figure 12f-1).

The measurements in Uithuizermeeden (GR-UHM-L1 and GR-UHM-L2) show comparable non-saline to slightly saline values in the root zone, with a maximum difference of 2 mS/cm (see Figure 13f). Location 1 is more saline at shallow depth up to 50 cm deep. However, location 2 is more saline at 150 cm depth. Location 1 was fertilized the day before, which might explain the higher EC in the topsoil. This is discussed in section 5.1.1. Saturation was reached for location 2 at 150 cm, and was not reached for location 1 (see Table 5, Appendix A), which might explain the salinity difference at 150 cm depth. The low salinity measurements in Uithuizermeeden would suggest infiltration, matching the infiltration area in the seepage-infiltration map (see Figure 12f-2)

4.1.2 Flevoland Coast

The locations in Flevoland are shown in Figure 17. By zooming in to the specific locations, the seepage-infiltration map is shown (Janssen et al., 2020), to compare these maps to the salinity profiles of the soil moisture in depth (see Figure 18) with similar indices. The seepage map shows clear seepage in most of the ditches and in part of the parcels, but other parcels are located in an infiltration area.

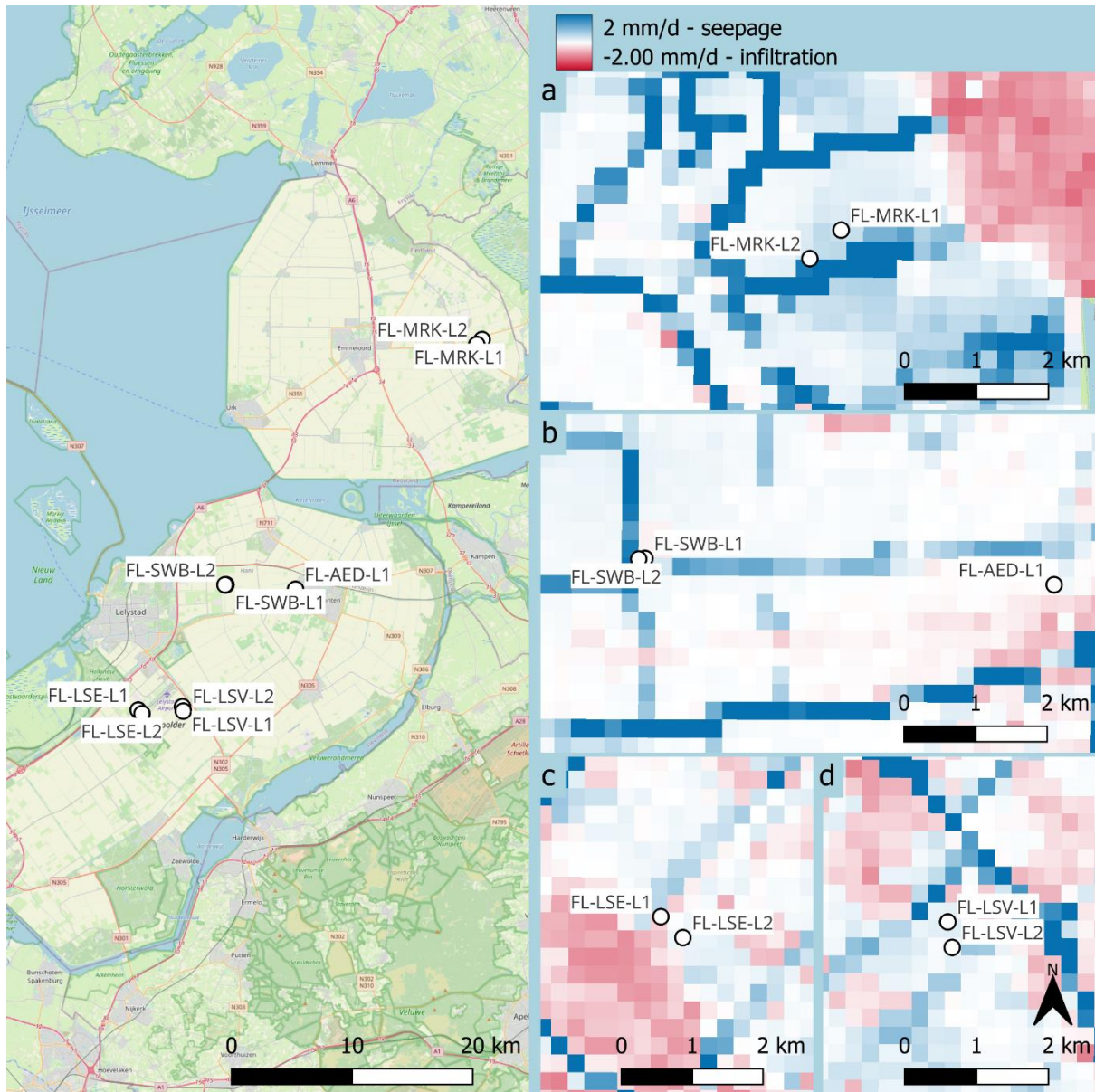


Figure 17: Map showing the locations along the Flevoland coast, and maps zooming in on the locations on the seepage-infiltration map (Janssen et al., 2020). The numbering a-f corresponds with the numbering in Figure 18.

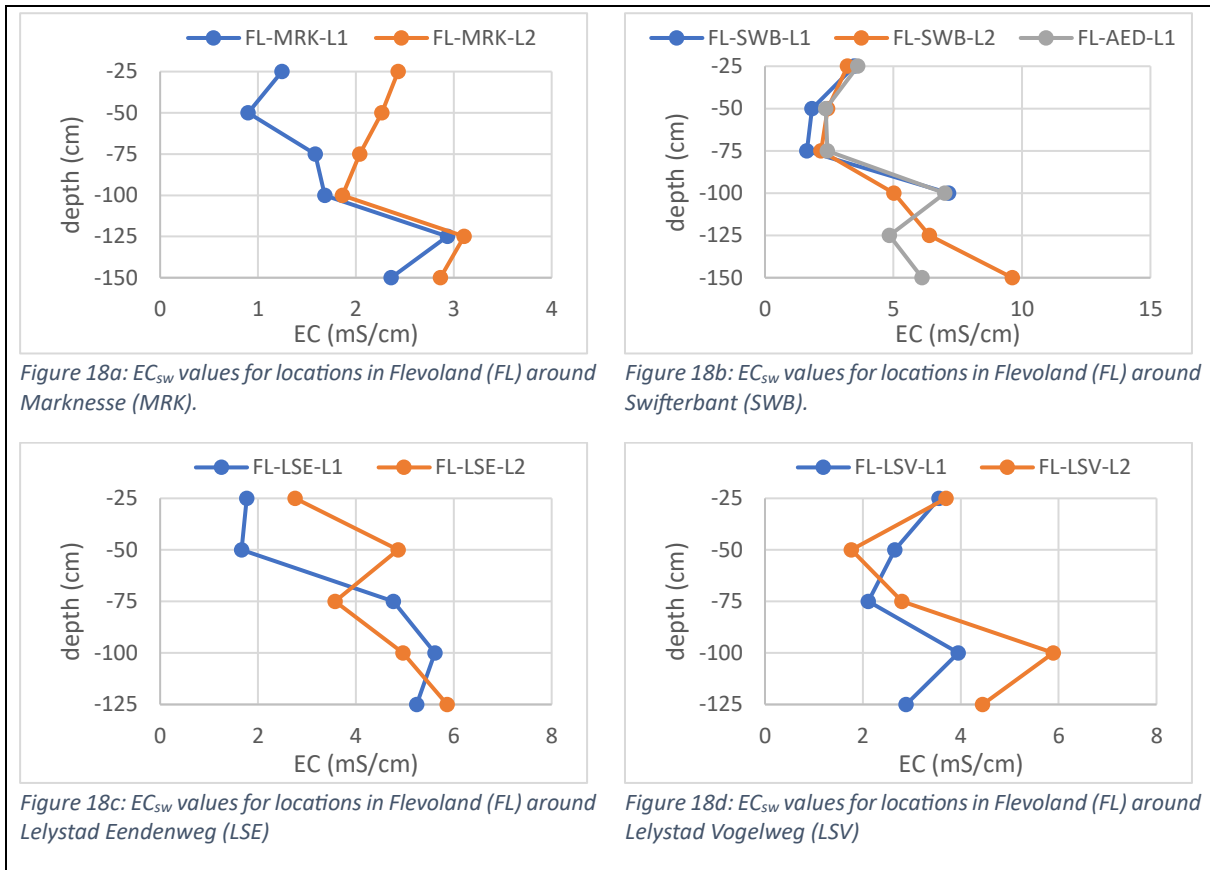


Figure 18: EC_{sw} values over depth for various locations along the Flevoland coast during the autumn of 2023.

The soil moisture in the top soil of location 2 in Marknesse (FL-MRK-L1 and FL-MRK-L2) shows slightly higher salinities compared to location 1, but overall non-saline to slightly saline values are found (see Figure 18a). Salinity profiles at depths of 100 cm and below are similar for both locations. Infiltration is mainly expected near the dike and the 2-meter higher elevated old land (Data Feed - Digital Terrain Model (DTM) 0.5m, 2023), while seepage is expected at the measurement locations. Location 2 is located in a stronger seepage zone than location 1 (see Figure 17a). Additionally, the western part of the ditch, closer to location 2, shows higher salinity compared to the eastern part near location 1 (Table 6, Appendix A), aligning with the seepage-infiltration map. The salinity difference between both locations can be explained by the difference in seepage, and irrigation with saline ditch water. The ditch at location 2 contained iron-rich seepage water with higher salinities compared to location 1 and was used for irrigation. This difference was also visible by the orange iron color on the netting above the trees due to irrigating with ditch water, which was not found for the netting at location 1 where ditch water was less saline (personal communication with landowner on 5 October 2023).

Salinity profiles near Swifterbant (FL-SWB-L1 and FL-SWB-L2) and Aeres Hogeschool Dronten (FL-AED-L1) show similar patterns with slightly to moderately saline values (see Figure 18b). Swifterbant shows salinities significantly increasing with depth. This suggests seepage, matching the seepage-infiltration map (see Figure 17b). Near Dronten however, the salinity decreases after 100 cm. Gley is observed at this location, which might also indicate saline seepage, as elaborated in section 5.1.2 (van Enk, 2016), but this location is not located in a particular seepage or infiltration zone (see Figure 17b). Location 1 in Swifterbant showed gley as well, and reached saturation at 100 cm depth, while location 2, with saturation at 125 cm, did not show gley (see Table 5, Appendix A). This suggests a relationship between saturation level and subsoil salinity, as elaborated in section 5.1.2, which might explain the higher salinity at 100 cm for location 2 in Swifterbant, even though deeper measurements were not possible.

The TEC-probe profile for location 1 in Swifterbant indicates a potential fresh-saline interface (see Figure 19), but the interface is less clear with lower salinities compared to TEC-profiles near Anna Paulowna and Kerkwerve (see sections 4.1.3 and 4.1.4). In previous research in this area, seepage dominance in ditches was observed (see Figure 36, Appendix B, showing the situation in the field during the autumn), particularly in the southern ditch, the Overijsselsetocht (Schipper et al., 2022). This underscores the significance of seepage dynamics in this area, although this study mainly focuses on root zone salinity.

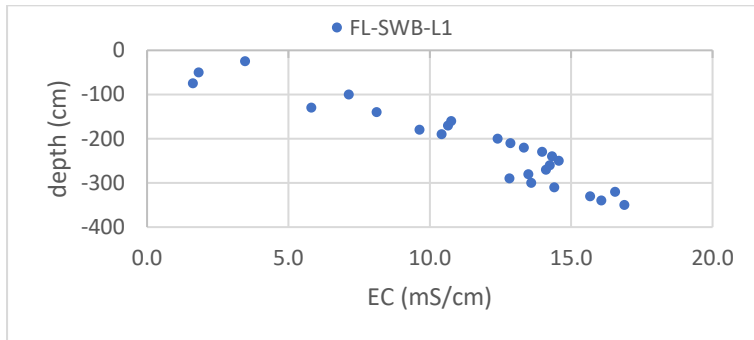


Figure 19: TEC-probe data showing the EC_{sw} values in depth for a location near Swifterbant, FL-SWB-L1 for September 2023, including soil sample measurements.

Salinities along the Eendenweg near Lelystad (FL-LSE-L1 and FL-LSE-L2) are slightly to moderately saline. Location 2 shows higher salinity in the topsoil compared to location 1, with comparable salinities at 75 cm depth and deeper (see Figure 18c). Location 1 is irrigated in the beginning of 2023, whereas location 2 is not irrigated in 2023 (personal communication with landowner on 13 September 2023). However, this could not explain the lower salinity in the topsoil of location 1. This might be because of leaching of salts from irrigation water towards the subsoil, due to expected infiltration (Patel et al., 2000), matching the irrigation area of location 1 as found on the seepage-infiltration map (see Figure 17c). The higher topsoil salinity at location 2 is likely attributed to saline water reaching the root zone via seepage, matching the seepage area of location 2 as found on the seepage-infiltration map (see Figure 17c).

Salinity profiles for parcels along the Vogelweg near Lelystad (FL-LSV-L1 and FL-LSV-L2) show slightly saline values, with location 2 showing moderately saline soil moisture at greater depths (see Figure 18d). Gley is observed at both locations, indicating seepage at these locations, matching the seepage as found on the seepage-infiltration map (see Figure 17d). However, gley is observed at greater depth for location 1 (see Table 5, Appendix A), potentially indicating less seepage compared to location 2, explaining the higher salinity of location 2, as is elaborated in section 5.1.2 (van Enk, 2016). Additionally, location 1 is irrigated in 2023 (personal communication with landowner on 13 September 2023), potentially contributing to slightly higher topsoil salinity at this location (Chen et al., 2010).

4.1.3 Holland Coast

The locations along the Holland coast are shown in Figure 20. By zooming in to the specific locations, the seepage-infiltration map is shown (Janssen et al., 2020), to compare these maps to the salinity profiles of the soil moisture in depth (see Figure 21) with similar indices.

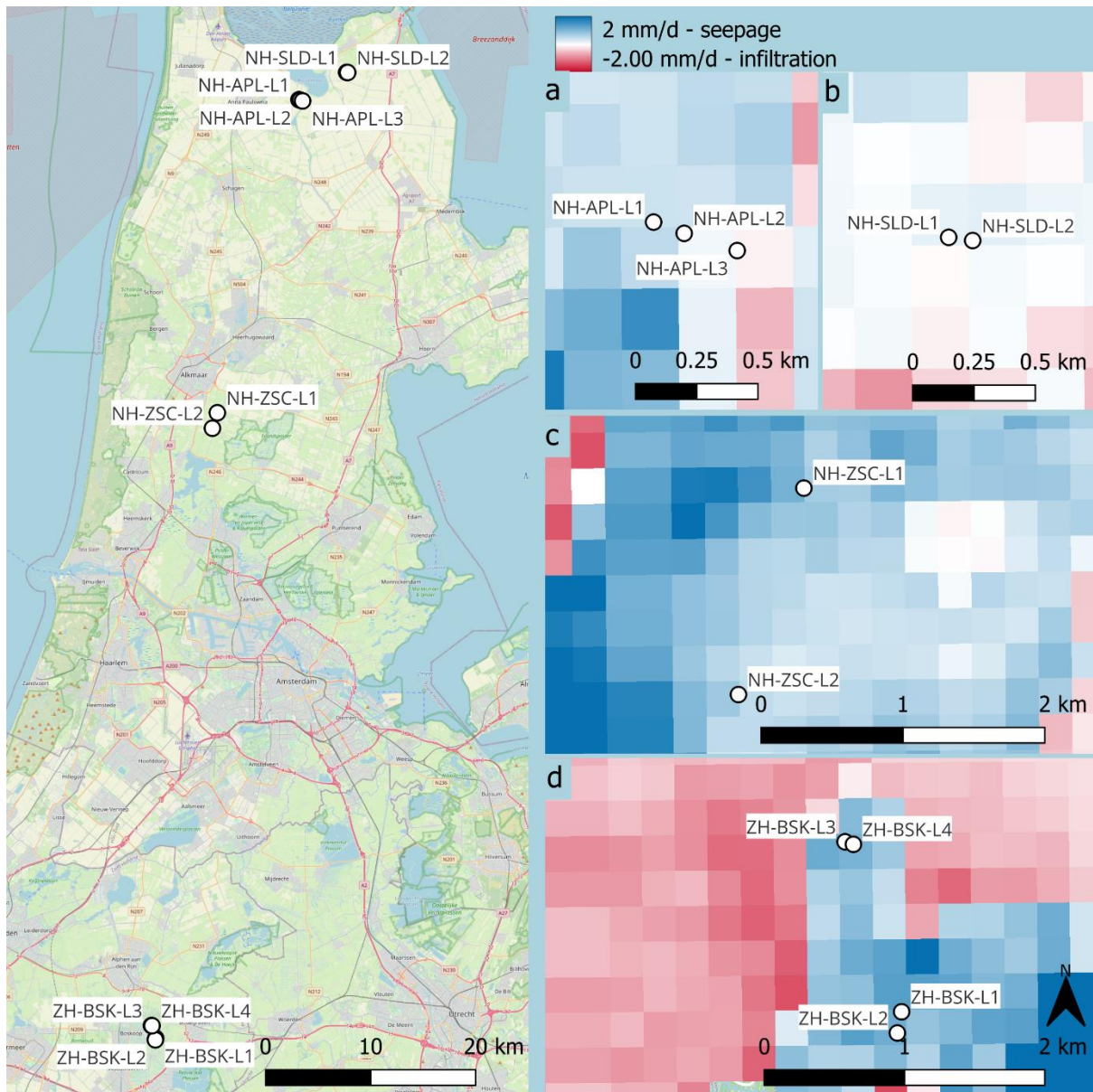


Figure 20: Map showing the locations along the Holland coast, and maps zooming in on the locations on the seepage-infiltration map (Janssen et al., 2020). The numbering a-f corresponds with the numbering in Figure 21.

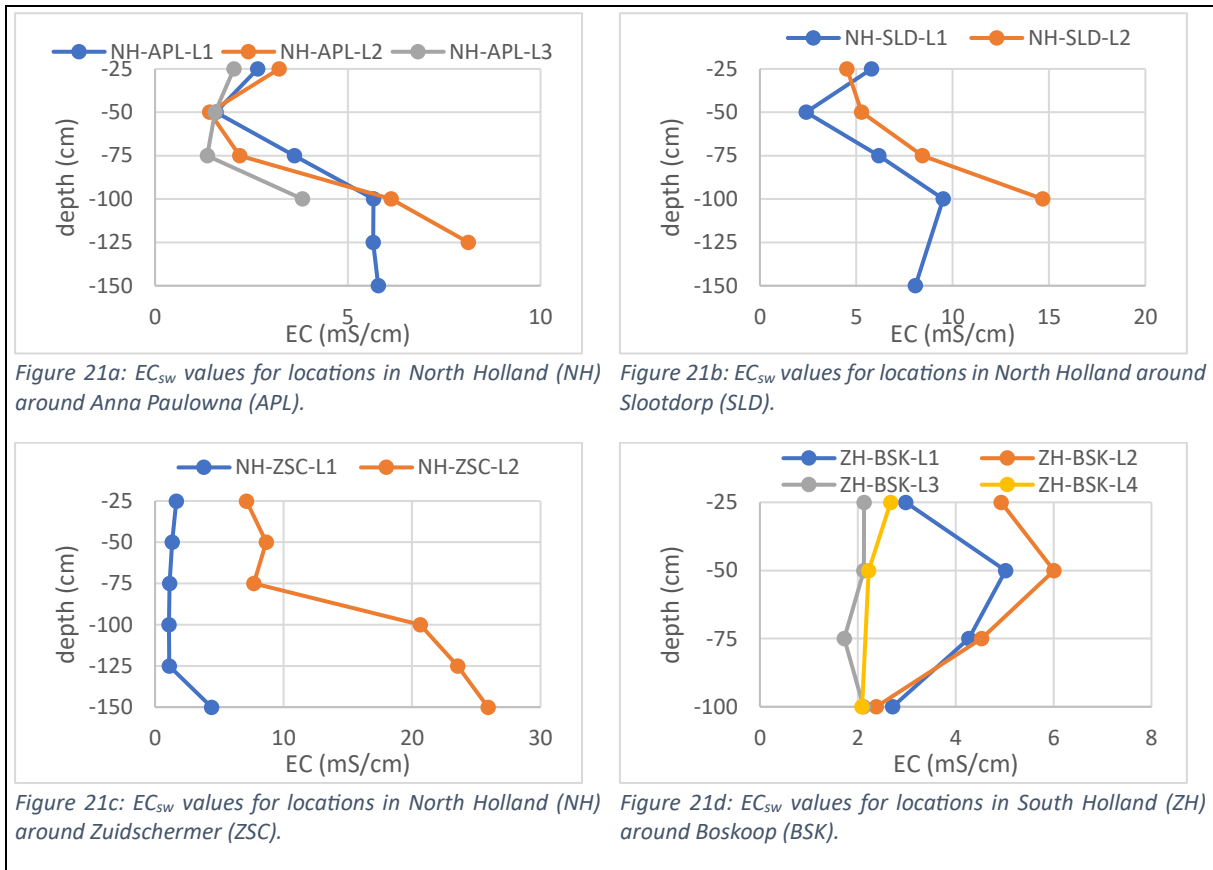


Figure 21: EC_{sw} values over depth for various locations along the Holland coast during the autumn of 2023.

Salinity profiles near Anna Paulowna (NH-APL-L1, NH-APL-L2 and NH-APL-L3) show slightly saline values, with moderate salinity observed at greater depths (see Figure 21a). These locations are located on a higher elevated tidal levee (*BRO Geomorfologische Kaart (GMM) WMS, 2023; Data Feed - Digital Terrain Model (DTM) 0,5m, 2023*). This would suggest infiltration at these locations, while the soil salinity measurements would suggest seepage, which agrees with the seepage-infiltration map (see Figure 20a). Location 3, close to a large ditch in the east, shows lower salinity and shallower saturation compared to the other locations (see Table 5, Appendix A), which could be explained due to its location closer to the infiltration area (see Figure 20a). In contrast, location 1 and 2 show similar profiles, with location 2 showing shallower saturation and higher subsoil salinity compared to location 1 (see Table 5, Appendix A). This suggests a relationship between the saturation level and the salinity level, as elaborated in section 5.1.2. Additionally, the shallower fresh-saline interface as found for location 2 in the TEC-probe profiles, match the higher salinity in the subsoil of location 2 (see Figure 22).

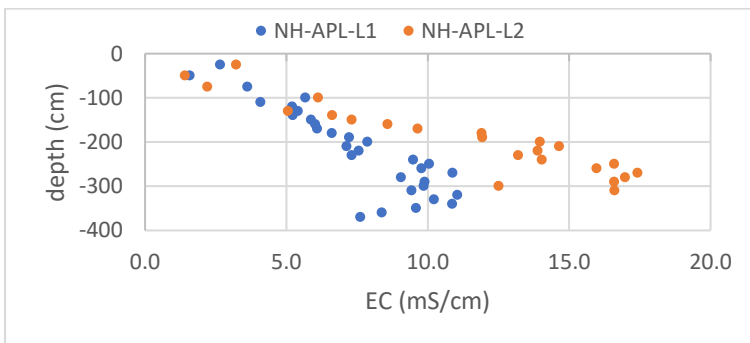


Figure 22: TEC-probe data showing the EC_{sw} values in depth for locations near Anna Paulowna (NH-APL-L1 and NH-APL-L2) for September 2023 (Data from Project - "Zoetwaterboeren" 2022 - 2025. n.d.), including soil sample measurements.

Slootdorp (NH-SLD-L1 and NH-SLD-L2) shows moderately to strongly saline soil moisture, increasing with depth (see Figure 21b). The topsoil of location 1 has higher salinity, possibly influenced by irrigation with water of 1.5 to 2 mS/cm (personal communication with landowner on 11 September 2023), while location 2, which was less saline, was not irrigated. Both locations have deeper elevation compared to the surrounding parcels (*Data Feed - Digital Terrain Model (DTM) 0,5m, 2023*). Together with the increase in salinity with depth, this suggests seepage at both locations, matching the seepage-infiltration map (see Figure 20b). Location 1 was saturated around 120 cm, while Location 2 was saturated around 100 cm (see Table 5, Appendix A). This suggests a relationship between saturation level and salinity level in the subsoil, as elaborated in section 5.1.2.

Slootdorp generally shows higher salinity compared to Anna Paulowna, which correlates with a model simulation by a salinization study of water board Hollands Noorderkwartier (see Figure 37, Appendix B), which showed that the salt load in Slootdorp was significantly higher than in Anna Paulowna (Velstra et al., 2013). This corresponds to the higher salinity in the soil moisture in Slootdorp. Additionally, the salt load increased towards the west in Anna Paulowna (see Figure 37, Appendix B), which corresponds to the higher salinity levels for location 1 and 2 (Velstra et al., 2013).

Salinity profiles in the Zuidermeer area (NH-ZSC-L1 and NH-ZSC-L2) vary significantly, with location 1 being non-saline, and location 2 being strongly to very strongly saline according to both the soil sample (see Figure 21c) and the ditch measurements (see Table 6, Appendix A). Measurements would suggest stronger seepage at location 2, but both areas are situated in a seepage area, and location 1 might even have stronger seepage according to the seepage-infiltration map (see Figure 20c). This correlates with a salinization study of water board Hollands Noorderkwartier (see Figure 37, Appendix B), indicating stronger seepage and a higher salt load for location 1 (Velstra et al., 2013). It is suggested that a local seepage boil exists at location 2, but exact boil locations are still unidentified. Current models lack sufficient data and contain too much uncertainty to accurately predict boil locations (P. G. B. de Louw, 2013).

Measurements in the deep polder near Boskoop (ZH-BSK-L1, ZH-BSK-L2, ZH-BSK-L3 and ZH-BSK-L4), show slightly to moderately saline values (see Figure 20), with the southern parcel (location 1 and 2) showing higher salinities compared to the northern parcel (location 3 and 4, see Figure 20d and Figure 21d). The ditch salinity levels in the southern area are more saline as well, but not as significant as the soil moisture (see Table 6, Appendix A). Soil salinities decrease with depth, and deeper measurements were not possible due to saturation (see Table 5, Appendix A). This area is located in a deep polder, with approximately 3.5 meters lower elevation compared to surrounding parcels (*Data Feed - Digital Terrain Model (DTM) 0,5m, 2023*), which suggests seepage at these locations, matching the seepage-infiltration map (see Figure 20d). Location 3 and 4 show comparable salinity profiles, but with lower salinity compared to location 1 and 2, suggesting more seepage at location 1 and 2. Additionally, location 2, adjacent to a seepage puddle with different vegetation (see Table 5, Appendix A), showed higher salinity compared to location 1, suggesting more seepage explaining the higher salinity at location 2 (see Figure 21d).

4.1.4 Delta Coast

The locations along the Waddenzee are shown in Figure 23. By zooming in to the specific locations, the seepage-infiltration map is shown (Janssen et al., 2020), to compare these maps to the salinity profiles of the soil moisture in depth (see Figure 24) with similar indices.

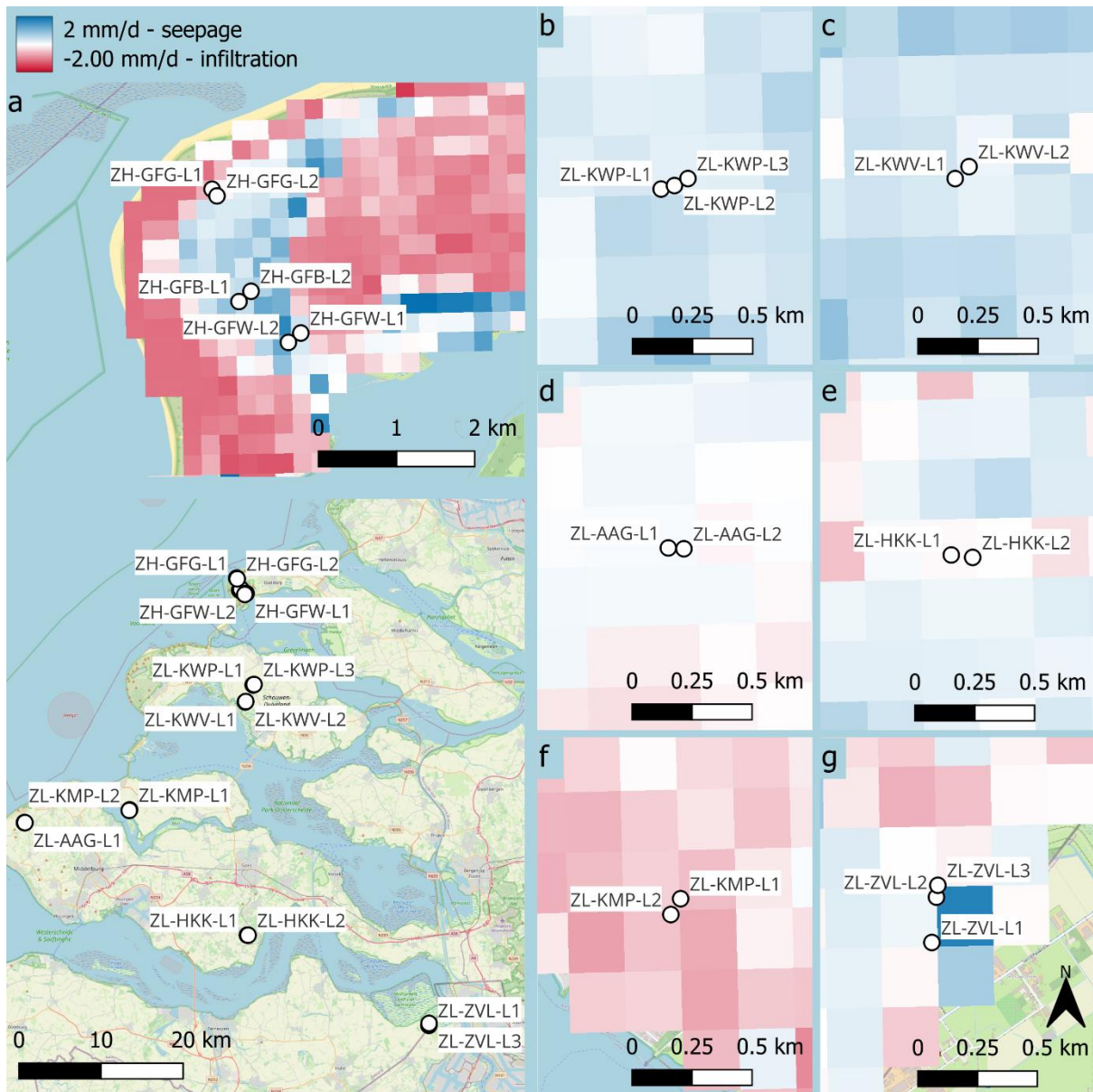


Figure 23: Map showing the locations along the Delta coast, and maps zooming in on the locations on the seepage-infiltration map (Janssen et al., 2020). The numbering a-f corresponds with the numbering in Figure 24.

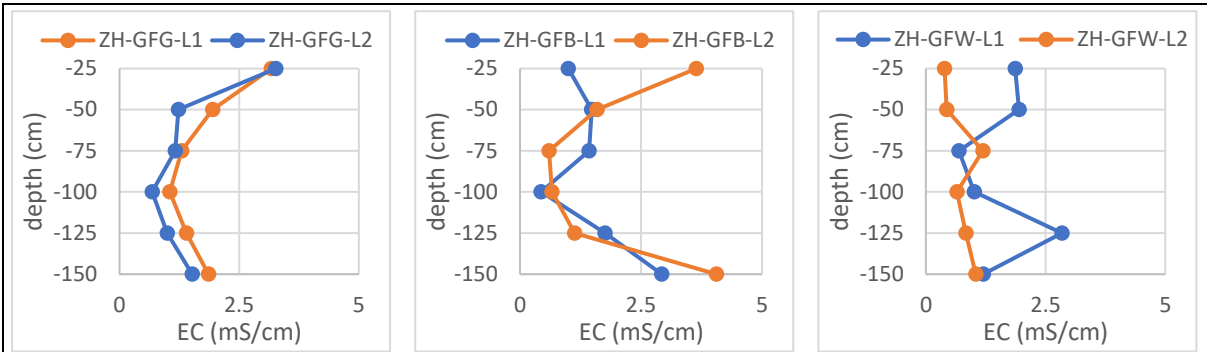


Figure 24a-1: EC_{sw} values for locations in South Holland (ZH) at Goeree-Overflakkee around the Groenedijk (GFG).

Figure 24a-2: EC_{sw} values for locations in South Holland (ZH) at Goeree-Overflakkee around the Boutweg (GFB).

Figure 24a-3: EC_{sw} values for locations in South Holland (ZH) at Goeree-Overflakkee around the Westduinweg (GFW).

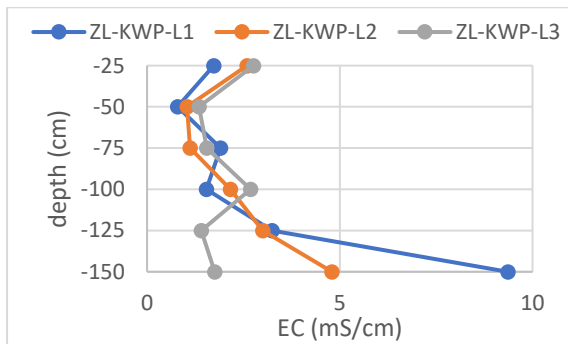


Figure 24b: EC_{sw} values for locations in Zeeland (ZL) around Kerkwerve, the Papeweg (KWP).

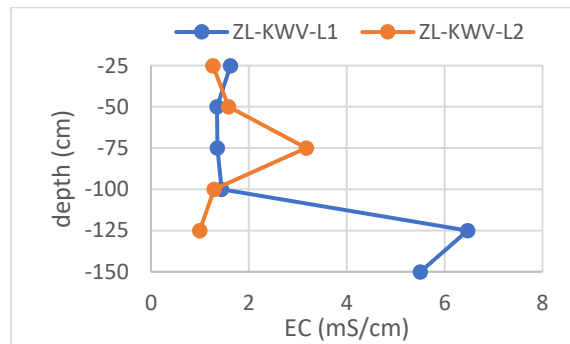


Figure 24c: EC_{sw} values for locations in Zeeland (ZL) around Kerkwerve, the Verseputseweg (KVV).

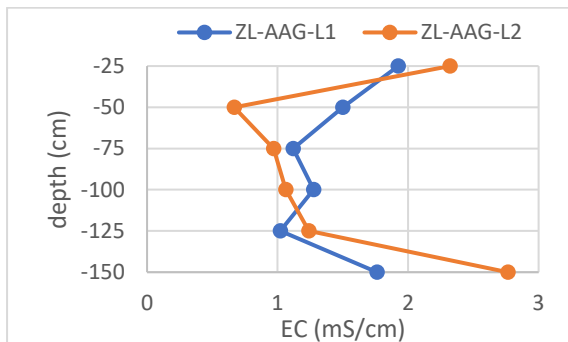


Figure 24d: EC_{sw} values for locations in Zeeland (ZL) around Aagtekerke (AAG).

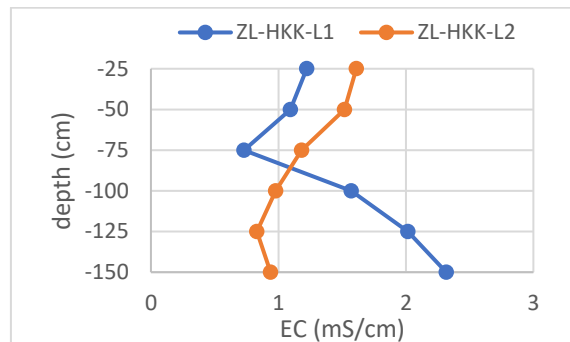


Figure 24e: EC_{sw} values for locations in Zeeland (ZL) around Hoedekenskerke (HKK).

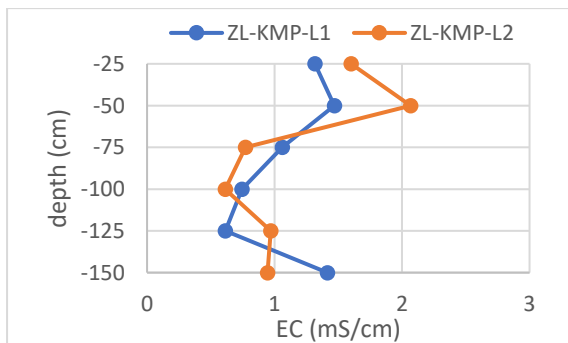


Figure 24f: EC_{sw} values for locations in Zeeland (ZL) around Kamperland (KMP).

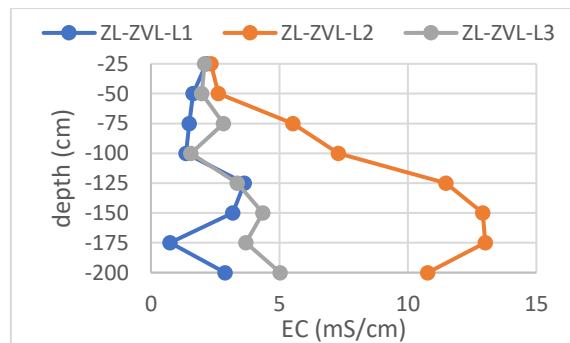


Figure 24g: EC_{sw} values for locations in Zeeland (ZL) in Zeeuws Vlaanderen (ZVL).

Figure 24: EC_{sw} values over depth for various locations along the Delta coast during the autumn of 2023.

The salinity profiles for parcels on Goeree-Overflakkee near Ouddorp show minor variations in salinity (see Figure 24a-1, Figure 24a-2 and Figure 24a-3). Between 50 and 125 cm only non-saline conditions are found for all locations. While slightly saline conditions are measured in the topsoil at locations around the Groeneweg (ZH-GFG-L1 and ZH-GFG-L2) and one location at the Boutweg (ZH-GFB-L2), greater depths show slightly saline values at the Boutweg as well (ZH-GFB-L1 and ZH-GFB-L2). Measured ditch salinities near the Boutweg are higher compared to those around the Groeneweg and Westduinweg (ZH-GFW-L1 and ZH-GFW-L2, see Table 6, Appendix A), aligning with previous Deltares research (*Data from Internal Database Deltares, n.d.*), indicating higher ditch salinity in the middle of the island (see Figure 25). This matches the higher salinity in soil moisture measurements at greater depth for the Boutweg. Seepage is expected on the lower elevated middle part of the island (*Data Feed - Digital Terrain Model (DTM) 0,5m, 2023*), close to the Boutweg, while infiltration is expected on the higher elevated parts on the sides close to the dunes and east of the parcels, close to the Groeneweg and Westduinweg (see Figure 25). This agrees with the seepage-infiltration map (see Figure 23a) and possibly explains the difference in subsoil salinity.

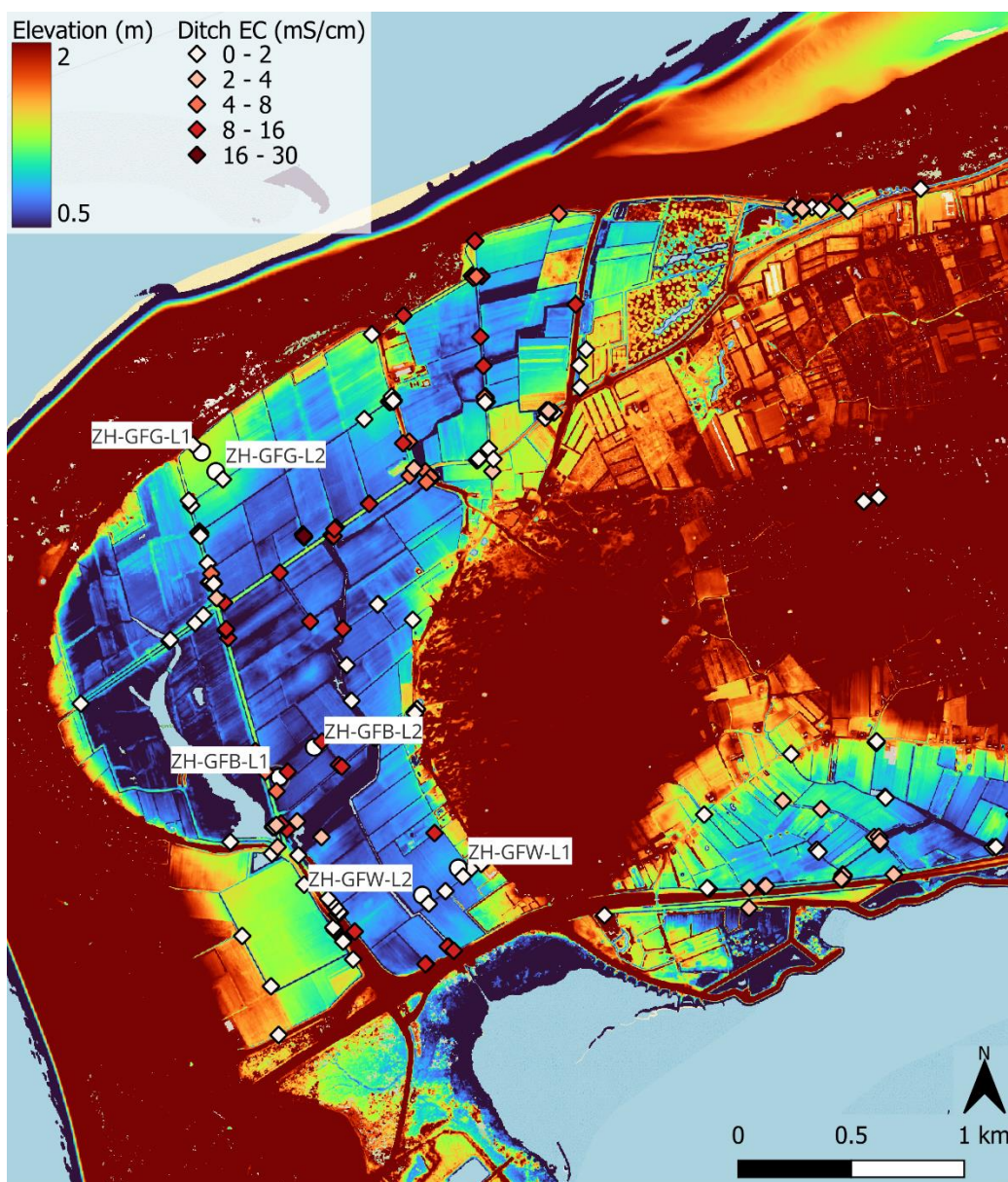


Figure 25: Ditch EC_w values (mS/cm) for Goeree-Overflakkee (*Data from Internal Database Deltares, n.d.*) and Digital Terrain Model showing the elevation on Goeree-Overflakkee (*Data Feed - Digital Terrain Model (DTM) 0,5m, 2023*).

Fresh-saline interface depths in Zeeland are obtained from FRESHEM data (*FRESHEM Zeeland Grensvlakken*, 2017), based on chloride concentrations of 1 g/L, corresponding to an EC_w of 4 mS/cm (P. G. B. de Louw et al., 2011) (see Figure 26, and Table 8 in Appendix A, which shows the depth for specific locations, including the depth for a concentration of 3 g/L, corresponding to an EC_w of 9.5 mS/cm). Shallow depths are found for locations near Kerkwerve and Hoedekenskerke. Conversely, significant differences within a parcel are found in Zeeuws-Vlaanderen, with location 2 showing a shallow interface as well. Locations near Aagtekerke and Kamperland have deeper interfaces. These interface depths help in understanding and explaining salinity distributions and salinity profiles.

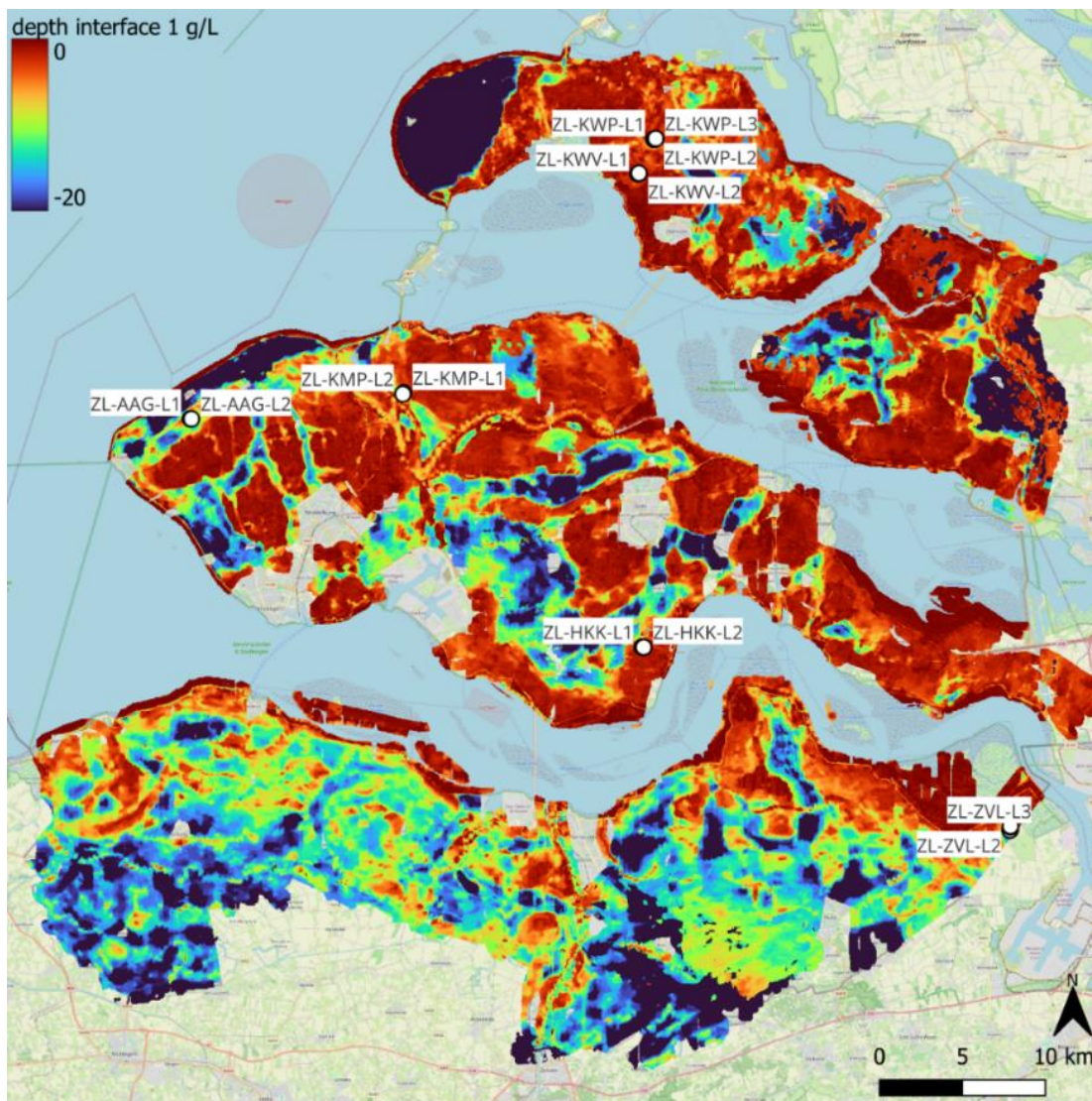


Figure 26: Depth of the fresh-saline interface on Zeeland for a chloride concentration of 1 g/L (*FRESHEM Zeeland Grensvlakken*, 2017).

The three locations for the Papeweg near Kerkwerve (ZL-KWP-L1, ZL-KWP-L2 and ZL-KWP-L3) show similar profiles with non-saline to slightly saline values in the topsoil. At 150 cm depth, salinity levels are separating, with location 3, closest to the ditch, being the least saline, location 2 reaching moderately saline values, and location 1, furthest from the ditch, reaching strongly saline values (see Figure 24b). These salinity patterns in depth, together with decreasing elevation towards the ditch (*Data Feed - Digital Terrain Model (DTM) 0,5m*, 2023), would indicate increasing seepage towards the ditch. The expected seepage matches the seepage-infiltration map (see Figure 23b). This, together with saturation occurring at shallower depths further from the ditches (see Table 5, Appendix A), likely

affects salinity concentrations, as elaborated in section 5.1.2. The shallow depth of the fresh-salt interface from FRESHM data (*FRESHM Zeeland Grensvlakken, 2017*) indicates occurrence of saline water close to the surface (see Figure 26 and Table 8, Appendix A). TEC-probe data (Data from Project - “Samenwerken Voor Zoetwater: Innovatieve Drainage Demonstreren, Monitoren En Evalueren” 2022-2024. n.d.) shows a shallower depth of the fresh-saline interface, especially for location 1 and 2, as can be seen by the small slope in Figure 27. This matches the higher salinity as measured in the soil moisture at greater depth for location 1 and 2.

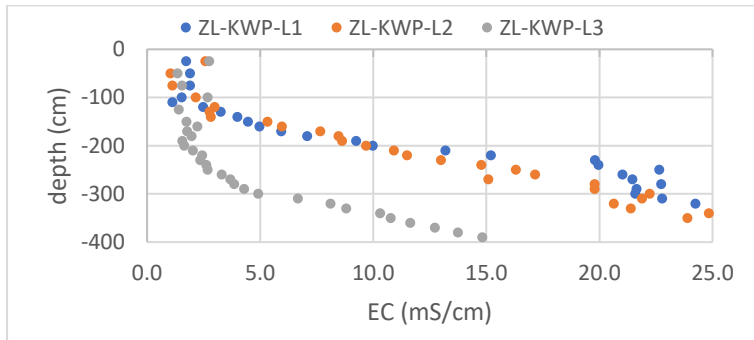


Figure 27: TEC-probe data showing the EC_{sw} values in depth for locations in Zeeland near Kerkwerve, the Papeweg (ZL-KWP-L1, ZL-KWP-L2 and ZL-KWP-L3) for September 2023 (Data from Project - “Samenwerken Voor Zoetwater: Innovatieve Drainage Demonstreren, Monitoren En Evalueren” 2022-2024. n.d.), including soil sample measurements.

The topsoil EC values along the Verseputseweg near Kerkwerve (ZL-KWV-L1 and ZL-KWV-L2) are similar and non-saline (see Figure 24c). Location 1 shows increasing salinity at greater depth, reaching moderately saline levels, whereas location 2 does not show this trend, and measurements were not possible deeper than 125 cm due to saturation (see Table 5, Appendix A). The increase in salinity with depth for location 1 would expect seepage. The seepage-infiltration map agrees with the stronger seepage at location 1 but shows that both areas are in a seepage area (see Figure 23c). However, TEC-probe profiles for location 1 and 2 contradict this (Data from Project - “Samenwerken Voor Zoetwater: Innovatieve Drainage Demonstreren, Monitoren En Evalueren” 2022-2024. n.d.). The fresh-saline interface is shallower for location 2, as seen by the sharp increase around 2 to 3 meters depth with high concentrations, which is not found for location 1 (see Figure 28). The fresh-salt interface from FRESHM is shallow as well, especially for location 2 (*FRESHM Zeeland Grensvlakken, 2017*), agreeing with the TEC-probe data (see Figure 26 and Table 8, Appendix A). Soil moisture measurements do not align with the shallow interface for location 2, as location 1 is more saline in the subsoil measurements. Nonetheless, due to saturation no deeper salinity measurements were possible for location 2, and thus possibly dependence on the shallow interface depth cannot be investigated in more detail.

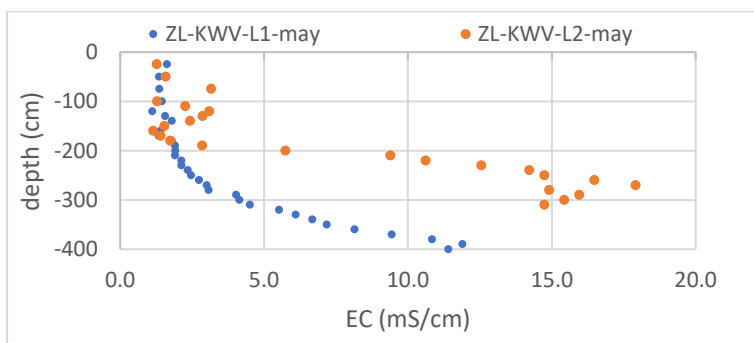


Figure 28: TEC-probe data showing the EC_{sw} values in depth for locations in Zeeland near Kerkwerve, the Verseputseweg (ZL-KWV-L1 and ZL-KWV-L2) for May 2023 (Data from Project - “Samenwerken Voor Zoetwater: Innovatieve Drainage Demonstreren, Monitoren En Evalueren” 2022-2024, n.d.), including soil sample measurements.

The salinity profiles near Aagtekerke (ZL-AAG-L1 and ZL-AAG-L2) show similar patterns with non-saline soil moisture (see Figure 24d). The topsoil is slightly more saline than the subsoil and at greater depth an increase is found, where location 2 reaches slightly saline values. The higher salinity in the topsoil might be because of irrigation with saline water, but no irrigation data is available. The increase at greater depth might be related to seepage, yet soil moisture remains relatively fresh, and the seepage-infiltration map does not show a clear seepage zone (see Figure 23d), probably due to its location at the interface of a creek ridge and a salt marsh (*BRO Geomorfologische Kaart (GMM) WMS, 2023*). This, together with a deep fresh-salt interface from FRESHEM data (*FRESHEM Zeeland Grensvlakken, 2017*), explains that saline water is not expected to reach the root zone, explaining the low salinity (see Figure 26 and Table 8, Appendix A).

Salinity profiles for parcels near Hoedekenskerke (ZL-HKK-L1 and ZL-HKK-L2) show non-saline soil moisture (see Figure 24e), attributed to expected freshwater infiltration at the creek ridge with sandier soils (*BRO Geomorfologische Kaart (GMM) WMS, 2023*), being 1 meter higher elevated compared to the surrounding salt marshes (Data Feed - Digital Terrain Model (DTM) 0.5m, 2023). No clear pattern and insignificant differences are found between both locations. However, the fresh-saline interface from the FRESHEM data (*FRESHEM Zeeland Grensvlakken, 2017*) is quite shallow (see Figure 26 and Table 8, Appendix A), meaning that salt is found close to the surface. However, because of expected infiltration at the creek ridge, saline water does reach the root zone, explaining the low salinity measurements. Contradictory, no significant infiltration zone is found on the seepage-infiltration map (see Figure 23e).

Locations near Kamperland (ZL-KMP-L1 and ZL-KMP-L2) show non-saline soil moisture, with the topsoil being slightly more saline than the subsoil (see Figure 24f). The low salinity and absence of pattern with depth suggests infiltration, matching the seepage-infiltration map (see Figure 23f), even though it is located on a salt marsh (*BRO Geomorfologische Kaart (GMM) WMS, 2023*). The fresh-salt interface is quite deep in this area (see Figure 26 and Table 8, Appendix A), indicating that saline water is not expected to reach the root zone.

Measurements in the Hedwigepolder in Zeeuws-Vlaanderen were conducted at similar distances from a ditch in the east (ZL-ZVL-L1, ZL-ZVL-L2 and ZL-ZVL-L3). Location 1 and 3 show similar non-saline to slightly saline profiles, with no significant changes in depth (see Figure 24g). However, location 2, situated in the middle, shows a significantly more saline profile, with increasing salinity up to strongly saline conditions. This parcel is deeper compared to the 0.5-to-1.0-meter higher elevated surrounding parcels (Data Feed - Digital Terrain Model (DTM) 0.5m, 2023), suggesting seepage. This matches the seepage-infiltration map (see Figure 23g). According to the FRESHEM data (*FRESHEM Zeeland Grensvlakken, 2017*), the fresh-salt interface is significantly shallower for location 2 (see Figure 26 and Table 8, Appendix A). This, combined with stronger seepage in this area, may explain the higher salinity at this location. Salinity measurements in this study align with conductivity-depth profiles from prior research in the Hedwigepolder (P. G. B. de Louw & Bootsma, 2020). Profiles for ZL-ZVL-L1 (MP6), ZL-ZVL-L2 (MP5) and ZL-ZVL-L3 (MP4) are available (see Figure 38, Appendix B). MP6 shows significantly lower conductivity in depth, correlating with the lower salinity at location 1 (see Figure 41, Appendix B). MP5 shows higher conductivity in the topsoil (see Figure 40, Appendix B), but comparable conductivity at greater depth compared to MP4 (see Figure 39, Appendix B), which matches the higher salinity as measured in the root zone for location 2.

4.2 Salinity in the Model Results

4.2.1 Salinity Index

The salinity index for 2019 (Delsman & America, 2022) indicates areas prone to salinization, including parts of the delta coast, including Schouwen-Duiveland, some deep polders in the coastal area of North and South Holland, including the Schermer polder, and part of the Waddenzee area (see Figure 29). Soil moisture measurements at 100 cm depth generally align with these regions, showing low salinity values for low salinization risks and high salinity for high risks. However, discrepancies exist, with some areas like the Flevopolder, Wieringermeerpolder, Zeeuws-Vlaanderen and parts of Friesland and Groningen showing significant saline soil moisture at 100 cm depth, while no salinization risk was expected. Conversely, Schouwen-Duiveland shows less saline soil moisture values than expected, although strongly saline values were found at greater depth as well (see section 4.1.3).

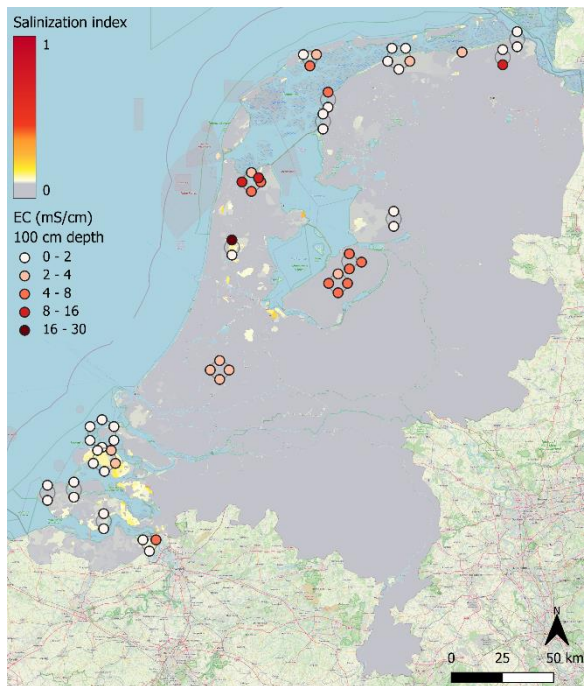


Figure 29: Measured EC_{sw} (mS/cm) for soil samples over the Dutch coastal area at 100 cm depth in the autumn of 2023 overlying the salinity index for 2019 as calculated from the LHM model (Delsman & America, 2022).

4.2.2 Salt Fronts and Concentrations

Solute concentrations are modelled across various depths for all soil sample measurement locations. Figure 30 shows the average depths of these salt fronts and the average concentration at this depth between 2010 and 2019 (Janssen et al., 2023). Salinization of the soil moisture is expected when high solute concentrations are found at shallow salt front depths.

Based on soil moisture measurements, 23 locations show moderately to strongly saline conditions (EC larger than 4 mS/cm), which are shown by the light grey bars in Figure 30 (see Table 4, Appendix A). Assuming that soil moisture salinization is expected for moderately saline solute concentrations exceeding 1 g/L (equivalent to an EC larger than 4 mS/cm) at shallow depths (less than 4 meters), 9 locations are of interest according to the TRANSOL results: FL-LSV-L1, FR-TRS-L1, FR-TRS-L3, NH-ZSC-L1, NH-ZSC-L2, ZL-KWP-L1L2L3, ZL-KWV-L1, ZL-KWV-L2 and ZL-ZVL-L1L2 (see Figure 30). Considering moderately saline conditions (greater than 4 mS/cm) in both field measurements and TRANSOL results, FR-TRS-L1, NH-ZSC-L1, NH-ZSC-L2, ZL-KWP-L1, ZL-KWP-L2, ZL-ZVL-L1 and ZL-ZVL-L2 are identified as risk locations, which are shown by the dark grey bars in Figure 30 (see Table 4, Appendix A).

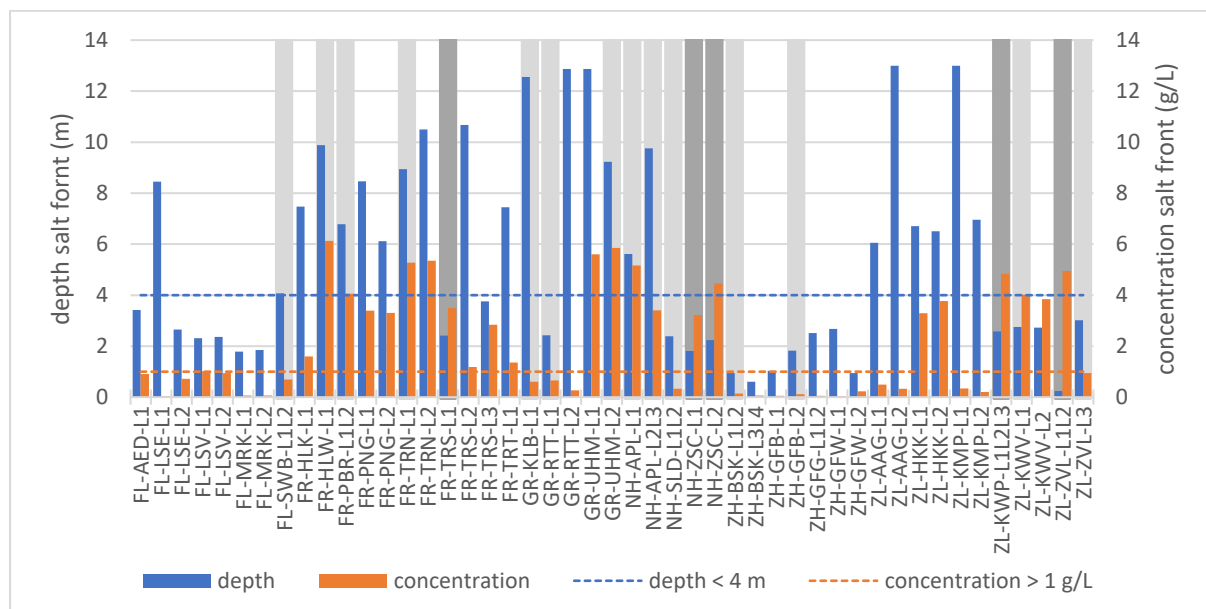


Figure 30: Average salt front depth and concentration over 2010-2019 for the locations of the soil sample measurements as output from the TRANSOL model, grey indicates locations where soil moisture measurements indicated a salinization risk (EC_{sw} larger than 4 mS/cm), and dark grey indicates locations where both TRANSOL and soil moisture measurements indicated a salinization risk (EC_{sw} larger than 4 mS/cm and salt front shallower than 4 meters) (Janssen et al., 2023).

First, simulated salinity depth profiles are compared with soil moisture measurements for locations where salinization is expected according to both the field measurements, being moderately to strongly saline, and TRANSOL simulations, with moderately to strongly saline salt fronts at shallow depth. If available, salinity depth profiles are compared to TEC-probe data as well. The salinity depth profiles are output from the TRANSOL model and show the depth (y-axis) against the simulated solute concentrations in the root zone (x-axis). Three different dates are plotted (10-01-2010, 20-09-2019 and 31-12-2019) to compare the beginning of the simulations to the end of the simulations, and one date at the end of summer, which is expected to be comparable to the field situation. The salt front is found at the depth where a strong increase in solute concentration is found (see Figure 42 to Figure 53, Appendix C). Conversion of chloride concentrations to EC_w values follows the relationship from P. G. B. de Louw et al. (2011), as elaborated in section 2.

FR-TRS-L1 showed strongly saline soil moisture (see Table 4, Appendix A). This aligns with a relatively shallow salt front depth as found for FR-TRS-L1 and FR-TRS-L3 (2.41 m and 3.76 m respectively), with high concentrations (3.5 g/L and 2.8 g/L, corresponding to EC values of 11.0 and 9.1 mS/cm respectively) in the model simulations (see Figure 44 and Figure 45, Appendix C). Location 3 appears to be more saline compared to location 2 in previous TEC-probe measurements (see Table 7, Appendix A), although this is not found in the soil moisture measurements, where location 2 was more saline (see Table 4, Appendix A). The TEC-probe data for location 2 and 3, together with the higher soil moisture salinity measurements for location 1, possibly explains why only location 1 and 3 show shallower salt front depths with higher concentrations.

NH-ZSC-L1 showed moderately saline conditions in the subsoil, while NH-ZSC-L2 reached very strongly saline conditions (see Table 4, Appendix A). This matches the relatively shallow salt fronts as found for NH-ZSC-L1 and NH-ZSC-L2 (1.8 m and 2.2 m respectively) with high concentrations (3.2 g/L and 4.5 g/L, corresponding to EC values of 10.1 mS/cm and 13.6 mS/cm respectively, see Figure 50 and Figure 51, Appendix C). Although location 1 has a slightly shallower salt front, location 2 shows significantly higher simulated solute concentrations, which matches the higher soil moisture measurements as found at location 2.

ZL-KWP-L1 showed strongly saline conditions in the subsoil, while ZL-KWP-L2 showed moderately saline conditions (see Table 4, Appendix A). The model simulation for ZL-KWP-L1L2L3 showed a relatively shallow salt front depth (2.6 m) with high concentrations (4.8 g/L, corresponding to EC values of 14.7 mS/cm, see Figure 52, Appendix C). This matches the moderately to strongly saline soil moisture measurements at location 1 and 2. However, location 3 did not show such high salinities in the subsoil measurements. TEC-probe data indicated shallower fresh-saline interfaces for location 1 and 2 and deeper interfaces for location 3, but no model results are available for individual locations. However, the interface of 2.6 m as found by the model is comparable to the interface for location 1 and 2 from the TEC-probe data (see Figure 27, section 4.1.4).

ZL-ZVL-L2 showed strongly saline soil moisture in the subsoil, while ZL-ZVL-L1 showed moderately saline conditions (see Table 4, Appendix A). Additionally, the model simulation for ZL-ZVL-L1L2 showed a shallow salt front (0.25m) with high concentrations (4.9 g/L, corresponding to EC values of 15.0 mS/cm). However, this salt front is remarkably shallow and the curve displays an abnormal pattern (see Figure 53, Appendix C). This cell is a model boundary, which possibly explains the irregularities in the results, and are thus expected to be unreliable for comparison with field measurements.

Next to these locations where salinization was expected according to both the field measurements and the TRANSOL simulations, there are also locations where salinization was expected due to high concentrations in the soil moisture measurements, which was not captured by the model simulations. For some locations with large discrepancies between the measurements and the model, this is elaborated below.

FL-SWB-L2 shows strongly saline soil moisture in the subsoil, particularly at 150 cm depth (up to 10 mS/cm, see Table 4, Appendix A). The model simulations shows a moderate salt front depth (4.1 m) with slightly saline concentrations (0.7 g/L, corresponding to EC values of 3.2 mS/cm, see Figure 42, Appendix C). TEC-probe data shows significantly higher salinities around 17 mS/cm at 3.5 m depth agreeing with the high subsoil salinity. However, a similar curve with significantly lower concentrations is found at the simulation on the 10th of January of 2010 (see Figure 19, section 0). However, this curve is not found for both simulations in 2019.

FR-PBR-L2 showed very strongly saline soil moisture in the subsoil (up to 18 mS/cm), significantly higher than location 1 (see Table 4, Appendix A). However, the model simulations shows a deep salt front (6.8 m) with very strong salinity (4.1 g/L, corresponding to EC values of 12.5 mS/cm, see Figure 43, Appendix C). As the cell covers both locations, distinctions between the locations in the model results are unclear. Both locations are in a seepage area, but there might be local seepage from greater depths, contributing to higher salinity at location 2.

GR-RTT-L1 shows very strongly saline soil moisture in the subsoil measurements (up to 26 mS/cm, see Table 4, Appendix A). However, the model simulation shows a shallow depth (2.4 m), with low concentrations (0.7 g/L, corresponding to EC values of 3.0 mS/cm, see Figure 46, Appendix C). The salt front for location 2 is deeper with comparable concentrations, potentially explaining the difference in measurements between both locations, as location 2 showed less saline soil moisture (see Figure 30).

NH-SLD-L1 and NH-SLD-L2 only show strongly saline soil moisture in the subsoil (up to 15 mS/cm, see Table 4, Appendix A). The model indicates a shallow salt front depth (2.4 m), with low concentrations (0.3 g/L, corresponding to EC values of 2.2 mS/cm, see Figure 49, Appendix C). The model does thus not predict the high values as found in the root zone.

NH-APL-L2 showed strongly saline soil moisture in the measurements (up to 8 mS/cm). NH-APL-L1 showed moderately saline soil moisture in the measurements (up to 6 mS/cm, see Table 4, Appendix A). However, the model shows a shallower depth for the salt front at location 1, compared to location 2 and 3 (5.6 m for location 1 and 9.8 m for location 2 and 3), with higher concentrations (5.1 g/L for location 1 and 3.4 g/L for location 2 and 3, corresponding to EC values of 15.6 mS/cm and 10.7 mS/cm respectively, see Figure 47 and Figure 48, Appendix C). This suggests that location 1 is a greater risk zone. However, location 2 and 3 represent the same cell in the model, and as indicated by the measurements, higher concentrations with more seepage were observed further from the ditch, whereas location 3, closest to the ditch, showed lower salinities. This possibly accounts for lower solute concentrations as found in the model at location 2 and 3. However, the TEC-probe data indicates a shallower interface for location 2 (see Figure 22, section 4.1.3), contradicting the deeper interface simulated by the model for location 2 and 3. However, no TEC-probe profile is available for location 3, which is expected to have a deeper interface because of the lower measured salinity in the subsoil. This discrepancy may explain the deeper interface with lower concentrations in the model results for location 2 and 3, representing the same cell in the model, while location 2 showed higher salinity in the soil moisture with a shallow fresh-saline interface according to TEC-probe data.

Besides the high-risk zones for salinization, TRANSOL results also identify areas where no salinization is expected (see Figure 30). These include regions with deep salt fronts, which are found along the coast in Groningen (GR-KLB-L1, GR-RTT-L2, GR-UHM-L1 and GR-UHM-L2), along the coast in Friesland (FR-HLK-L1, FR-HLW-L1, FR-PBR-L1L2, FR-PNG-L1, FR-PNG-L2, FR-TRN-L1, FR-TRN-L2 and FR-TRT-L1), one location on Terschelling (FR-TRS-L2), one location in the Wieringermeerpolder (NH-APL-L2L3), and in Zeeland (ZL-AAG-L1, ZL-AAG-L2, ZL-HKK-L1, ZL-HKK-L2, ZL-KMP-L1 and ZL-KMP-L2). Additionally, there are areas with shallow salt fronts, but with low concentrations, which are found in Flevoland (FL-LSE-L1, FL-MRK-L1 and FL-MRK-L2) and in South Holland (ZH-BSK-L1L2, ZH-BSK-L3L4, ZH-GFB-L1, ZH-GFB-L2, ZH-GFG-L1L2, ZH-GFW-L1 and ZH-GFW-L2). These areas generally show non-saline to slightly saline soil moisture in the subsoil, as indicated in Figure 9 (section 4.1) and Table 4 (Appendix A), and have low salinization risks according to the salinization index (see Figure 29, section 4.2.1). Exceptions are found for FR-PBR-L1L2, with strongly saline soil moisture in the subsoil for location 2, and NH-APL-L2L3, which shows strongly saline soil moisture for location 2. However, these discrepancies are likely limitations of the LHM model, which cannot distinguish between locations within the same cell.

4.2.3 Salt Concentrations in the Root Zone

The TRANSOL model also simulates root zone depths and solute concentrations (Janssen et al., 2023), which vary spatially and temporarily. Figure 54 in Appendix C provides the yearly averaged root zone depth, to give a general overview of the spatial variation. Additionally, the model simulates salt concentrations within the root zone. As mentioned in section 4.1, several locations show saline soil moisture in the root zone, therefore it is interesting to compare this with TRANSOL results. Figure 31 shows the average solute concentration for the root zone from 2010 to 2019, indicating that most locations show no salt accumulation in the root zone according to the model. However, FL-LSE-L2, FL-LSV-L1, FL-MRK-L1, FL-MRK-L2, FL-SWB-L1L2 and GR-UHM-L1 show some solute in the yearly-averaged solute concentrations in the root zone (see Figure 31). Especially, FL-LSE-L2 and FL-LSV-L1 show relevant salinity concentrations with clear seasonal patterns (see Figure 32), while FL-MRK-L1 and FL-MRK-L2 show seasonality as well, but their concentrations are negligible (see Figure 56, Appendix C). Conversely, FL-SWB-L1L2 and GR-UHM-L1 show sporadic peaks in salinity concentration, without any seasonal trends (see Figure 55, Appendix C), likely suggesting simulation errors.

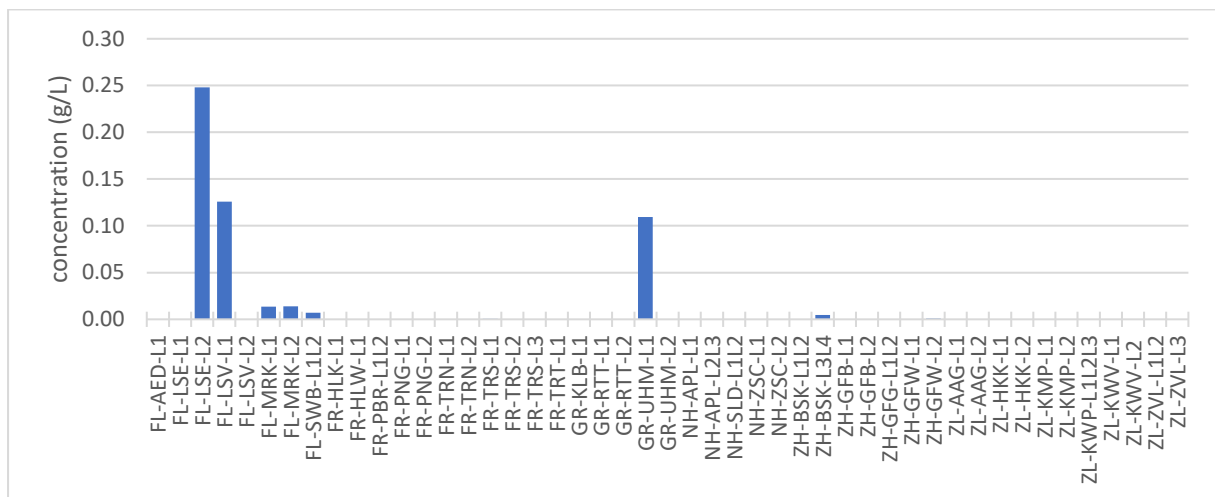


Figure 31: Yearly averaged solute concentrations in the root zone over 2010-2019 for the locations of the soil sample measurements as output from the TRANSOL model (Janssen et al., 2023).

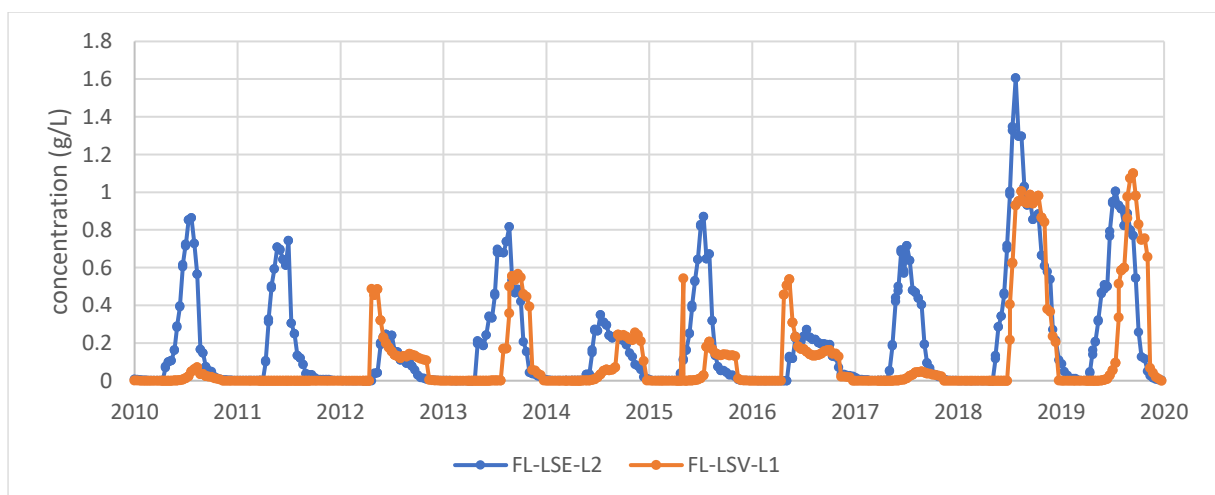


Figure 32: Solute concentrations in the root zone for locations in Flevoland: Eendenweg location 2 (FL-LSE-L2) and Vogelweg location 1 (FL-LSV-L1) as output from the TRANSOL model (Janssen et al., 2023).

In Flevoland, both FL-LSE-L2 and FL-LSV-L1 show clear seasonal patterns, with minimal root zone salinity during winter, and slightly saline values during summer (around 0.5-1 g/L, corresponding to EC values of 2.6-4 mg/L, (see Figure 32). Soil sample measurements confirm higher salinity values in the root zone (at 30-40 cm depth according to TRANSOL output) for location 2 along the Eendenweg compared to location 1 (2.8-4.9 mS/cm for location 2 compared to 3.6-2.7 mS/cm for location 1 at 25 and 50 cm depth respectively, see Table 4, Appendix A). Also, higher salinity values are found in the root zone (at 40-45 cm depth according to TRANSOL output) for location 1 along the Vogelweg compared to location 2 (2.7 mS/cm for location 1, compared to 1.8 mS/cm for location 2 at 50 cm depth, see Table 4, Appendix A). These locations show similarities between the salinity as measured in the root zone and the TRANSOL simulations, but for other samples no significant solute concentrations were simulated, while saline water was measured in the root zone (see Table 4, Appendix A).

Figure 33 shows solute concentration in the root zone for the 20th of September 2019, after a dry period (Janssen et al., 2023). Although certain locations show higher concentrations, no clear spatial patterns were found with especially deviations on pixel-scale. This shows that there can be significant inaccuracy when zooming in to specific pixels, therefore it might be better to look into multiple pixels. Most sampled locations show low concentrations corresponding to Figure 31, while surrounding areas may have slightly higher simulated concentrations (see Figure 33). The TRANSOL simulation indicates higher concentrations around Boskoop, Zuidscherm, part of the Wieringermeerpolder, Flevoland and Goeree-Overflakkee. However, discrepancies are found as highly saline soil moisture was measured in parcels in Pietersbierum, Terschelling, Rottum, Anna Paulowna, Slootdorp, Zuidscherm, Kerkwerf, Zeeuws-Vlaanderen and Swifterbant, which is not found in the TRANSOL simulation. Thus, while Zuidscherm, the Wieringermeer and part of Flevoland show high root zone salinities as indicated by the model, the accuracy in simulating highly saline conditions in the root zone is questionable.

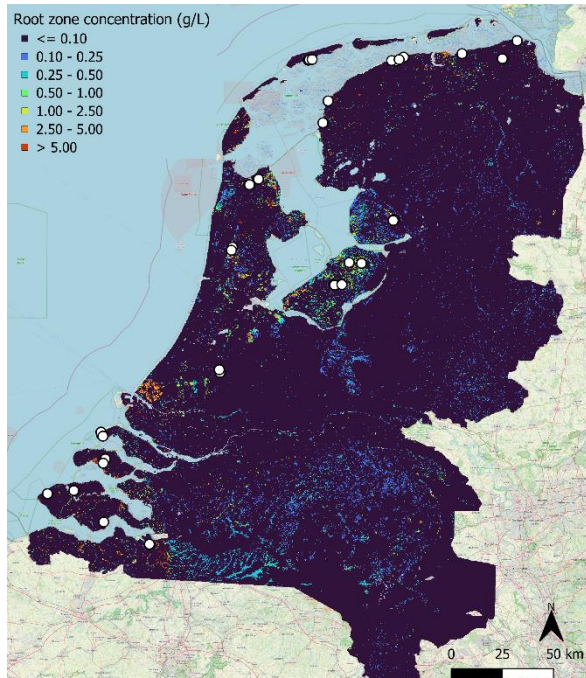


Figure 33: Solute concentration in the root zone for the Netherlands as output from the TRANSOL model (Janssen et al., 2023).

5 Discussion and recommendations

5.1 Discussion Relevant Processes

5.1.1 Soil Moisture Salinity Levels

The soil moisture shows significant variability in salinity over depth. A curve with higher salinity in the topsoil at 25 cm for several locations, followed by a slight decrease, and a significant increase deeper than 100 cm is found for most of the samples. However, this curve is not consistent across all measurements, showing significant variability between locations and even within individual parcels.

Higher topsoil salinity is found for several locations (FL-AED-L1, FL-LSV-L1, FL-LSV-L2, FL-SWB-L1, FL-SWB-L2, FR-HLW-L1, GR-UHM-L1, GR-UHM-L2, NH-APL-L1, NH-APL-L2, NH-APL-L3, NH-SLD-L1, ZH-GFB-L2, ZH-GFG-L1, ZH-GFG-L2, ZL-AAG-L1, ZL-AAG-L2, ZL-KWP-L1, ZL-KWP-L2 and ZL-KWP-L3, see Figure 13, Figure 18, Figure 21 and Figure 24 in sections 4.1.1 to 4.1.4), especially after dry periods without precipitation (see Table 9 and Figure 34, Appendix A) when evapotranspiration dries the soil and leaves salts in the upper soil layer. Lower salinity is expected after rainfall, due to leaching and dilution of salts. Even though precipitation data comes from a weather station in de Bilt instead of the specific fields, it serves as a good first indicator for weather conditions during soil sampling. Higher salinity in the topsoil may thus be influenced by evapotranspiration during dry periods, combined with seepage and capillary rise, or saline irrigation. Moreover, root water extraction might lead to salt accumulation in the root zone (Blanco & Folegatti, 2002; Nishida & Shiozawa, 2010). Fertilization or pesticide usage possibly increases EC values as well due to addition of ions, as elaborated in section 5.1.5 (Jurinak & Wagenet, 1981; Möller & Schultheiß, 2015), which possibly explains the difference in Uithuizermeeden where only location 1 was fertilized. Furthermore, irrigation with saline water brings salts in the root zone (Nachshon, 2018). Saline groundwater comes up into the root zone as well, by seepage and capillary rise. Evapotranspiration consequently dries the soil and leaves salts in the root zone, increasing the salinity (D. L. Carter, 1975; Chen et al., 2010; Nachshon, 2018; Provin & Pitt, 2001; Yusefi et al., 2020). Further research into effects of fertilization, pesticides usage and irrigation during different seasons in the Netherlands is recommended, to understand their impact on soil salinity.

Higher salinity in the subsoil might be influenced by dilution and leaching of salts from the topsoil during large precipitation events. In seepage areas, capillary rise and seepage lead to higher salinities in the subsoil (P. G. B. de Louw, 2013). Conversely, infiltration areas show leaching of salts through macropores (P. G. B. de Louw, 2013; Patel et al., 2000). However, some salts may remain in the upper soil due to capillary rise through micropores, while leaching mainly occurs via macropores.

5.1.2 Saturation Level Dependency

The results show considerable variability in salinity between locations within parcels. A relationship is found between saturation level and salinity in seepage areas, with higher salinity observed at shallower depth, for locations with shallower saturation levels. The presence of gley, often found in seepage areas with higher salinity, might be an indicator for saline soil moisture as well. Gley indicates seepage of saline, iron-rich groundwater or fluctuating groundwater levels, raising the subsoil salinity. Groundwater fluctuations cause iron oxidation during dry periods and reduction during wet periods, resulting in the characteristic orange and grey colors respectively (Hewitt et al., 2021; van Enk, 2016).

Pietersbierum, situated in a seepage zone, shows higher salinity for the location with a deeper groundwater level. However, this location contained gley starting at 50 cm, while no gley was observed for the less saline location. Salt is expected to come up by fluctuating groundwater levels or seepage, while salts remain in the unsaturated zone during evaporation (P. G. B. de Louw, 2013). This probably explains the salinity difference in Pietersbierum, as gley is only found at the more saline location.

In various seepage areas in Swifterbant, the Vogelweg near Lelystad, Anna Paulowna, Sloodorp and the Papeweg near Kerkwerf, higher subsoil salinities were observed at shallower depth, coinciding with shallower saturation levels and often accompanied by gley. This suggests that seepage or capillary rise reaches shallower depths in areas with shallower saturation levels, leading to increased subsoil salinities compared to locations with deeper saturation levels and lower salinities. Further research is needed to explore the relationship between saturation levels and subsoil salinity on field-scale.

5.1.3 Drain Locations

Drains are used to prevent waterlogging and saturation, facilitating crop growth by removing excess water. However, drains affect saturation levels and salinity dynamics within a field. Drain locations provide insights into the spatial variability within a field (P. G. B. de Louw, Eeman, et al., 2013; Velstra et al., 2011), with seepage and capillary rise near drains increasing salinity, while drains discharge seepage and excess precipitation water. In between drains, shallow rainwater lenses develop above the saline groundwater (Maljaars et al., 2006; Velstra et al., 2011). The lack of data on drain locations, types and saturated zone salinity limits understanding of field-scale processes and the hypothesized relationship between salinity and saturated zones as explained in section 5.1.2. Future research should investigate the influence of drain locations on the variability of salinity within a field, and their impact on salinity in the unsaturated zone. Enhanced knowledge of drain locations and associated processes is crucial for understanding of processes, validating of models and improving modeling accuracy.

5.1.4 Ditch Dependence

Ditch measurements were conducted adjacent to parcels of soil sampling, but this was not feasible for some ditches due to limited ditch water or vegetation obstruction. Additionally, external data showed significant variability over time, while some locations lack recent data. This introduces uncertainty since ditch salinity is only relevant at the time of soil sampling, and can vary due to various factors such as influx from freshwater sources to flush saline water (P. G. B. de Louw, 2013), precipitation causing dilution of salts (P. G. B. de Louw, 2013; Delsman et al., 2014; Schipper et al., 2022), and droughts leading to higher concentrations due to saline seepage and evapotranspiration (P. G. B. de Louw, 2013; Schipper et al., 2022). Despite this, most ditch data did not correlate well with soil moisture salinity, and ditch salinities were only mentioned in the results when it helped in understanding soil salinity. In certain locations, such as Anna Paulowna, the Papeweg near Kerkwerf and Zeeuws-Vlaanderen, soil salinity seemed dependent on the distance from the ditch. Further research is recommended to explore whether this relates to ditch proximity, saturation levels or other influencing factors.

5.1.5 EC as Salinity Indicator

EC serves as a conductivity measure and salinity indicator, but its value and reliability is questioned due to dependence on soil type, temperature and ion composition (M. R. Carter & Gregorich, 2007; Friedman, 2005; Johnson et al., 2001; Klein & Santamarina, 2003). However, it is only a valid salinity indicator for EC values larger than 2 mS/cm, where chloride and sodium dominate. For smaller values, conductivity may be dominated by other anions, complicating salinity assessment (Miller, n.d.).

Despite its limitations, research suggests that EC is a reasonable salinity estimator (M. R. Carter & Gregorich, 2007). EC is widely used, particularly within the Deltares database, and is useful both in field and laboratory settings. However, chloride concentration is used as salinity indicator as well, posing challenges in conversion to EC, due to nonlinear relationships, ion composition dependence and temperature variations (P. G. B. de Louw et al., 2011; Maljaars et al., 2006; Stuyt et al., 2013). The relationship as proposed by P. G. B. de Louw et al. (2011) is used in this study due to its alignment with field measurements (see section 2), but it is only valid for EC values larger than 2 mS/cm (P. G. B. de Louw et al., 2011; P. G. B. de Louw, Vandenbohede, et al., 2013; Delsman et al., 2018).

5.2 Recommendations

5.2.1 Spatial and Temporal Variability

The soil sampling method could introduce uncertainty requiring further research. Sampling was limited to coastal areas where salinity issues were expected based on the salinity index (see section 3.2.4) and consultations with water boards and local landowners. However, this approach did not cover the entire coastal zone extensively, potentially overlooking areas being susceptible to salinization as well. Moreover, only one or two measurements were taken per parcel, raising questions about their representativeness given the high spatial variability of soil salinity as results and previous research show (Heselmans et al., 2017; Oude Essink et al., 2018). It is crucial to measure salinity even in areas where no salinization is expected, to understand the spatial variability along the entire coast.

Sampling was conducted during the autumn of 2023, but soil salinity shows dynamic seasonal fluctuations (P. G. B. de Louw, 2013). Precipitation events lead to rapid decrease in macropore salinity through leaching to groundwater, drains and ditches (Delsman et al., 2014), while evapotranspiration leaves salts in the soil pores, and capillary rise brings salts into the micropores (P. G. B. de Louw, 2013; Delsman et al., 2014; Oude Essink et al., 2018; Stofberg et al., 2017; Velstra et al., 2011). These seasonal variations, coupled with individual meteorological processes contribute to significant temporal variability in soil moisture salinity (P. G. B. de Louw, Eeman, et al., 2013; Stofberg et al., 2017).

Validating models requires comprehensive field data covering the entire coastal area at multiple moments in time, to capture seasonality adequately. Even though the current field measurements provide valuable insights into the root zone salinity, more representative data for model validation is recommended, emphasizing the need for additional field research.

5.2.2 Saturated Paste Method

The saturated paste method may introduce uncertainty due to factors affecting how easily salts may dissolve, such as the amount of distilled water added, saturation equilibrium time, mixing method and soil type (Wang et al., 2023). While existing research is mainly focused on uncertainty in converting EC values from other methods to the laboratory EC_{sw} as obtained from the saturated paste method, limited information is available regarding the uncertainty in the saturated paste method itself (Aboukila & Norton, 2017; Rhoades et al., 1989; Slavich & Petterson, 1993; Wang et al., 2023; Wittler et al., 2006). Although a consistent methodology is used across all soil samples, small outliers and fluctuations in depth are identified (GR-KLB-L1, GR-RTT-L1, FR-TRN-L1 and FL-LSE-L2 at 50 cm depth, ZL-KWV-L2 at 75 cm depth). Therefore, investigating uncertainty in the saturated paste method and potential contributing processes to outliers at this depth could enhance the reliability of this method.

5.2.3 Seepage-Infiltration Map

The yearly-averaged seepage-infiltration map does not capture seasonal variations in seepage and infiltration processes which might affect salinization in certain areas. During winter, infiltration might dominate due to increased precipitation, while seepage might dominate during dry periods in summer (de Ville et al., 2017; Jansen et al., 2007; Velstra et al., 2011). This introduces uncertainty, especially since soil salinity was measured at the end of summer under dry conditions. Additionally, the theoretical approximations of this model might overlook certain field processes. Also, the low resolution limits its ability to capture differences within a field, especially because of the large pixel-size of 250x250 meters. Therefore, it is suggested to look at seepage or infiltration areas of several pixels instead of individual pixels, to exclude small-scale deviations. However, this limits the capability to look into variations within a parcel. Enhancing the map with a higher resolution and summer- and winter averaged versions could provide better insights into seasonal dynamics and field-level salinity variations.

5.2.4 TEC-Probe Data

TEC-probe data provides valuable insights into the salinity of the shallow saturated zone, providing indicators for the depth of the fresh-saline interface and rainwater lens patterns. Previous research has investigated the accuracy of TEC-probe measurements and showed reliable agreements with other conductivity methods measuring the EC and ionic ratios using water and soil sampling methods and the Continuous Vertical Electrical Sounding (CVES) method (Barendregt et al., 2004; Jager et al., 2011; Schouwenberg & van Wirdum, 1997; Van Wirdum, 1991; Velstra et al., 2008). However, TEC-probe data is only available for a few parcels and for limited moments in time, while temporal variability in subsoil salinity is expected. The absence of TEC-probe data at the moment of soil sampling raises uncertainty, as field conditions may have changed over time, influenced by seasonal variations and responses to wet and dry periods in rainwater lenses (P. G. B. de Louw, Eeman, et al., 2013; P. G. B. de Louw et al., 2011; Schot et al., 2004; Velstra et al., 2011). Future research should investigate temporal variability of TEC-probe data in areas like the Netherlands, ideally at the moment of soil sampling for comparison. Increasing the spatial and temporal coverage of TEC-probe data could help in understanding of variability of the fresh-saline interface and could improve and validate models.

5.2.5 Bulk Density

Bulk density measurements were done as well, as soil physical properties were expected to affect leaching of soluble salts, and subsequently salinity (Roy & Chowdhury, 2020). However, significant uncertainty arose due to the disturbed soil samples being placed in sample rings, while field-density could not be obtained. Moreover, excess demineralized water was added to ensure sufficient water available for extraction using rhizons for the EC measurements, therefore the maximum water content and the porosity, as described in the adjusted saturated paste method (Oude Essink et al., 2018), could not be determined. Consequently, bulk density measurements were excluded from this study. Future research could explore alternative methods for determining the bulk density and other soil physical properties at various depths, thereby offering insights into soil properties and providing more knowledge in processes affecting the root zone salinity.

5.2.6 TRANSOL Simulations

The LHM simulations, and in particular TRANSOL simulations focusing on salt transport in the unsaturated and shallow saturated zone, show significant inconsistencies between model results and field observations. The model itself contains uncertainty in parameters and coupling of models, but there is also lack of validation with field measurements in the root zone, explaining discrepancy between the model and field results. This emphasizes the importance of validation data for model improvement.

TRANSOL is a sub-model of the LHM model, and receives seepage fluxes from MODFLOW, groundwater recharge from MetaSWAP and discharge of water via ditches from MOZART. These sub-models are schematizations of reality, based on numerical calculations of water balances for a cell size of 250x250 meters (Janssen et al., 2023). The pixel-based resolution of the model limits its ability to capture variations on field-scale due to both input parameter quality and computational constraints. This means that zooming in to specific locations leads to uncertainty. Certain cells might include multiple soil sampling locations due to the large cell size, and significant differences are found between individual cells, as highlighted in section 4.2.2 and 4.2.3 as well. Therefore, it is suggested to look into multiple pixels, by zooming in to a certain area and use a pixel-averaging method to reduce small-scale outliers, instead of focusing on individual pixels. Even though this approach may pose challenges in distinguishing between specific locations, it significantly enhances understanding of particular regions. Consequently, it leads to more accurate identification of salinization risk zones by correct model implementation and validation.

The results indicate that salt front depths and concentrations serve as reliable indicators for identifying salinization risk zones. However, accurately predicting salinity levels from TRANSOL simulations poses notable difficulties. Additionally, notable discrepancies exist between the TRANSOL simulations and field measurements at specific locations, lacking consistent patterns indicating accurately predicted salinization risk areas.

Additionally, the results show that concentrations in the root zone were underestimated in the model, as compared to field measurements and prior research (van Doorn & Velstra, 2021). Assumptions regarding flow depth and drain characteristics in the model contribute to this discrepancy and are insufficiently accounted for (P. G. B. de Louw, Eeman, et al., 2013; P. G. B. de Louw et al., 2011; van Doorn & Velstra, 2021). Furthermore, inaccuracies in boundary conditions may contribute to uncertainties, for example insufficient detailed spatial knowledge about groundwater salinity and irrigation with saline water, which is insufficiently accounted for (Delsman & America, 2022; van Doorn & Velstra, 2021). Moreover, clay cracks are not incorporated in the model, which can locally alter the root zone salinity significantly (Delsman et al., 2022). This emphasizes the need for model validation with accurate field data with high spatial coverage.

Furthermore, while the model spans from 2010 to 2019, this study used averaged values to compare simulations of various locations, overlooking seasonality. Future research should focus on specific periods when salinization is a concern and consider effects of individual meteorological events on model results as well. Therefore, acquiring more temporal field data and accounting for seasonality is crucial for model validation.

6 Conclusion

In conclusion, this research investigates salinization in the soil moisture of Dutch coastal areas, addressing the necessity for field measurements in order to validate the existing TRANSOL model within LHM. The aim was to investigate to what extent salinization is found in the root zone in Dutch coastal areas, focusing both on soil sample measurements and comparing these results with TRANSOL model output. The research showed presence of saline soil moisture along almost the entire Dutch coast, characterized by higher values in the topsoil, followed by a small decline and subsequently a, for some locations major, increase in salinity with depth. Notably, significant spatial variability was observed, both on field-scale and between different types of polders.

Clear patterns were found in sub-recent transgression areas in Groningen, Friesland and the South west delta area, which contain both seepage and infiltration areas. Seepage areas showed clear increasing salinity with depth sometimes even up to strongly saline salinities, while infiltration areas showed lower and less variable salinities, mainly being non-saline to slightly saline. Localized high concentrations were found in deep polders in North Holland, South Holland and Flevoland. These deep polders mainly consist of seepage areas, with localized preferential saline seepage via boils leading to locally high concentrations in soil moisture.

In addition to soil moisture measurements, ditch salinities were expected to be a potential indicator for salinity in the root zone. However, correlation between soil moisture and ditch salinities were not consistent across the whole coastal area. For most of the locations, the ditch salinities did not match the soil moisture salinities, except for some locations in the deep polders near Zuidermeer and Boskoop, and locations on Goeree-Overflakkee in a sub-recent transgression area. This suggests that there is no reliable relationship between soil moisture and ditch salinities. However, this also indicates that it is important to consider multiple factors for understanding the variability of soil moisture salinity.

Comparison with TRANSOL model simulations demonstrated agreement in some areas, but also discrepancies between soil moisture measurements and model results are found. The salinization index from the LHM model is a good indicator of risk-zones for salinization, but not all locations are identified correctly. The modelled salt fronts from TRANSOL were a quite good indicator, where in general high concentrations with shallow salt fronts matched the high concentrations in the root zone, and either low concentrations or deep salt fronts matched the low concentrations in the root zone generally. However, the model inaccurately simulated absence of salt in the root zone for most of the coastal area, contradicting the variability in saline soil moisture in field measurements.

The observed high spatial variability in soil moisture salinity and discrepancy with the model results emphasizes the need for more research to understand both the temporal and spatial patterns. Especially additional field research with larger temporal and spatial coverage is recommended for accurate validation and improvement of the model, to obtain more accurate model predictions for soil moisture salinity in the future. However, this study not only contributes to advancing knowledge in soil moisture salinization dynamics, but also emphasizes the need for more research to improve models and investigate effective soil management practices in coastal regions to minimize salinization.

References

- Aboukila, E. F., & Norton, J. B. (2017). Estimation of Saturated Soil Paste Salinity From Soil-Water Extracts. *Soil Science*, 182(3), 107–113. <https://doi.org/10.1097/SS.000000000000197>
- Abrol, I. P., Yadav, J. S. P., & Massoud, F. I. (1988). *Salt-affected soils and their management* (Vol. 39). Food & Agriculture Org.
- America, I., Kaandorp, V., Drontmann, P., van Veelen, P., & van Berkum, J. (2023). *Verzilting bij zeespiegelstijging - Achtergrond document bij doorsnedes verzilting zeespiegelstijging – waterkerend landschap Ouwerkerk*.
- Barendregt, A., Beltman, B., Schouwenberg, E., & van Wirdum, G. (2004). *Effectgerichte maatregelen tegen verdroging, verzuring en stikstofdepositie op trilvenen (Noord-Holland, Utrecht en Noordwest-Overijssel)*. Expertisecentrum LNV.
- Blanco, F. F., & Folegatti, M. V. (2002). Salt accumulation and distribution in a greenhouse soil as affected by salinity of irrigation water and leaching management. *Revista Brasileira de Engenharia Agrícola e Ambiental*, 6(3), 414–419. <https://doi.org/10.1590/S1415-43662002000300006>
- Boer, H. C., & Radersma, S. (2011). *Verzilting in Nederland: oorzaken en perspectieven*.
- Bonte, M., & Biesheuvel, A. (2006). The application of the SEAWAT variable density code for the Lake Wieringen project, the Netherlands. *Proceedings of the 1st SWIM-SWICA Joint Saltwater Intrusion Conference, Cagliari-Chia Laguna, Italy*, 24–29.
- BRO Bodemkaart (SGM) WMS. (2023, July 31). PDOK. <https://www.pdok.nl/ogc-webservices/-/article/bro-bodemkaart-sgm->
- BRO Geomorfologische Kaart (GMM) WMS. (2023, August 2). PDOK. <https://www.pdok.nl/introductie/-/article/bro-geomorfologische-kaart-gmm->
- Carter, D. L. (1975). *Problems of Salinity in Agriculture* (pp. 25–35). https://doi.org/10.1007/978-3-642-80929-3_3
- Carter, M. R., & Gregorich, E. G. (2007). *Soil sampling and methods of analysis*. CRC press.
- Chen, W., Hou, Z., Wu, L., Liang, Y., & Wei, C. (2010). Evaluating salinity distribution in soil irrigated with saline water in arid regions of northwest China. *Agricultural Water Management*, 97(12), 2001–2008. <https://doi.org/10.1016/j.agwat.2010.03.008>
- Chloridekaart - Wetterskip Fryslân. (2014, June 14). Wetterskip Fryslân. <https://www.wetterskipfryslan.nl/kaarten/chloride-kaart>
- Condon, L. E., Atchley, A. L., & Maxwell, R. M. (2020). Evapotranspiration depletes groundwater under warming over the contiguous United States. *Nature Communications*, 11(1), 873.
- CORINE Land Cover - CLC 2018. (2019). <https://land.copernicus.eu/pan-european/corine-land-cover/clc2018?tab=mapview>
- Costall, A. R., Harris, B. D., Teo, B., Schaa, R., Wagner, F. M., & Pigois, J. P. (2020). Groundwater Throughflow and Seawater Intrusion in High Quality Coastal Aquifers. *Scientific Reports*, 10(1), 9866. <https://doi.org/10.1038/s41598-020-66516-6>

- Dagwaarden van weerstations (25-08-2023 to 11-10-2023) - de Bilt.* (n.d.). Koninklijk Nederlands Meteorologisch Instituut. Retrieved February 6, 2024, from <https://daggegevens.knmi.nl/>
- Dajic, Z. (2006). *Physiology and molecular biology of stress tolerance in plants: Salt stress*. Springer Netherlands.
- Data Feed - Digital Terrain Model (DTM) 0,5m.* (2023, April 12). PDOK. https://service.pdok.nl/rws/ahn/atom/dtm_05m.xml
- Data from internal database Deltares.* (n.d.). Deltares.
- Data from project - "Samenwerken voor Zoetwater: innovatieve drainage demonstreren, monitoren en evalueren" 2022-2024.* (n.d.). Deltares.
- Data from project - "Toekomstperspectief Polder Terschelling" 2021-2026.* (n.d.). Deltares.
- Data from project - "Zoetwaterboeren" 2022 - 2025.* (n.d.). Deltares.
- de Louw, P. G. B. (2013). *Saline seepage in deltaic areas: Preferential groundwater discharge through boils and interactions between thin rainwater lenses and upward saline seepage.*
- de Louw, P. G. B., & Bootsma, H. (2020). *Nulmeting grondwater Hedwigepolder.*
- de Louw, P. G. B., Eeman, S., Oude Essink, G. H. P., Vermue, E., & Post, V. E. A. (2013). Rainwater lens dynamics and mixing between infiltrating rainwater and upward saline groundwater seepage beneath a tile-drained agricultural field. *Journal of Hydrology*, 501, 133–145. <https://doi.org/10.1016/j.jhydrol.2013.07.026>
- de Louw, P. G. B., Eeman, S., Siemon, B., Voortman, B. R., Gunnink, J., van Baaren, E. S., & Oude Essink, G. H. P. (2011). Shallow rainwater lenses in deltaic areas with saline seepage. *Hydrology and Earth System Sciences*, 15(12), 3659–3678. <https://doi.org/10.5194/hess-15-3659-2011>
- de Louw, P. G. B., Vandenbohede, A., Werner, A. D., & Oude Essink, G. H. P. (2013). Natural saltwater upconing by preferential groundwater discharge through boils. *Journal of Hydrology*, 490, 74–87. <https://doi.org/10.1016/j.jhydrol.2013.03.025>
- de Ville, N., Le, H. M., Schmidt, L., & Verbanck, M. A. (2017). Data-mining analysis of in-sewer infiltration patterns: seasonal characteristics of clear water seepage into Brussels main sewers. *Urban Water Journal*, 14(10), 1090–1096. <https://doi.org/10.1080/1573062X.2017.1363252>
- de Vries, A., & Veraart, J. A. (2009). Fresh and salt water in the delta. In *Climate Research Netherlands-Research Highlights* (pp. 46–49).
- Delsman, J. R. (2015). *Saline groundwater-Surface water interaction in coastal lowlands* (Vol. 15). IOS Press.
- Delsman, J. R., & America, I. (2022). *Zoutmodellering in het LHM - Een overzicht van processen en beoordeling van de toepasbaarheid van zoutmodellering voor landelijke beleidsanalyse zoetwater.*
- Delsman, J. R., America, I., & Mulder, T. (2022). *Grondwaterverziltting en watervraag bij een stijgende zeespiegel.*

- Delsman, J. R., Groen, M. M. A., Groen, J., & Stuyfzand, P. J. (2014). Investigating summer flow paths in a Dutch agricultural field using high frequency direct measurements. *Journal of Hydrology*, *519*, 3069–3085.
- Delsman, J. R., van Baaren, E. S., Siemon, B., Dabekaussen, W., Karaoulis, M. C., Pauw, P. S., Vermaas, T., Bootsma, H., de Louw, P. G. B., Gunnink, J. L., Dubelaar, C. W., Menkovic, A., Steuer, A., Meyer, U., Revil, A., & Oude Essink, G. H. P. (2018). Large-scale, probabilistic salinity mapping using airborne electromagnetics for groundwater management in Zeeland, the Netherlands. *Environmental Research Letters*, *13*(8), 084011. <https://doi.org/10.1088/1748-9326/aad19e>
- Deltares Nitrate App.* (n.d.). Deltares. Retrieved December 18, 2023, from <https://nitrate-app.deltares.nl/index>
- Donkers, H., & Köbber, B. J. (2018, December 1). Zoet water in tijden van droogte. *Geografie November/December 2018*.
- EC metingen - Provincie Zeeland.* (n.d.). Provincie Zeeland. Retrieved December 18, 2023, from <https://kaarten.zeeland.nl/map/ec>
- Eeman, S., Leijnse, A., Raats, P. A. C., & van der Zee, S. E. A. T. M. (2011). Analysis of the thickness of a fresh water lens and of the transition zone between this lens and upwelling saline water. *Advances in Water Resources*, *34*(2), 291–302. <https://doi.org/10.1016/j.advwatres.2010.12.001>
- Ernst, L. F. (1969). Groundwater flow in the Netherlands Delta area and its influence on the salt balance of the future Lake Zeeland. *Journal of Hydrology*, *8*(2), 137–172. [https://doi.org/10.1016/0022-1694\(69\)90119-X](https://doi.org/10.1016/0022-1694(69)90119-X)
- Fokker, Peter. A., van Leijen, Freek. J., Orlic, B., van der Marel, H., & Hanssen, Ramon. F. (2018). Subsidence in the Dutch Wadden Sea. *Netherlands Journal of Geosciences*, *97*(3), 129–181. <https://doi.org/10.1017/njg.2018.9>
- FRESHM Zeeland grensvlakken.* (2017, January 5). Provincie Zeeland & Waterschap Scheldestromen. <https://dataportaal.zeeland.nl/dataportaal/srv/dut/catalog.search?node=srv#/metadata/8bdd4aff-5349-4ae5-a9f7-43276ee820af?tab=general>
- Friedman, S. P. (2005). Soil properties influencing apparent electrical conductivity: a review. *Computers and Electronics in Agriculture*, *46*(1–3), 45–70. <https://doi.org/10.1016/j.compag.2004.11.001>
- Goes, B. J. M., Oude Essink, G. H. P., Vernes, R. W., & Sergi, F. (2009). Estimating the depth of fresh and brackish groundwater in a predominantly saline region using geophysical and hydrological methods, Zeeland, the Netherlands. *Near Surface Geophysics*, *7*(5–6), 401–412. <https://doi.org/10.3997/1873-0604.2009048>
- Heselmans, G., de Louw, P., Kempenaar, C., Ahlrichs, E., Terpstra, I., Delsman, J. R., Ball, S., van Kempen, C., van Baaren, E., & van Wesemael, J.-P. (2017). *Zouttolerantie aardappel binnen Regionaal bod Proeftuin Zoet Water*.
- Hewitt, A. E., Balks, M. R., Lowe, D. J., Hewitt, A. E., Balks, M. R., & Lowe, D. J. (2021). Gley Soils. *The Soils of Aotearoa New Zealand*, 73–85.
- Hilarides, A. (2019). *Dealing with salinization in “Fryslan”, an elaboration of costs and benefits of applying “SeepCat.” technology*. <http://essay.utwente.nl/80380/>

- Hoeksema, R. J. (2007). Three stages in the history of land reclamation in the Netherlands. *Irrigation and Drainage*, 56(S1), S113–S126. <https://doi.org/10.1002/ird.340>
- Jacobs, P. (2007). Zout vanuit zee: Verzilting van de rijkswateren in Midden-West Nederland nu en in de toekomst. In P. de Louw (Ed.), *Verzilting in Nederland* (pp. 71–83). Nederlandse Hydrologische Vereniging (NHV).
- Jager, T. D., van der Veen, K., & Bijkerk, W. (2011). *Monitoring plaggen en vrijstellen drijftillen in De Wieden*.
- Jansen, P. C., Querner, E. P., & Kwakernaak, C. (2007). *Effecten van waterpeilstrategieën in veenweidegebieden: een scenariostudie in het gebied rond Zegveld*. Alterra.
- Janssen, G., van Walsum, P., America, I., Pouwels, J., Hunink, J., Vermeulen, P., Meshgi, A., Prinsen, G., Mulder, N., Visser, M., & Kroon, T. (2020). *Veranderingsrapportage LHM 4.1 - Beheer en onderhoud van de landelijke toepassing van het NHI*.
- Janssen, G., van Walsum, P., Vermeulen, P., Meeusen, R., Pouwels, J., Prinsen, G., America, I., Mes, E., Delsman, J. R., Kok, H., & Kroon, T. (2023). *Veranderingsrapportage LHM 4.3 - Actualisatie van het landelijk hydrologisch model in 2022 en 2023*.
- Johnson, C. K., Doran, J. W., Duke, H. R., Wienhold, B. J., Eskridge, K. M., & Shanahan, J. F. (2001). Field-Scale Electrical Conductivity Mapping for Delineating Soil Condition. *Soil Science Society of America Journal*, 65(6), 1829–1837. <https://doi.org/10.2136/sssaj2001.1829>
- Jurinak, J. J., & Wagenet, R. J. (1981). Fertilization and salinity. *Salinity in Irrigation and Water Resources*, 103–119.
- Klein, K. A., & Santamarina, J. C. (2003). Electrical conductivity in soils: Underlying phenomena. *Journal of Environmental & Engineering Geophysics*, 8(4), 263–273.
- KNMI. (2014). *KNMI Klimaatscenario's*.
- Kok, A., Auken, E., Groen, M., Ribeiro, J., & Schaars, F. (2010). Using Ground based Geophysics and Airborne Transient Electromagnetic Measurements (SkyTEM) to map Salinity Distribution and Calibrate a Groundwater Model for the Island of Terschelling–The Netherlands 21st SWIM conference. *21st Salt Water Intrusion Meeting, Azores, Portugal*.
- Kroes, J. G., & Rijtema, P. E. (1996). *TRANSOL, a dynamic simulation model for transport and transformation of solutes in soils*. DLO Winand Staring Centre.
- Kroes, J. G., & Supit, I. (2011). Impact analysis of drought, water excess and salinity on grass production in The Netherlands using historical and future climate data. *Agriculture, Ecosystems & Environment*, 144(1), 370–381. <https://doi.org/10.1016/j.agee.2011.09.008>
- Maljaars, P. S., Wils, R. A., de Louw, P. G. B., Oude Essink, G. H. P., & van Wirdum, G. (2006). *TNO-rapport - Regenwaterlenzen in zoute kwelsystemen*. www.tno.nl
- Meetpunten Chloride - Waterschap Hollandse Delta*. (2019, January 30). Waterschap Hollandse Delta. <https://hub.arcgis.com/datasets/WSHD::wshd-meetpunten-chloride/about>
- Miller, R. O. (n.d.). *Soil testing: saturated paste interpretation*.
- Minnema, I. B., Kuijper, M. J. M., Essink, G. H. P. O., & Maas, C. (2004). Bepaling toekomstige verzilting van het grondwater in Zuid-Holland. *TNO-Rapport NITG*, 4–189.

- Möller, K., & Schultheiß, U. (2015). Chemical characterization of commercial organic fertilizers. *Archives of Agronomy and Soil Science*, 61(7), 989–1012. <https://doi.org/10.1080/03650340.2014.978763>
- Nachshon, U. (2018). Cropland Soil Salinization and Associated Hydrology: Trends, Processes and Examples. *Water*, 10(8), 1030. <https://doi.org/10.3390/w10081030>
- Nishida, K., & Shiozawa, S. (2010). Modeling and Experimental Determination of Salt Accumulation Induced by Root Water Uptake. *Soil Science Society of America Journal*, 74(3), 774–786. <https://doi.org/10.2136/sssaj2008.0425>
- Oude Essink, G. H. P. (2007). Regionale modellering zoet-zout grondwater in het Nederlandse kustgebied. In P. de Louw (Ed.), *Verzilting in Nederland* (pp. 41–53). Nederlandse Hydrologische Vereniging (NHV).
- Oude Essink, G. H. P., Klepper, C., de Louw, P. G. B., & van Baaren, E. S. (2008). Zoet en zout Grondwater in de Provincie Flevoland. *Stromingen*, 14(3).
- Oude Essink, G. H. P., Pauw, P. S., van Baaren, E. S., Zuurbier, K. G., Louw, P. G. B. de, Veraart, J. A., MacAteer, E., van der Schoot, M., Groot, N., & Cappon, H. (2018). *GO-FRESH: valorisatie kansrijke oplossingen voor een robuuste zoetwatervoorziening: rendabel en duurzaam watergebruik in een zilte omgeving*. Utrecht: GO-FRESH.
- Oude Essink, G. H. P., Post, V. E. A., Kuijper, M. J. M., & Minnema, B. (2004). *Land subsidence and sea level rise threaten the coastal aquifer of Zuid-Holland, the Netherlands*.
- Patel, R. M., Prasher, S. O., & Bonnell, R. B. (2000). Effects of watertable depth, irrigation water salinity, and fertilizer application on root zone salt buildup. *Canadian Agricultural Engineering*, 42(3), 111–116.
- Post, V. E. A., Van der Plicht, H., & Meijer, H. A. J. (2003). The origin of brackish and saline groundwater in the coastal area of the Netherlands. *Netherlands Journal of Geosciences*, 82(2), 133–147.
- Provin, T., & Pitt, J. L. (2001). Managing soil salinity. *Texas FARMER Collection*.
- Raats, P. A. C. (2015). Salinity management in the coastal region of the Netherlands: A historical perspective. *Agricultural Water Management*, 157, 12–30. <https://doi.org/10.1016/j.agwat.2014.08.022>
- Rengasamy, P. (2006). World salinization with emphasis on Australia. *Journal of Experimental Botany*, 57(5), 1017–1023. <https://doi.org/10.1093/jxb/erj108>
- Rhoades, J. D., Manteghi, N. A., Shouse, P. J., & Alves, W. J. (1989). Estimating Soil Salinity from Saturated Soil-Paste Electrical Conductivity. *Soil Science Society of America Journal*, 53(2), 428–433. <https://doi.org/10.2136/sssaj1989.03615995005300020019x>
- Ritchie, J. T. (1981). Water dynamics in the soil-plant-atmosphere system. *Plant and Soil*, 81–96.
- Ritzema, H. P., & Stuyt, L. C. P. M. (2015). Land drainage strategies to cope with climate change in the Netherlands. *Acta Agriculturae Scandinavica, Section B — Soil & Plant Science*, 65(sup1), 80–92. <https://doi.org/10.1080/09064710.2014.994557>
- Roy, S., & Chowdhury, N. (2020). Effects of leaching on the reclamation of saline soils as affected by different organic and inorganic amendments. *Journal of Environmental Science and Sustainable Development*, 3(2). <https://doi.org/10.7454/jessd.v3i2.1075>

- Schipper, P. N. M., Groenendijk, P., van Gerven, L. P. A., Lukacs, S., & Rozemeijer, J. (2022). *Monitoring en modellering in twee pilotgebieden voor gebiedsgerichte aanpak: onderdeel KIWK-project Nutriënten: welke landbouwmaatregelen snijden hout?* Stowa.
- Schot, P. P., Dekker, S. C., & Poot, A. (2004). The dynamic form of rainwater lenses in drained fens. *Journal of Hydrology*, 293(1–4), 74–84. <https://doi.org/10.1016/j.jhydrol.2004.01.009>
- Schouwenberg, E., & van Wirdum, G. (1997). *Effectgerichte maatregelen tegen verzuring in De Weerribben; monitoring van kraggenvennen in de periode 1991-1996*. IBN-DLO.
- Slavich, P., & Petterson, G. (1993). Estimating the electrical conductivity of saturated paste extracts from 1:5 soil, water suspensions and texture. *Soil Research*, 31(1), 73. <https://doi.org/10.1071/SR9930073>
- Stofberg, S. F., Essink, G. H. P. O., Pauw, P. S., de Louw, P. G. B., Leijnse, A., & van der Zee, S. E. A. T. M. (2017). Fresh Water Lens Persistence and Root Zone Salinization Hazard Under Temperate Climate. *Water Resources Management*, 31(2), 689–702. <https://doi.org/10.1007/s11269-016-1315-9>
- Stuurman, R., Essink, G. O., Broers, H. P., & van der Grift, B. (2006). *Monitoring zoutwaterintrusie naar aanleiding van de Kaderrichtlijn Water" verzilting door zoutwaterintrusie en chloridevervuiling"*. TNO Bouw en Ondergrond.
- Stuyfzand, P. J. (1995). The impact of land reclamation on groundwater quality and future drinking water supply in the netherlands. *Water Science and Technology*, 31(8). [https://doi.org/10.1016/0273-1223\(95\)00356-R](https://doi.org/10.1016/0273-1223(95)00356-R)
- Stuyfzand, P. J. (2007). Oorzaken van verzilting, hun herkenning en de risicofactoren voor de drinkwatervoorziening. In P. De Louw (Ed.), *Verzilting in Nederland* (pp. 1–26). Nederlandse Hydrologische Vereniging (NHV).
- Stuyt, L., Van Bakel, P. J. T., Delsman, J. R., Massop, H. T. L., Kselik, R. A. L., Paulissen, M., Essink, G. H. P. O., Hoogvliet, M., & Schipper, P. N. M. (2013). *Zoetwatervoorziening in het Hoogheemraadschap van Rijnland: onderzoek met hulp van € ureyopener 1.0*. Alterra.
- van Alphen, J., Haasnoot, M., & Diermanse, F. (2022). Uncertain Accelerated Sea-Level Rise, Potential Consequences, and Adaptive Strategies in The Netherlands. *Water*, 14(10), 1527. <https://doi.org/10.3390/w14101527>
- van den Brink, M., Huismans, Y., Blaas, M., & Zwolsman, G. (2019). Climate Change Induced Salinization of Drinking Water Inlets along a Tidal Branch of the Rhine River: Impact Assessment and an Adaptive Strategy for Water Resources Management. *Climate*, 7(4), 49. <https://doi.org/10.3390/cli7040049>
- van Doorn, A., & Velstra, J. (2021). *Validatie en toetsing LHM 4.1 - Deelrapport 4: Verzilting*.
- van Duinen, R., Filatova, T., Geurts, P., & van der Veen, A. (2015). Coping with drought risk: empirical analysis of farmers' drought adaptation in the south-west Netherlands. *Regional Environmental Change*, 15(6), 1081–1093. <https://doi.org/10.1007/s10113-014-0692-y>
- van Enk, R. (2016). Iedere generatie zijn eigen oerbank? Gebruik en gedrag van ijzer in de Nederlandse ondergrond. *Grondboor & Hamer*, 70(2), 48–54.
- van Walsum, P. E. V. (2023). *SIMGRO V8.1.2.2, Input and output reference manual - Metaswap manual*.

- Van Wirdum, G. (1991). *Vegetation and hydrology of floating rich-fens*. Geert van Wirdum.
- Velstra, J., Groen, J., & De Jong, K. (2011). Observations of salinity patterns in shallow groundwater and drainage water from agricultural land in the Northern part of the Netherlands. *Irrigation and Drainage*, 60, 51–58. <https://doi.org/10.1002/ird.675>
- Velstra, J., van Diepen, R., Hoogmoed, M., Groen, K., & Groen, M. (2008). *Aanvullend veldonderzoek Groot Mijdrecht Noord*.
- Velstra, J., Van Staveren, G., Oosterwijk, J., Van der Werff, R., Tolk, L., & Groen, J. (2013). Verziltingsstudie Hoogheemraadschap Hollands Noorderkwartier. *Eindrapport. Acacia Water*, 175.
- Veraart, J. A., & Klostermann, J. E. M. (2013). *De rol van onzekerheid in kennis in de MER procedure van het Volkerak-Zoommeer. Achtergrond document*. Alterra.
- Verburg, R. W., Bezlepina, I., Chen, L., & Bogaardt, M. J. (2011). *Adaptation to climate change on arable farms in the Dutch province of Flevoland. An inventory for the AgriAdapt project*. LEI, part of Wageningen UR.
- Vogelzang, T., Smit, B., Kuiper, P. P., & Gillet, C. (2019). *Grond in beweging: ontwikkelingen in het grondgebruik in de provincie Flevoland in de periode tot 2025 en 2040* (Issues 2019–003). Wageningen Economic Research.
- Wang, Q., Li, X., Zhao, C., Pei, L., & Wan, S. (2023). Evaluation analysis of the saturated paste method for determining typical coastal saline soil salinity. *Soil and Tillage Research*, 225, 105549. <https://doi.org/10.1016/j.still.2022.105549>
- Wittler, J. M., Cardon, G. E., Gates, T. K., Cooper, C. A., & Sutherland, P. L. (2006). Calibration of Electromagnetic Induction for Regional Assessment of Soil Water Salinity in an Irrigated Valley. *Journal of Irrigation and Drainage Engineering*, 132(5), 436–444. [https://doi.org/10.1061/\(ASCE\)0733-9437\(2006\)132:5\(436\)](https://doi.org/10.1061/(ASCE)0733-9437(2006)132:5(436))
- Yusefi, A., Farrokhian Firouzi, A., & Aminzadeh, M. (2020). The effects of shallow saline groundwater on evaporation, soil moisture, and temperature distribution in the presence of straw mulch. *Hydrology Research*, 51(4), 720–738. <https://doi.org/10.2166/nh.2020.010>
- Zhang, X., Ye, P., Wu, Y., & Zhai, E. (2022). Experimental study on simultaneous heat-water-salt migration of bare soil subjected to evaporation. *Journal of Hydrology*, 609, 127710. <https://doi.org/10.1016/j.jhydrol.2022.127710>
- Zoutgehalte - Waterschap Zuiderzeeland. (2022, January 9). Waterschap Zuiderzeeland. <https://geo-zzl.opendata.arcgis.com/maps/a8ff455c661444d58a4c4dc1221038da/explore?location=52.544130%2C5.677300%2C10.57>

Appendices

Appendix A

Table 4: Soil sample measurements (each 25 cm): EC values (mS/cm) for the coastal zone of the Netherlands including coordinates.

Code	Latitude	Longitude	EC _{sw} 25 cm depth	EC _{sw} 50 cm depth	EC _{sw} 75 cm depth	EC _{sw} 100 cm depth	EC _{sw} 125 cm depth	EC _{sw} 150 cm depth	EC _{sw} 175 cm depth	EC _{sw} 200 cm depth	Unit
FL-AED-L1	52.53133	5.676592	3.61	2.36	2.42	7.00	4.85	6.12			mS/cm
FL-LSE-L1	52.4422	5.485937	1.77	1.66	4.77	5.61	5.24				mS/cm
FL-LSE-L2	52.43955	5.490525	2.76	4.86	3.58	4.96	5.87				mS/cm
FL-LSV-L1	52.44469	5.539598	3.56	2.66	2.11	3.95	2.89				mS/cm
FL-LSV-L2	52.44145	5.540497	3.70	1.77	2.80	5.89	4.45				mS/cm
FL-MRK-L1	52.71492	5.902739	1.24	0.90	1.58	1.68	2.93	2.36			mS/cm
FL-MRK-L2	52.71137	5.896292	2.43	2.26	2.04	1.86	3.11	2.86			mS/cm
FL-SWB-L1	52.53464	5.592365	3.47	1.83	1.63	7.15					mS/cm
FL-SWB-L2	52.53455	5.591068	3.22	2.43	2.18	5.02	6.40	9.63			mS/cm
FR-HLK-L1	53.37527	5.914727	0.99	1.30	1.85	1.88	1.88	1.71			mS/cm
FR-HLW-L1	53.37753	5.884991	2.67	1.88	1.24	2.91	7.78	7.08			mS/cm
FR-PBR-L1	53.20915	5.443903	1.79	1.88	1.67	1.51	3.10	1.40			mS/cm
FR-PBR-L2	53.21059	5.445437	1.48	2.36	2.52	6.89	15.62	18.17			mS/cm
FR-PNG-L1	53.11909	5.410093	1.53	0.88	1.49	1.56	0.88	1.67			mS/cm
FR-PNG-L2	53.11963	5.409264	1.17	1.50	1.86	1.76	1.66	1.57			mS/cm
FR-TRN-L1	53.39143	5.967121	1.50	5.32	1.08	1.06	1.25	1.33			mS/cm
FR-TRN-L2	53.39179	5.968496	1.46	1.46	1.52	1.29	1.17	1.07			mS/cm
FR-TRS-L1	53.37913	5.30816	1.85	1.41	3.11	7.90	8.78	14.46	15.13	15.05	mS/cm
FR-TRS-L2	53.38108	5.31549	1.42	0.96	1.64	2.18	2.51	3.82	5.34	4.98	mS/cm
FR-TRS-L3	53.38211	5.33442	2.61	1.52	1.24	1.85	2.28	3.10	2.49	1.51	mS/cm
FR-TRT-L1	53.38183	5.936802	1.30	1.11	1.05	1.45	1.48	1.59			mS/cm
GR-KLB-L1	53.40619	6.372398	3.17	5.14	2.60	2.60					mS/cm
GR-RTT-L1	53.38542	6.656187	2.49	11.23	5.14	9.96	23.36	25.65			mS/cm

Code	Latitude	Longitude	EC _{sw} 25 cm depth	EC _{sw} 50 cm depth	EC _{sw} 75 cm depth	EC _{sw} 100 cm depth	EC _{sw} 125 cm depth	EC _{sw} 150 cm depth	EC _{sw} 175 cm depth	EC _{sw} 200 cm depth	Unit
GR-RTT-L2	53.38536	6.651851	2.46	1.51	1.19	0.79	1.10	2.40			mS/cm
GR-UHM-L1	53.4602	6.754194	3.70	1.57	0.85	1.08	3.09	2.73			mS/cm
GR-UHM-L2	53.45941	6.753577	1.80	1.13	1.52	1.21	3.01	4.33			mS/cm
NH-APL-L1	52.86208	4.895725	2.66	1.58	3.62	5.67	5.66	5.79			mS/cm
NH-APL-L2	52.86167	4.897581	3.22	1.41	2.20	6.12	8.13				mS/cm
NH-APL-L3	52.86104	4.900797	2.04	1.56	1.35	3.82					mS/cm
NH-SLD-L1	52.88492	4.96184	5.79	2.40	6.18	9.51		8.07			mS/cm
NH-SLD-L2	52.8848	4.963295	4.52	5.28	8.43	14.68					mS/cm
NH-ZSC-L1	52.59941	4.782574	1.66	1.32	1.13	1.08	1.10	4.39			mS/cm
NH-ZSC-L2	52.58638	4.775769	7.11	8.65	7.67	20.64	23.54	25.91			mS/cm
ZH-BSK-L1	52.06986	4.697096	2.98	5.02	4.27	2.71					mS/cm
ZH-BSK-L2	52.0685	4.69665	4.93	6.01	4.53	2.38					mS/cm
ZH-BSK-L3	52.08071	4.691211	2.13	2.12	1.72	2.12					mS/cm
ZH-BSK-L4	52.08055	4.692079	2.67	2.22		2.09					mS/cm
ZH-GFB-L1	51.80117	3.877327	1.00	1.48	1.43	0.44	1.76	2.93			mS/cm
ZH-GFB-L2	51.80236	3.87956	3.65	1.59	0.60	0.66	1.13	4.06			mS/cm
ZH-GFG-L1	51.81405	3.872341	3.17	1.95	1.30	1.05	1.40	1.86			mS/cm
ZH-GFG-L2	51.81328	3.873253	3.26	1.23	1.16	0.68	1.00	1.52			mS/cm
ZH-GFW-L1	51.79757	3.888797	1.87	1.94	0.69	1.01	2.84	1.19			mS/cm
ZH-GFW-L2	51.7965	3.886491	0.39	0.44	1.19	0.65	0.84	1.04			mS/cm
ZL-AAG-L1	51.54962	3.501743	1.92	1.50	1.12	1.28	1.02	1.76			mS/cm
ZL-AAG-L2	51.54959	3.50268	2.32	0.67	0.97	1.06	1.24	2.76			mS/cm
ZL-HKK-L1	51.42742	3.890924	1.22	1.09	0.73	1.57	2.02	2.32			mS/cm
ZL-HKK-L2	51.42732	3.89221	1.61	1.52	1.18	0.98	0.83	0.94			mS/cm
ZL-KMP-L1	51.56347	3.685363	1.32	1.47	1.06	0.74	0.61	1.42			mS/cm
ZL-KMP-L2	51.56288	3.684775	1.60	2.07	0.77	0.61	0.97	0.94			mS/cm
ZL-KWP-L1	51.69881	3.90104	1.73	0.79	1.91	1.54	3.24	9.36			mS/cm
ZL-KWP-L2	51.69894	3.901844	2.59	1.04	1.12	2.16	3.00	4.80			mS/cm

Code	Latitude	Longitude	EC _{sw} 25 cm depth	EC _{sw} 50 cm depth	EC _{sw} 75 cm depth	EC _{sw} 100 cm depth	EC _{sw} 125 cm depth	EC _{sw} 150 cm depth	EC _{sw} 175 cm depth	EC _{sw} 200 cm depth	Unit
ZL-KWP-L3	51.69921	3.902652	2.76	1.35	1.55	2.68	1.41	1.75			mS/cm
ZL-KWV-L1	51.68033	3.887335	1.63	1.35	1.36	1.45	6.47	5.50			mS/cm
ZL-KWV-L2	51.68077	3.888168	1.27	1.58	3.17	1.29	1.00				mS/cm
ZL-ZVL-L1	51.32915	4.207798	2.16	1.64	1.49	1.37	3.64	3.18	0.75	2.89	mS/cm
ZL-ZVL-L2	51.33086	4.208073	2.34	2.63	5.52	7.30	11.49	12.92	13.01	10.77	mS/cm
ZL-ZVL-L3	51.3313	4.208157	2.09	1.98	2.82	1.56	3.36	4.36	3.70	5.03	mS/cm

Table 5: Comments for the soil sample measurements (each 25 cm) for the coastal zone of the Netherlands.

Code	Comments	25 cm depth	50 cm depth	75 cm depth	100 cm depth	125 cm depth	150 cm depth
FL-AED-L1		Sandy clay	Clayey, gley around 45 cm		Clayey around 85 cm, around 110 cm sand with iron oxidation	Sand	Peaty clay
FL-LSE-L1	Corn and grass field, corn irrigated in beginning of 2023	Clay with shells	Clay and beginning gley	More gley and sandy at 80 cm	Grey sand, saturated at 110 cm	Clayey sand	Clayey sand
FL-LSE-L2	Not irrigated during 2022/2023	Clay, beginning gley around 40 cm	Clay	Gray clay	Clearer gley, saturated at 110 cm with sandy clay	Sandy clay	Sandy clay
FL-LSV-L1	Spinach irrigated in 2022, and three times in 2023. 50 meters form a dry ditch	Clay	Clay	Clay, around 80 cm sand with gley	Sand	Saturated around 120 cm, and grey sand	Grey sand
FL-LSV-L2	Mustard plants, samples on location without plants on side of field. Not irrigated in 2022-2023	Clay with shells	Gley around 50 cm	Sand around 90 cm, gley	Sand with gley, saturated around 110 cm	Yellow sand	Sand
FL-MRK-L1	Fruit trees	Clay	Light clay	Gley around 60 cm, saturated around 80 cm	Grey clay	Peat with clay around 130 cm	Peat

Code	Comments	25 cm depth	50 cm depth	75 cm depth	100 cm depth	125 cm depth	150 cm depth
FL-MRK-L2	Fruit trees, iron-richer compared to L1 as seen in netting above trees, ditch water more saline	Light clay	Gley around 55 cm	Saturated around 75 cm, clay and gley	Clay and gley	Peat	Peat
FL-SWB-L1	Onion	Light clay, gley around 50 cm	Clay, shells, clayey sand around 60 cm	Sandy around 90 cm, gley	Saturated around 1m	Sand	Sand
FL-SWB-L2	Onion	Clay	Sand around 60 cm	Sand	Gray sand around 90 cm	Peaty pieces between grey sand, saturated around 125 cm	Sand
FR-HLK-L1		Heavy clay	Heavy clay	Gley around 80 cm	Gley around 1m, with pieces of sand in clay	Heavy clay with gley	Heavy grey clay, saturated around 135 cm
FR-HLW-L1	Close to salt marsh dike	Clay with light pieces of sand	Sand with gley	Clay, gley with shells, at 80 cm heavy clay with gley	Heavy clay	Heavy clay with gley and shells, saturated around 120 cm	around 140 cm sand with gley and shells
FR-PBR-L1	Grass field, no gley	Light clay	Light clay	Sandy clay (zavel)	Sandy clay (zavel), saturated around 110 cm	Sandy clay (zavel)	Grey sandy clay (zavel)
FR-PBR-L2	Grass field	Light clay	Clay, gley	Sandy clay (zavel)/clayey	Gley, sandy clay (zavel)	Sand, gley, saturated around 125 cm	Sandy clay (zavel)
FR-PNG-L1	Lower elevation compared to L2, next to dug ditch to discharge excess water	Light clay	Sandy clay (zavel) around 40 cm, more clayey around 60 cm	Heavy clay, gley	Heavy clay, gley	Heavy clay, gley, saturated around 125 cm	Grey clay

Code	Comments	25 cm depth	50 cm depth	75 cm depth	100 cm depth	125 cm depth	150 cm depth
FR-PNG-L2	Old salt marsh	Clay	Clay, sandy clay (zavel) around 60 cm	clayey sand, minimal gley around 60 cm	Clayey, gley	Heavy clay, gley	Heavy clay, gley, almost saturated
FR-TRN-L1	Herbal grassland in between dikes	Clay	Heavy clay	Heavy clay with some sand patches and shells, gley around 85 cm	Gley, clay	Grey clay	Grey clay
FR-TRN-L2		Clay	Clay with sand patches, gley around 55 cm	Shells with sand and clay, gley	Heavy clay	Heavy clay, grey, saturated somewhere between 125 and 150 cm	Grey clay, saturated
FR-TRS-L1	ReesN - Landerum	Sand	Clay, gley	Clayey sand, gley	Saturated around 100 cm, grey sand	Grey sand	Sandy clay (zavel), deeper than 150 cm sand
FR-TRS-L2	HWBZ - Formerum	Sand	Clay, gley	Sand, saturated around 75 cm	Grey sandy clay (zavel)	Grey sand	Grey sand
FR-TRS-L3	GrasN - Lies	Sand	sand/sandy clay (zavel), gley	clay	Clay, saturated around 100 cm	Sand	Sand
FR-TRT-L1		Heavy clay	Gley around 50 cm, sandy layer with clay	Sand	clay	Clay, saturated around 125 cm	Clay
GR-KLB-L1	Empty field, due to thunder no deeper or more measurements	Heavy clay, gley around 20 cm, sand around 30 cm	Clayey sand around 50 cm	Clayey sand, shells around 75 cm	Clayey sand, saturated around 90 cm		
GR-RTT-L1		Clay, shells	Clay, gley, shells	Clay	Clay, saturated around 100 cm	Clay	Clay
GR-RTT-L2		Clay, gley around 30 cm	Clay, grey sand around 60 cm	Sand with gley around 90 cm	Sand	Bit gley and grey sandy clay	Grey sandy clay

Code	Comments	25 cm depth	50 cm depth	75 cm depth	100 cm depth	125 cm depth	150 cm depth
GR-UHM-L1	Fertilized the day before	Sandy clay, sandier around 30 cm, around 45 cm grey sand	Grey sand	Grey sand	Grey sand	Grey sand	Grey sand, saturated around 150 cm
GR-UHM-L2		Top clay, sand after 15 cm	Sand	Sand	Sand	Sand	Sand
NH-APL-L1		Dark clay/peat	Peat	Grey clay	Grey clay	Grey clay	Grey clay, saturated around 125-150 cm
NH-APL-L2		Sandy clay	(sandy) clay	Peat	Separation peat and grey clay	Grey clay, saturated around 125 cm	Grey clay
NH-APL-L3		Clay	Peat around 40 cm	Clay around 70 cm	Clay, saturated around 100 cm	Clay	Clay
NH-SLD-L1	Irrigated with 1.5 to 2 mS/cm water, beginning of year, 5 to 7 times grey part not measurable.	Heavy clay	Heavy clay, shells	Heavy clay	Heavy clay, becomes more grey sea-clay, around 110 cm a sandy layer and after that peat, saturated around 120 cm	Too wet	Too wet
NH-SLD-L2	No irrigation for years, 50 meters from ditch with irrigation tube	Heavy clay	Heavy clay, shells around 60 cm	Heavy clay	Heavy clay, saturated around 100 cm	Deeper than 100 cm peat with pieces of wood	Peat
NH-ZSC-L1	Biological mixed field	Clay	Clay	Sandy, beginning gley	Sand	Sand, saturated around 115 cm	Sand, becomes greyer
NH-ZSC-L2	Biological grass field	clay, grey clay around 25 cm	Sandy clay	Sand, beginning gley around 70 cm	Sand, gley, saturated around 110 cm	Sand, gley	Sand, gley

Code	Comments	25 cm depth	50 cm depth	75 cm depth	100 cm depth	125 cm depth	150 cm depth
ZH-BSK-L1	Grass field, seepage expected here	Peat	Peat	Saturated grey clay around 60 cm	Saturated grey clay	Too wet	Too wet
ZH-BSK-L2	Grass field, next to seepage puddle	Peat	Peat, saturated after 50 cm and grey clay	Grey clay	Too wet	Too wet	Too wet
ZH-BSK-L3	Next to higher grass and well-growing plants, most in seepage area according to farmer	Peat	Peat, around 70 cm clayey peat with saturation	Clayey peat	Peaty clay	Too wet	Too wet
ZH-BSK-L4		Peat	Saturated around 50 cm, start grey clay	Grey clay	Grey clay	Too wet	Too wet
ZH-GFB-L1	Just ploughed, difficult to measure depth due to thick clay blocks, potato field	Heavy clay	Glau around 45 cm with sandy clay, sand around 55 cm	sand, saturated around 75 cm	Sand	Grey sand	Grey sand
ZH-GFB-L2	Just ploughed, difficult to measure depth due to thick clay blocks, potato field	Heavy clay	Sand with gley around 45 cm	Sand, saturated around 80 cm	Sand	Grey clay	Grey clay
ZH-GFG-L1	Potato field	Dark sand, with organic matter	Dark sand, lighter around 55 cm	Sand with gley around 70 cm	Grey sand around 90 cm	Saturated around 115 cm, grey sand	Grey sand
ZH-GFG-L2	Potato field	Sandy clay	Sand	Light clay around 80 cm	Saturated around 85-100 cm	Sandy clay (zavel) around 110 cm	Sandy clay (zavel)

Code	Comments	25 cm depth	50 cm depth	75 cm depth	100 cm depth	125 cm depth	150 cm depth
ZH-GFW-L1	Side just sown, green vegetation	Clay, sand around 35 cm	Gley around 50 cm	Saturated around 80 cm with gley	Sand	Grey sand at 120 cm, dark clay (almost looking like peat) around 130 cm	Dark sand
ZH-GFW-L2	Green vegetation	Heavy clay	Clayey sand/ Sandy clay (zavel) around 60 cm with gley	Saturated around 80 cm, sand with gley	Sand with gley	Grey sand	Grey sand
ZL-AAG-L1	Beets	Heavy clay	Heavy clay	Clay with beginning gley	Heavy clay with gley	Heavy clay, peat around 130 cm, saturated around 130 cm	Peat
ZL-AAG-L2	Middle of beet field, around 75 m from ditch	Heavy clay	Heavy clay, gley around 60 cm	Heavy clay, gley	Sandy with gley	Sand, peat and saturated around 140 cm	peat
ZL-HKK-L1	Between peer trees, creek ridge	Clay, Sandy clay (zavel) around 30 cm	Clayey sand/ Sandy clay (zavel) around 60 cm, gley around 60 cm	Clayey sand	Sand, gley	Sand, saturated around 140 cm	Sand
ZL-HKK-L2	Between apple trees, creek ridge	Light clay	Light clay, gley around 70 cm	Light clay, gley	Heavy clay around 90-100 cm, sand with gley around 110 cm	Sand with gley, saturated around 140 cm	Sand
ZL-KMP-L1	Grass field	Heavy clay	Clay, sandier with gley around 60 cm	Sand	Sand	Sand, saturated around 120-130 cm	Sand
ZL-KMP-L2	Grass, grows better than at location 1,	Heavy clay	Sandy clay with a bit of gley around 50 cm, sand	Around 75 cm a bit of gley,	Gley and sandy clayey (zavel),	Sand	Sand

Code	Comments	25 cm depth	50 cm depth	75 cm depth	100 cm depth	125 cm depth	150 cm depth
	location estimated from google maps		without gley around 60 cm	sandier clayey (zavel)	saturated around 1 m with gley		
ZL-KWP-L1	DH2	Heavy clay	Gley around 25-50 cm	Sandy clay	Saturated around 115-120 cm, around 130 cm clay to sandy clay (zavel)	Sandy clay (zavel)	zavel Sandy clay (zavel)
ZL-KWP-L2	DH4, sugar beets	Clay	Clay, gley between 40-60 cm	Sandy clay (zavel) around 80 cm	Sandy clay (zavel), saturated around 110 cm	Sandy clay (zavel)	Sandy clay (zavel)
ZL-KWP-L3	DH3, bare soil	Heavy clay	Heavy clay	Gley, sandy clay (zavel) glei around 90 cm	Sandy clay	Sandy clay (zavel)/light clay	Sandy clay (zavel)/light clay, saturated around 150 cm
ZL-KWV-L1	DB2, potato field	Clay, gley around 40 cm	Clay	Clay	Peat around 110 cm	Peat, saturated around 120 cm, sand around 140 cm	Sand
ZL-KWV-L2	DB4, potato field, just dug	Heavy clay	Peat between 50-70 cm	Clay	Clay	Clay	clay
ZL-ZVL-L1	mp6	Sand, gley	Sand, saturated around 75 cm	Sand	Sand	Sand	Sand, also deeper measurements
ZL-ZVL-L2	mp5	Sand, gley	Sand, saturated around 75 cm	Sand	Sand	Sand	Sand, also deeper measurements
ZL-ZVL-L3	mp4	Sand	Sandy clay, gley	Sand, saturated around 100 cm	Sand	Sand	Sand, also deeper measurements

Table 6: Ditch measurements: EC values (mS/cm) for the coastal zone of the Netherlands.

Code	Latitude	Longitude	Comments	EC _w (mS/cm)
FL-AED-L1	52.53131	5.675879		0.578
FL-LSE-L1	52.44251	5.48646		0.433
FL-LSE-L2	52.4399	5.49097		0.355
FL-LSV-L1	52.44498	5.540147	Dry	-
FL-MRK-L2	52.70939	5.89634	L1 around 1 mS/cm (personal communication with landowner on 5 October 2023).	3.28
FL-SWB-L1	52.53461	5.592904		1.741
FR-HLK-L1	53.37489	5.915224	Dead-ending ditch	1.658
FR-HLW-L1	53.37792	5.884517	Close to salt marsh dike	1.535
FR-PBR-L1	53.20892	5.44454		12
FR-PBR-L2	53.20963	5.445461		10.55
FR-PNG-L1	53.11991	5.409779		3.14
FR-PNG-L1	53.11932	5.410661		8.85
FR-PNG-L3	53.11834	5.411418		4.87
FR-TRN-L1	53.39122	5.968136		1.678
FR-TRN-L2	53.39161	5.967855		1.309
FR-TRT-L1	53.3815	5.937538		1.721
GR-KLB-L1	53.40605	6.373225	Close to Waddenzee dike	12.47
GR-RTT-L2	53.38536	6.651883	Dry	-
GR-UHM-L1	53.46033	6.753538	Close to Waddenzee dike	11.25
GR-UHM-L2	53.45947	6.752706	Too shallow to measure	15.14
NH-APL-L1	52.86051	4.901014		3.68
NH-APL-L2	52.86059	4.901331		3.55
NH-SLD-L1	52.8849	4.962558		3.17
NH-SLD-L2	52.88534	4.962718	Ditch flushed with freshwater	1.88
NH-ZSC-L1	52.59826	4.785679		5.62
NH-ZSC-L2	52.58594	4.775505		17.39
ZH-BSK-L1	52.06982	4.697327		2.96

ZH-BSK-L2	52.06987	4.696896		2.6
ZH-BSK-L3	52.0808	4.691283		2.05
ZH-BSK-L4	52.08059	4.691177		2.35
ZH-GFB-L1	51.80091	3.876772		7.98
ZH-GFB-L2	51.80157	3.876989		8.31
ZH-GFB-L3	51.80091	3.877677		7.82
ZH-GFB-L4	51.80258	3.880061		8.21
ZH-GFG-L1	51.81435	3.871786	Oily seepage firm, close to dunes	0.982
ZH-GFG-L2	51.81297	3.873709		0.88
ZH-GFW-L1	51.79723	3.889105		0.483
ZH-GFW-L2	51.79615	3.886909		1.275
ZL-AAG-L1	51.54999	3.501358		3.73
ZL-KMP-L1	51.56374	3.685219	Oily seepage firm	1.61
ZL-KMP-L2	51.56298	3.684351	Oily seepage firm	1.51
ZL-KWV-L2	51.67995	3.886924	Too shallow to measure	-

Table 7: Ditch EC values (mS/cm) for the coastal zone of the Netherlands from external sources.

Close to location	Date	EC _w (mS/cm)	Comment	Measurement id or description and source
FL-LSE	24-08-2023	3.18	Day of samples: 13-09-2023	Larservaart, Meerkoetenweg (Zoutgehalte - Waterschap Zuiderzeeland, 2022)
	26-09-2023	2.96		
FL-LSV	05-09-2023	1.35	Day of samples: 13-09-2023	Larsertocht, aflatwerk Vleetweg, hoge kant (Zoutgehalte - Waterschap Zuiderzeeland, 2022)
	19-09-2023	1.21		
FL-MRK	05-10-2023	1.31	Day of soil samples	Blokzijlerdwarstocht (Zoutgehalte - Waterschap Zuiderzeeland, 2022)
FL-SWB	12-09-2023	4.52	Day of samples: 11-09-2023	Vuursteentocht, Wisentweg (Zoutgehalte - Waterschap Zuiderzeeland, 2022)
FR-HLW	14-09-2023	1.80	Day of samples: 12-09-2023	NOCL 232 (Chloridekaart - Wetterskip Fryslân, 2014)
	12-10-2023	1.92		
FR-PBR	08-09-2023	2.74	Day of samples: 05-10-2023	NOCL 205 (Chloridekaart - Wetterskip Fryslân, 2014)
	02-10-2023	3.49		
FR-TRN	14-09-2023	1.54	Day of samples: 05-10-2023	NOCL 233 (Chloridekaart - Wetterskip Fryslân, 2014)
	12-10-2023	1.30		
FR-TRS-L2	31-05-2023	2.17	Ditch	Prikstokmeting10 and Prikstokmeting11 (Data from Project - "Toekomstperspectief Polder Terschelling" 2021-2026. n.d.)
		3.2	Average TEC-probe, L2	
FR-TRS-L3	31-05-2023	3.14	Ditch	Prikstokmeting1 and Prikstokmeting6 (Data from Project - "Toekomstperspectief Polder Terschelling" 2021-2026. n.d.)
		4.5	Average TEC-probe, L3	
FR-TRT-L1	14-09-2023	1.48	Day of samples: 05-10-2023	NOCL 050 (Chloridekaart - Wetterskip Fryslân, 2014)
	12-10-2023	1.22		
	14-09-2023	1.64		NOCL 051 (Chloridekaart - Wetterskip Fryslân, 2014)
	12-10-2023	1.52		
ZL-AAG	28-09-2023	2.9	Day of samples: 15-09-2023	Roosjesweg (Deltares Nitrate App, n.d.)
ZL-HKK	19-09-2023	11.49	Day of samples: 15-09-2023	Waardweg (Deltares Nitrate App, n.d.)
ZL-KWP	19-10-2023	2.58	Day of samples: 14-09-2023	Parcel Papeweg Kerkwerve (EC Metingen - Provincie Zeeland, n.d.)
	15-11-2023	2.83		Sloot naast diepe drain Leonard (Deltares Nitrate App, n.d.)
	15-11-2023	7.13		Onderste drain Leonard (Deltares Nitrate App, n.d.)
ZL-ZVL	06-07-2022	11.4	Day of samples: 22-09-2023	West in ditch,, Mariastraat (EC Metingen - Provincie Zeeland, n.d.)
	14-11-2022	10.3		East in ditch, Mariastraat (EC Metingen - Provincie Zeeland, n.d.)
	06-07-2022	4.9		
ZH-GFB/GFG/GFW (a lot of measurements available from Deltares database)				(Data from Internal Database Deltares, n.d.)

Table 8: FRESHEM and SkyTEM results for measurement locations (Data from Internal Database Deltares, *n.d.*; FRESHEM Zeeland Grensvlakken, 2017; Kok et al., 2010).

Code	Depth fresh-salt interface (m)	Chloride concentration (mg/l)	Depth fresh-salt interface (m)	Chloride concentration (mg/l)
FR-TRS-L1	5.7	8000	-	-
FR-TRS-L2	16.7	8000	-	-
FR-TRS-L3	9.8	8000	-	-
ZL-AAG-L1	6.6	3000	5.6	1000
ZL-AAG-L2	6.6	3000	6.6	1000
ZL-HKK-L1	4.2	3000	3.2	1000
ZL-HKK-L2	4.0	3000	3.5	1000
ZL-KMP-L1	6.7	3000	5.7	1000
ZL-KMP-L2	6.2	3000	5.7	1000
ZL-KWP-L1	3.7	3000	2.7	1000
ZL-KWP-L2	3.7	3000	2.7	1000
ZL-KWP-L3	3.8	3000	2.7	1000
ZL-KWV-L1	11.0	3000	3.0	1000
ZL-KWV-L2	2.9	3000	2.4	1000
ZL-ZVL-L1	29.1	3000	5.6	1000
ZL-ZVL-L2	5.6	3000	3.6	1000
ZL-ZVL-L3	6.2	3000	4.7	1000

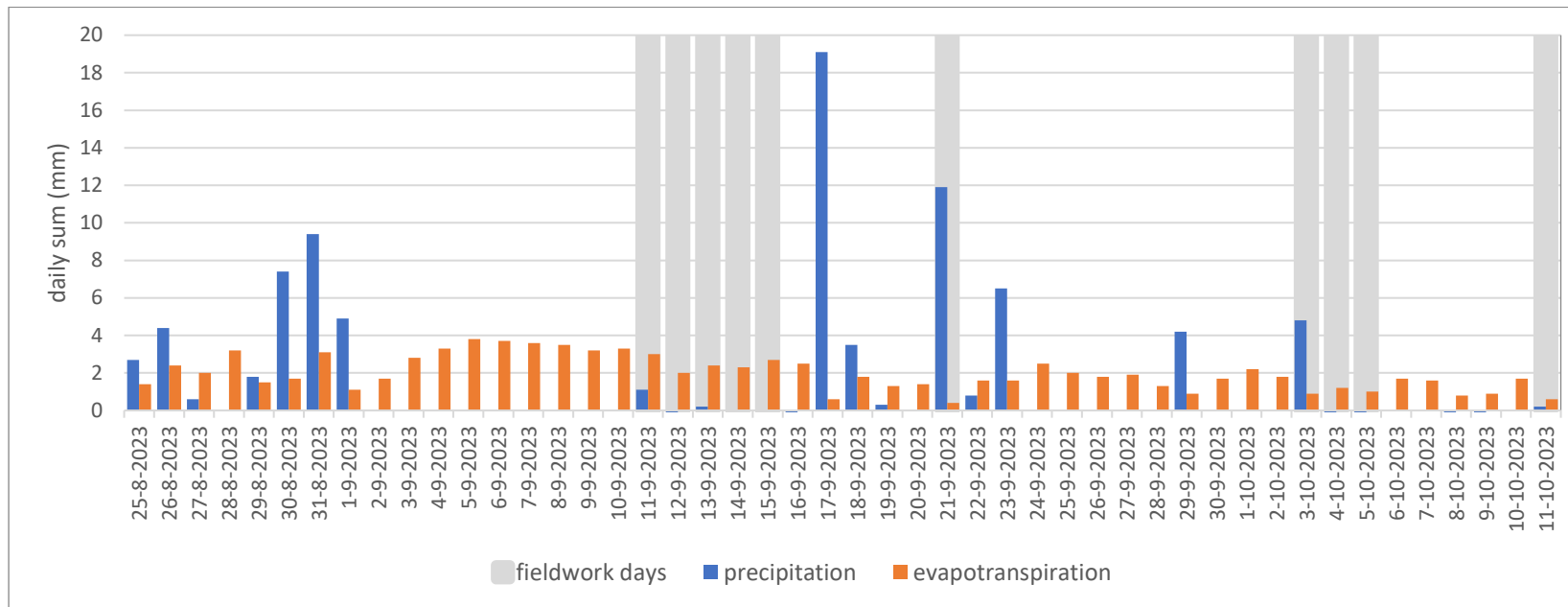


Figure 34: Precipitation and evapotranspiration during the fieldwork period from a weather station in de Bilt (Dagwaarden van Weerstations (25-08-2023 to 11-10-2023) - de Bilt, n.d.).

Table 9: Fieldwork dates per location.

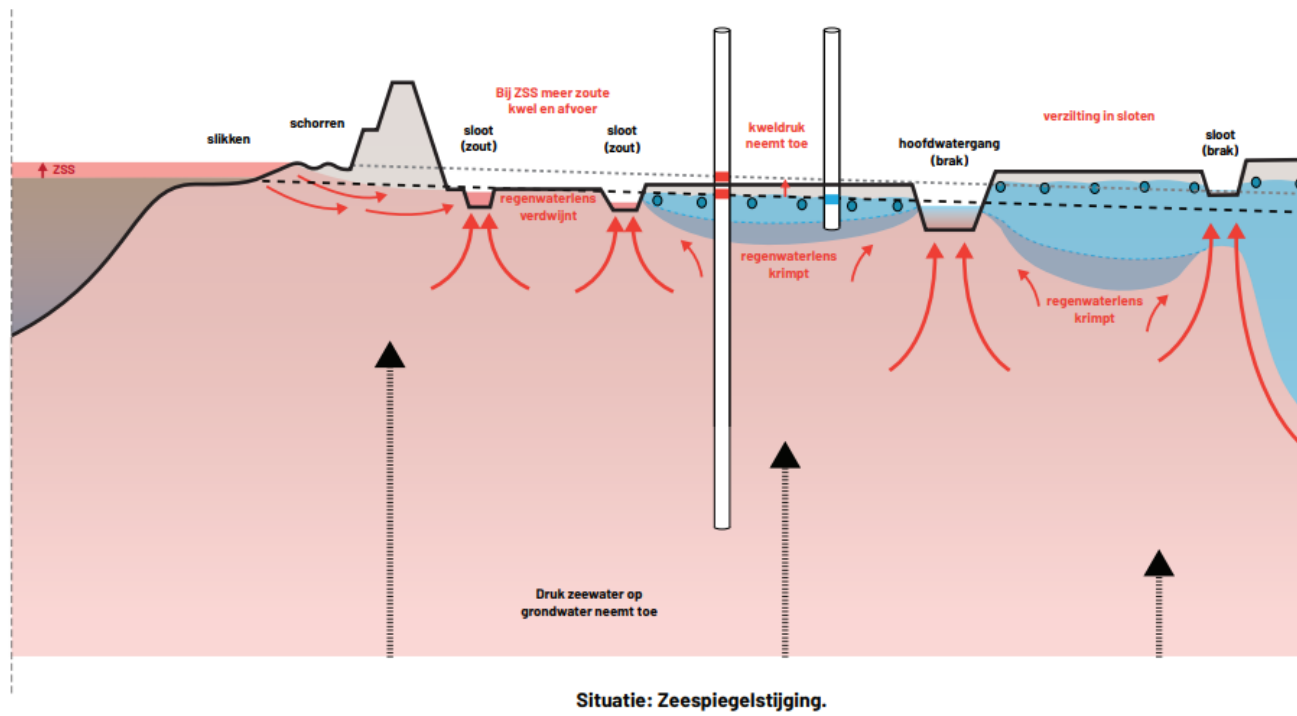
Date	Locations
11-09-2023	FL-AED; FL-SWB; NH-APL; NH-SLD
12-09-2023	FR-HLW; GR-KLB; GR-RTT; GR-UHM
13-09-2023	FL-LSE; FL-LSV
14-09-2023	ZL-KWP; ZL-KWV
15-09-2023	ZL-AAG; ZL-HKK; ZL-KMP
21-09-2023	ZL-ZVL
03-10-2023	NH-ZSC; ZH-BSK
04-10-2023	ZH-GFB; ZH-GFG; ZH-GFW
05-10-2023	FL-MRK; FR-HLK; FR-PBR; FR-PNG; FR-TRN; FR-TRT
11-10-2023	FR-TRS

Appendix B

Principe doorsnede 1: Hydrologische veranderingen bij zeespiegelstijging
Brede Waterkerende Landschappen Oosterschelde locatie Ouwkerk

Legenda

- maalveld
- huidige stijghoogte
- zoet water
- zout water
- ↑ zoute kwel
- - - - - stijghoogte bij ZSS



Situatie: Zeespiegelstijging.
Effecten: Druk zeewater op grondwater neemt toe. Meer zoute kwel en afvoer. Kweldruk neemt toe. Verzilting in sloten. Regenwaterlensen krimpen / verdwijnen.

Figure 35: Hydrological cross-section, showing the area with mudflats (slikken) and salt marshes (schorren), and the more saline 'seepage' ditches close to the dike (America et al., 2023).

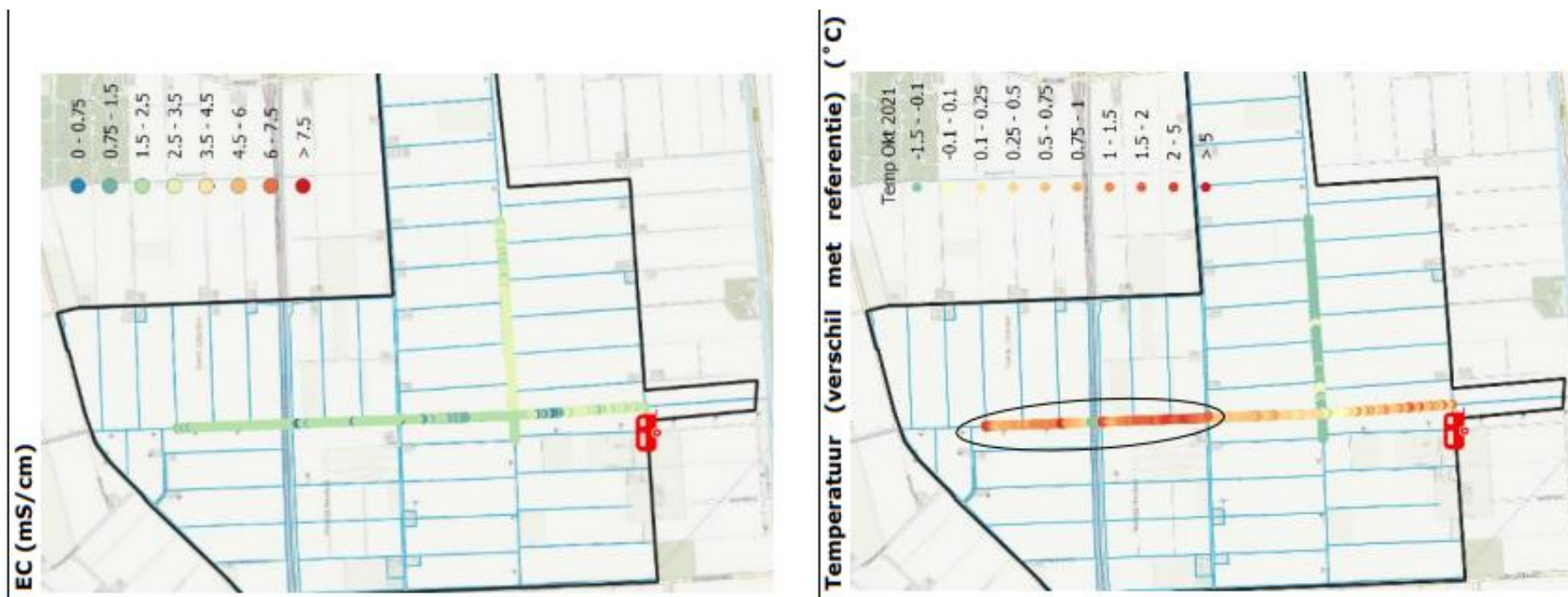


Figure 36: Results routing October 2021, showing seepage in the southern (horizontal) ditch and seepage in the encircled western (vertical) ditch (Schipper et al., 2022).

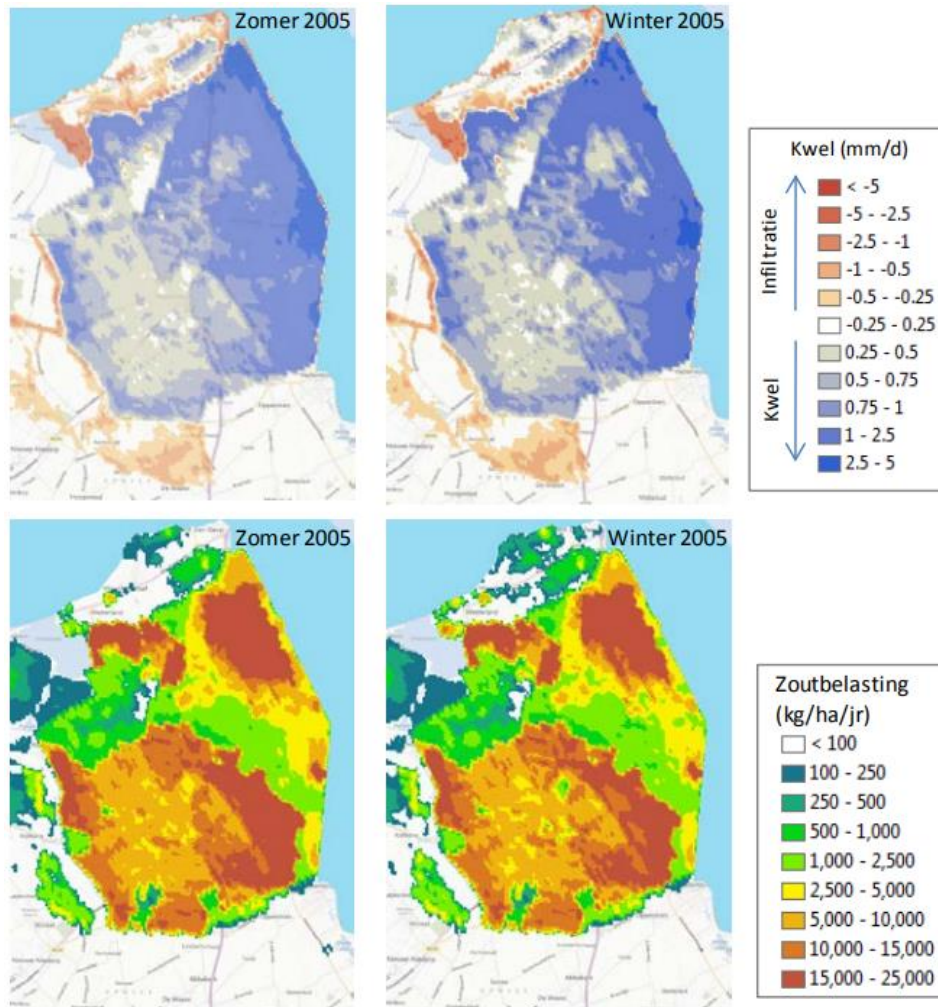


Figure 37: Simulated seepage and salt load for the Wieringermeerpolder in mm/d for the current situation. Upper figure shows the seepage-infiltration map, lower figure shows the salt load map for the mean summer and winter situation (Velstra et al., 2013).

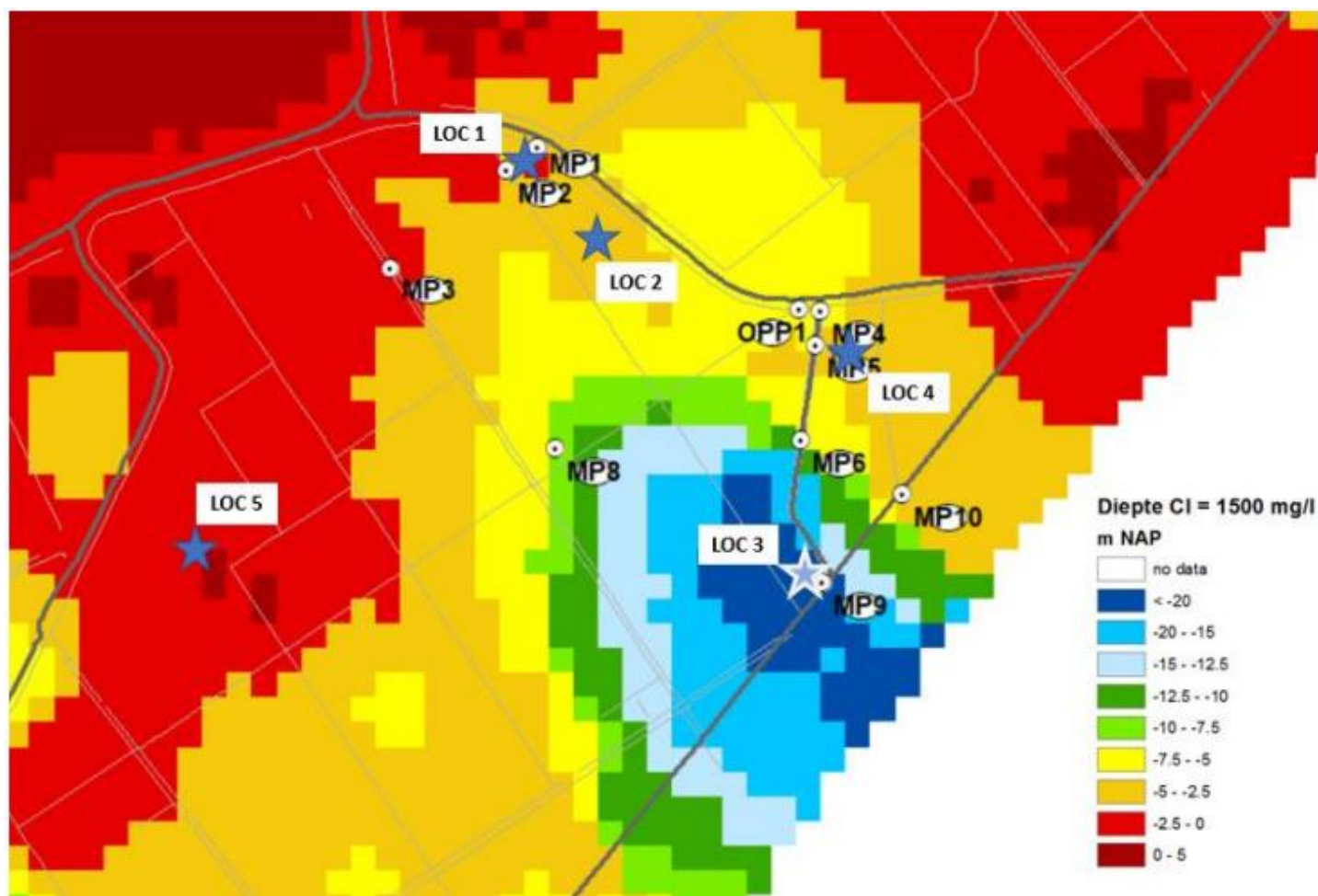


Figure 38: Depth of 1500 mg/L chloride concentration for the Hedwigepolder, with MP4 being ZL-ZVL-L3, MP5 being ZL-ZVL-L2 and MP6 being ZL-ZVL-L1 (P. G. B. de Louw & Bootsma, 2020).

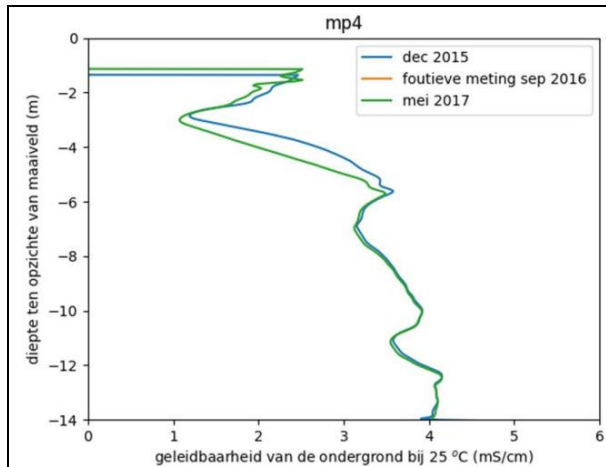


Figure 39: Conductivity of the subsurface with depth for mp4: ZL-ZVL-L3 (P. G. B. de Louw & Bootsma, 2020).

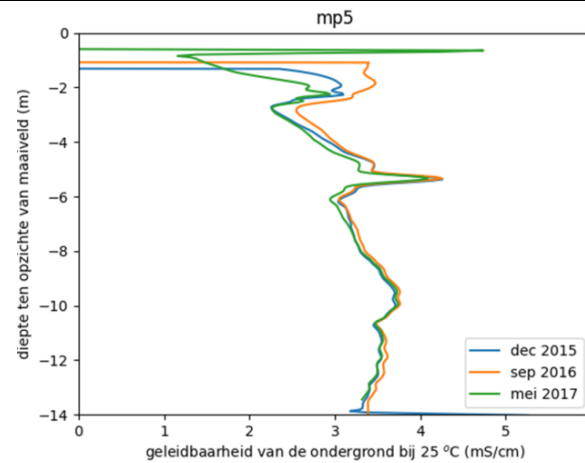


Figure 40: Conductivity of the subsurface with depth for mp5: ZL-ZVL-L2 (P. G. B. de Louw & Bootsma, 2020).

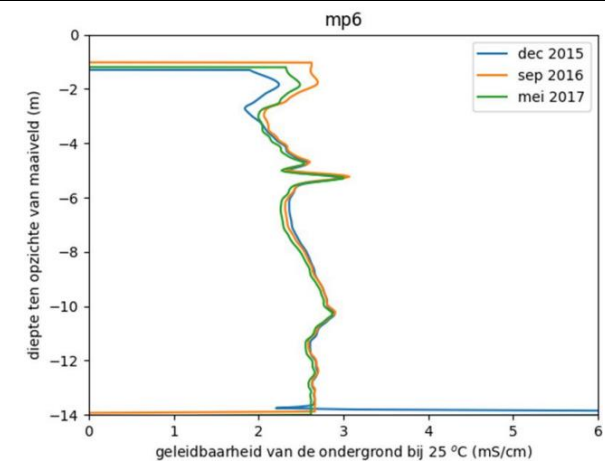


Figure 41: Conductivity of the subsurface with depth for mp6: ZL-ZVL-L1 (P. G. B. de Louw & Bootsma, 2020).

Appendix C

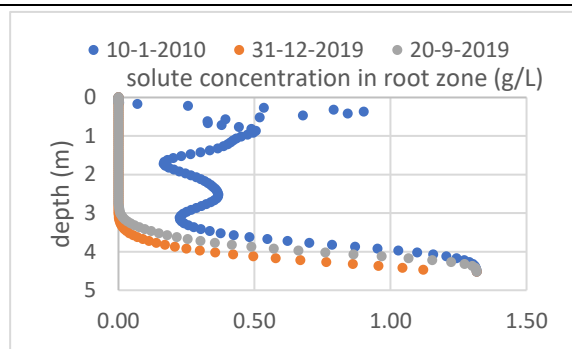


Figure 42: Solute concentrations modelled in depth for FL-SWB-L1L2 for three moments in time, at the start of the timeseries, the end of the timeseries and a measurement in September 2019 (Janssen et al., 2023).

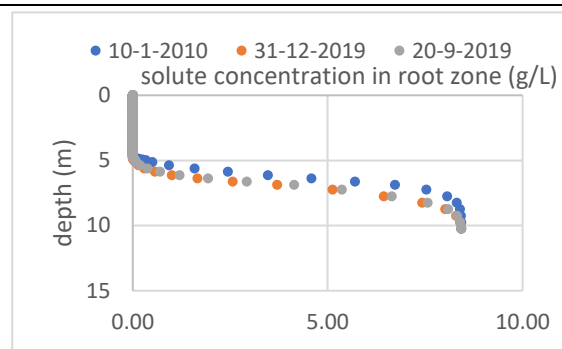


Figure 43: Solute concentrations modelled in depth for FR-PBR-L1L2 for three moments in time, at the start of the timeseries, the end of the timeseries and a measurement in September 2019 (Janssen et al., 2023).

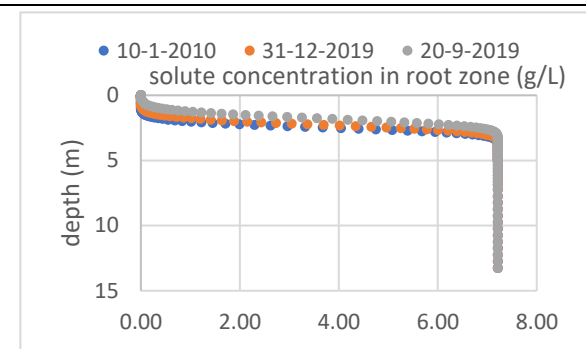


Figure 44: Solute concentrations modelled in depth for FR-TRS-L1 for three moments in time, at the start of the timeseries, the end of the timeseries and a measurement in September 2019 (Janssen et al., 2023).

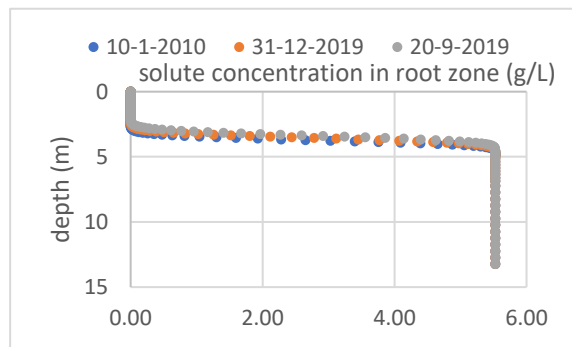


Figure 45: Solute concentrations modelled in depth for FR-TRS-L3 for three moments in time, at the start of the timeseries, the end of the timeseries and a measurement in September 2019 (Janssen et al., 2023).

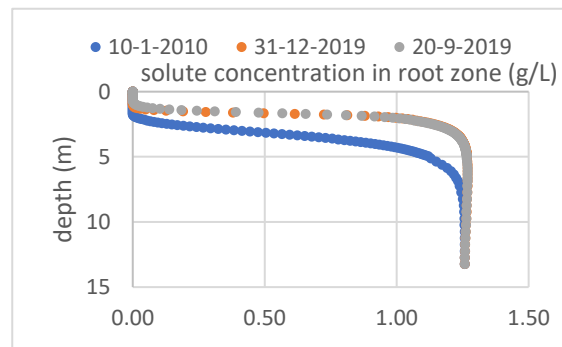


Figure 46: Solute concentrations modelled in depth for GR-RTT-L1 for three moments in time, at the start of the timeseries, the end of the timeseries and a measurement in September 2019 (Janssen et al., 2023).

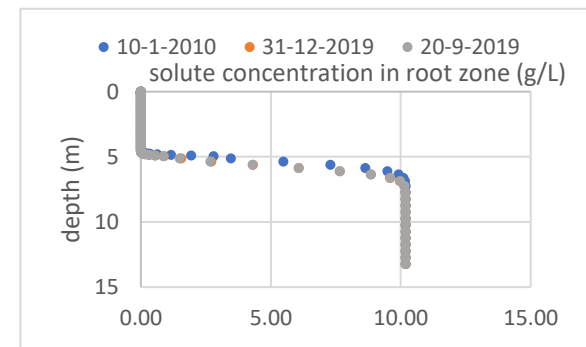


Figure 47: Solute concentrations modelled in depth for NH-APL-1 for three moments in time, at the start of the timeseries, the end of the timeseries and a measurement in September 2019 (Janssen et al., 2023).

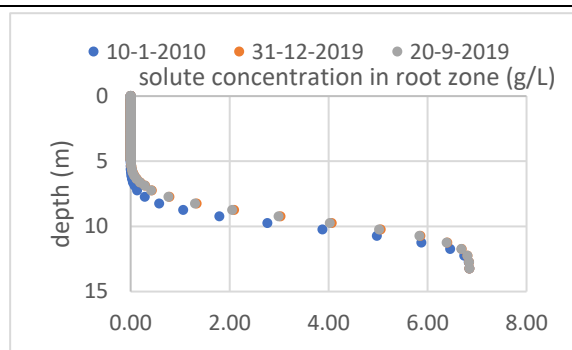


Figure 48: Solute concentrations modelled in depth for NH-APL-L2L3 for three moments in time, at the start of the timeseries, the end of the timeseries and a measurement in September 2019 (Janssen et al., 2023).

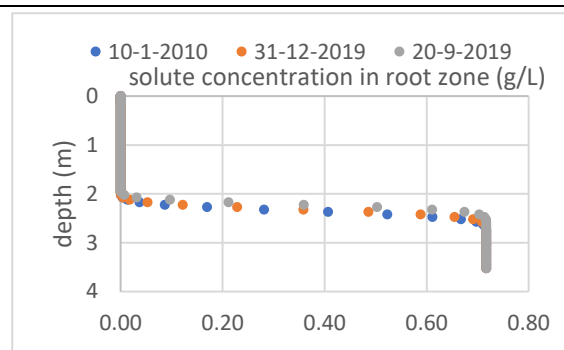


Figure 49: Solute concentrations modelled in depth for NH-SLD-L1L2 for three moments in time, at the start of the timeseries, the end of the timeseries and a measurement in September 2019 (Janssen et al., 2023).

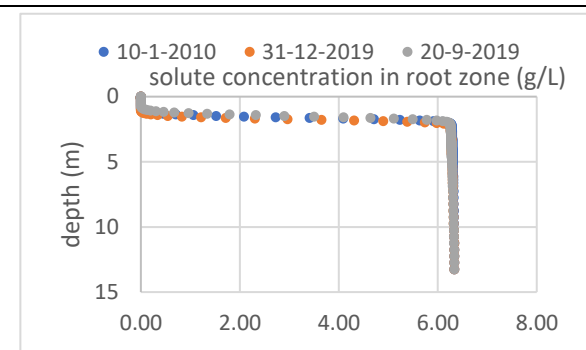


Figure 50: Solute concentrations modelled in depth for NH-ZSC-L1 for three moments in time, at the start of the timeseries, the end of the timeseries and a measurement in September 2019 (Janssen et al., 2023).

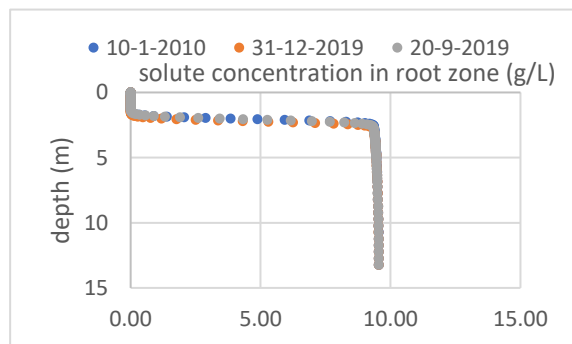


Figure 51: Solute concentrations modelled in depth for NH-ZSC-L2 for three moments in time, at the start of the timeseries, the end of the timeseries and a measurement in September 2019 (Janssen et al., 2023).

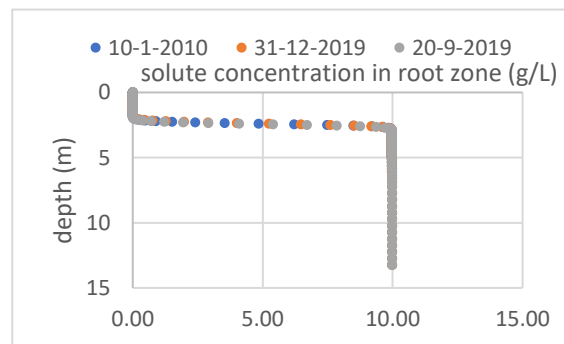


Figure 52: Solute concentrations modelled in depth for ZL-KWP-L1L2L3 for three moments in time, at the start of the timeseries, the end of the timeseries and a measurement in September 2019 (Janssen et al., 2023).

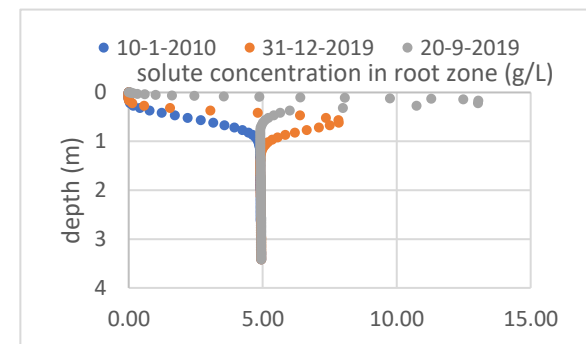


Figure 53: Solute concentrations modelled in depth for ZL-ZVL-L1L2 for three moments in time, at the start of the timeseries, the end of the timeseries and a measurement in September 2019 (Janssen et al., 2023).

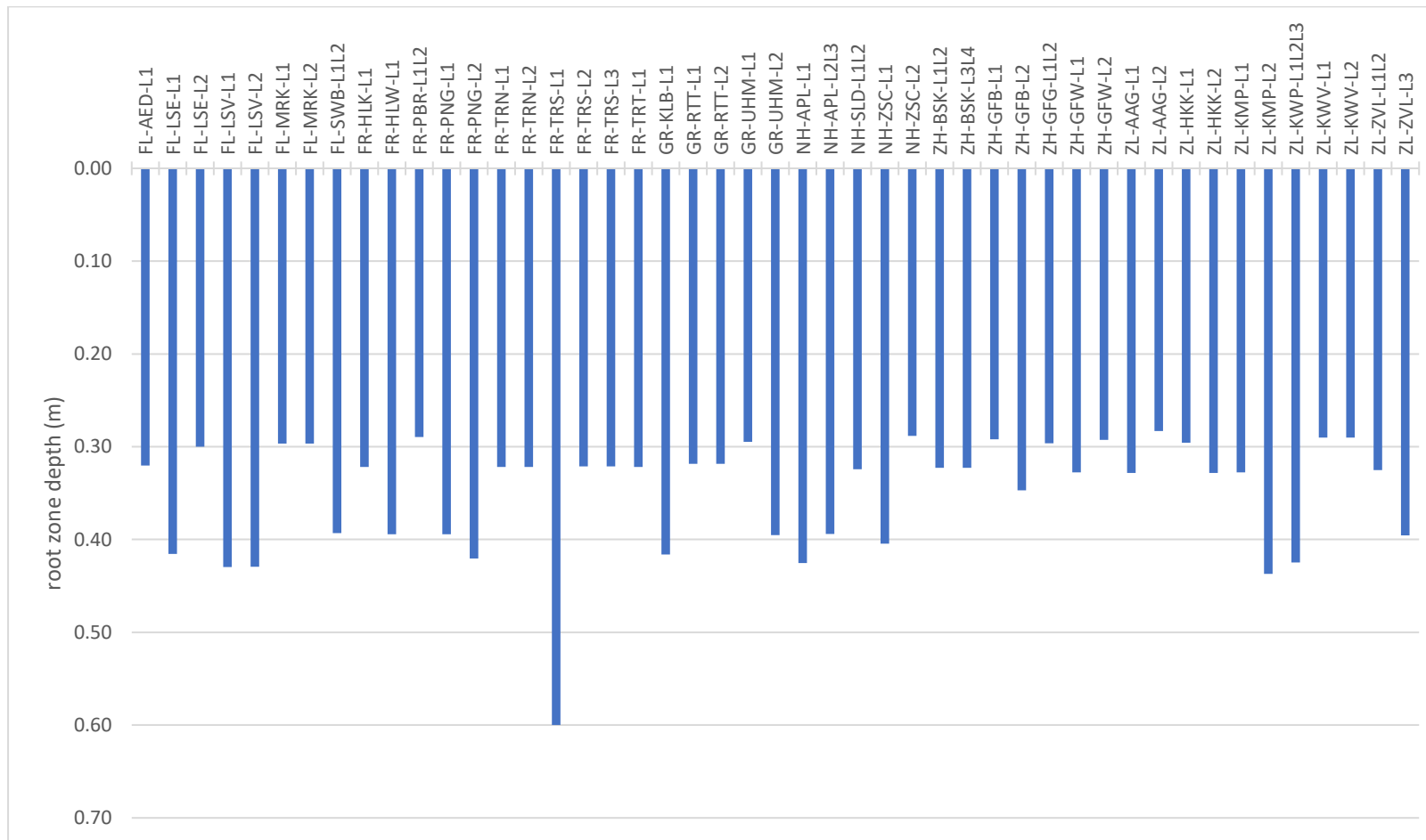


Figure 54: Yearly averaged root zone depths over 2010-2019 for the locations of the soil sample measurement as output from the TRANSOL model (Janssen et al., 2023).

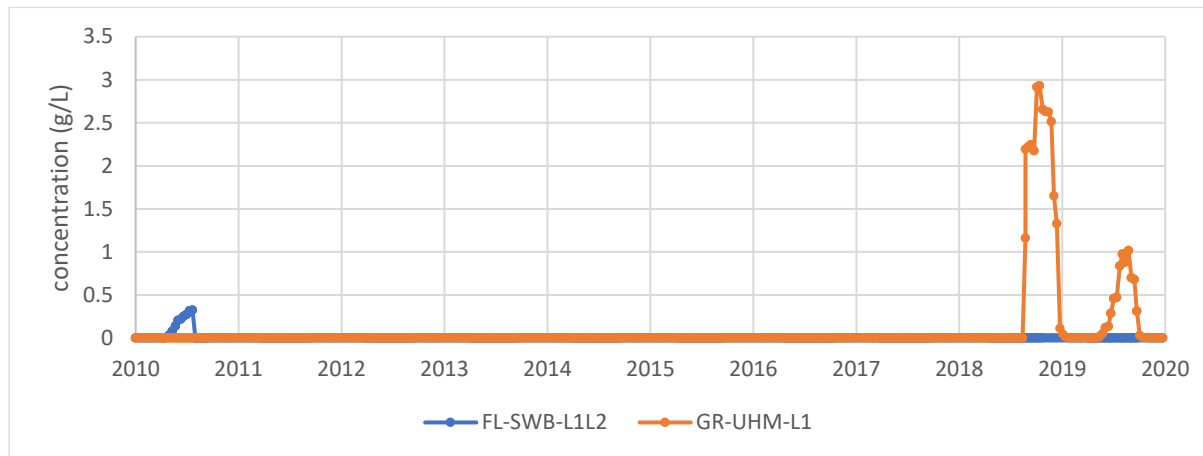


Figure 55: Solute concentrations in the root zone for a location in Flevoland: Swifterbant location 1 and 2 (FL-SWB-L1L2) and a location in Groningen: Uithuizermeeden location 1 (GR-UHM-L1) (Janssen et al., 2023).

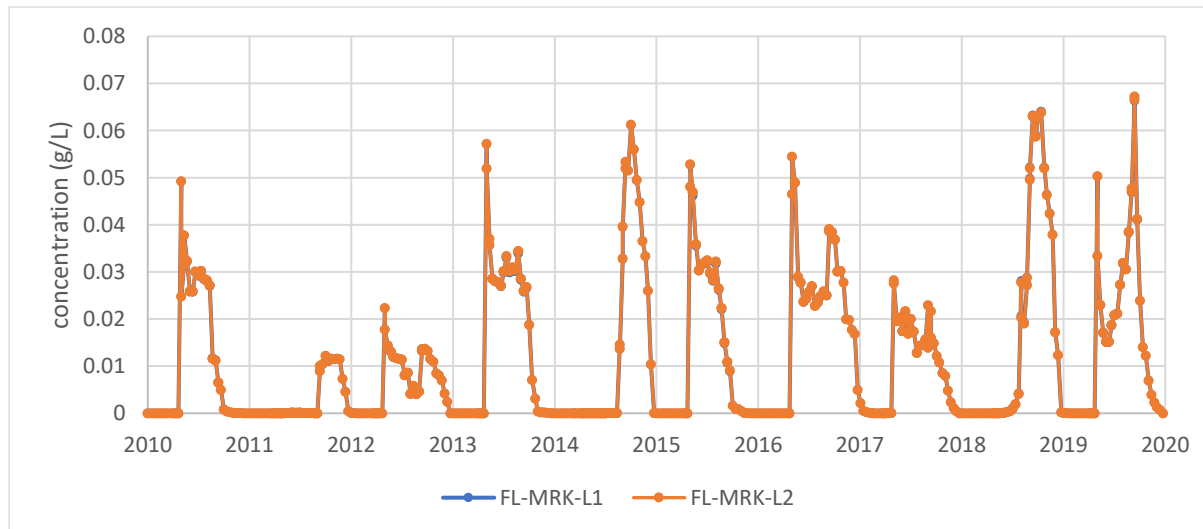


Figure 56: Solute concentrations in the root zone for locations in Flevoland: Marknesse location 1 (FL-MRK-L1) and location 2 (FL-MRK-L2) (Janssen et al., 2023).